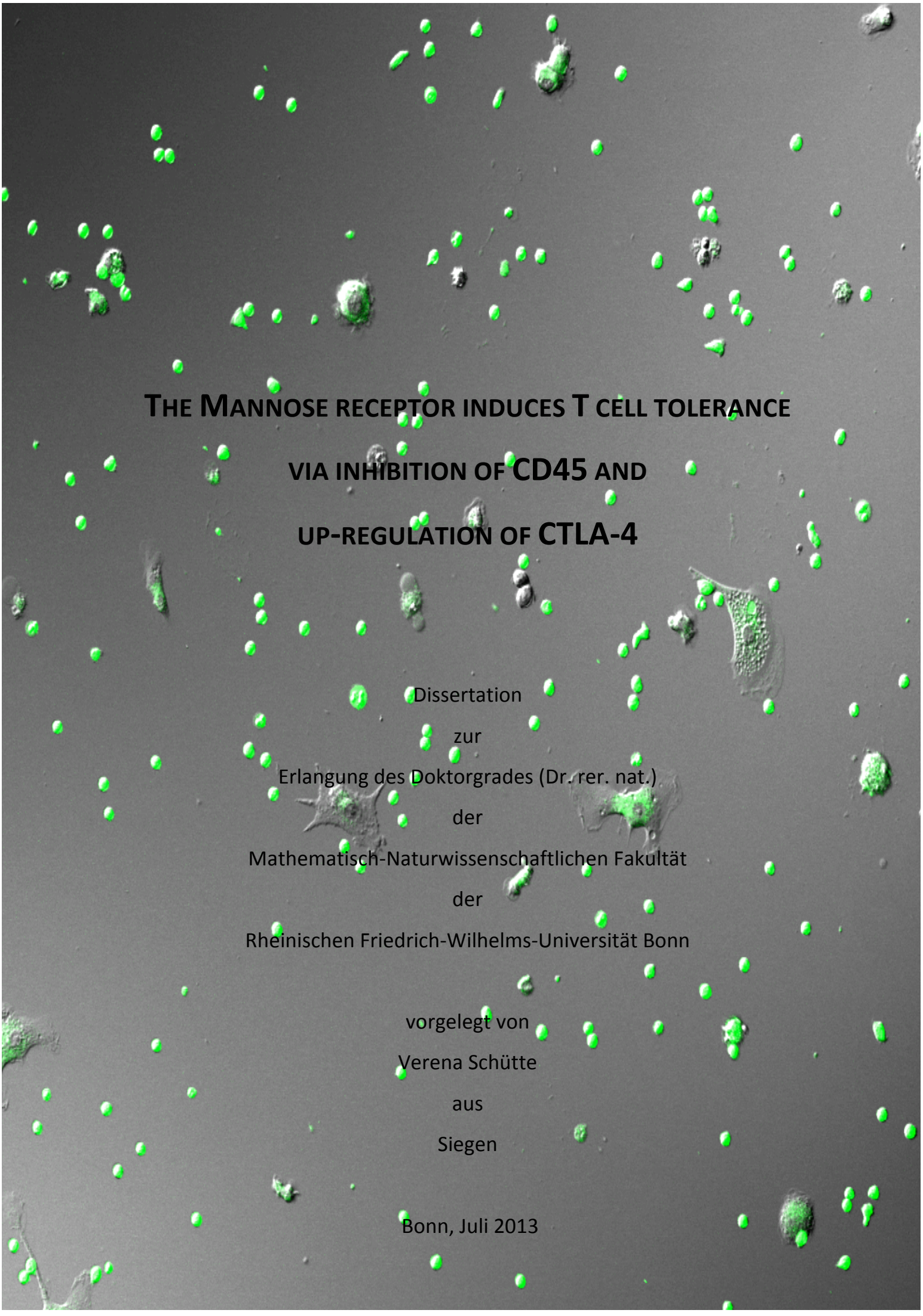

THE MANNOSE RECEPTOR INDUCES T CELL TOLERANCE VIA INHIBITION OF CD45 AND UP-REGULATION OF CTLA-4

Dissertation

zur

Erlangung des Doktorgrades (Dr. rer. nat.)

der

Mathematisch-Naturwissenschaftlichen Fakultät

der

Rheinischen Friedrich-Wilhelms-Universität Bonn

vorgelegt von

Verena Schütte

aus

Siegen

Bonn, Juli 2013

THE MANNOSE RECEPTOR INDUCES T CELL TOLERANCE VIA INHIBITION OF CD45 AND UP-REGULATION OF CTLA-4

Dissertation

zur

Erlangung des Doktorgrades (Dr. rer. nat.)

der

Mathematisch-Naturwissenschaftlichen Fakultät

der

Rheinischen Friedrich-Wilhelms-Universität Bonn

vorgelegt von

Verena Schütte

aus

Siegen

Bonn, Juli 2013

Angefertigt mit Genehmigung der Mathematisch-Naturwissenschaftlichen Fakultät der
Rheinischen Friedrich-Wilhelms-Universität Bonn

1. Gutachter: Prof. Dr. Sven Burgdorf

2. Gutachter: Prof. Dr. Waldemar Kolanus

Tag der Promotion: 14.10.2013

Erscheinungsjahr: 2014

In der Dissertation eingebunden:

Zusammenfassung (Abstract)

Für Steven.

„Leider läßt sich eine wahrhafte Dankbarkeit
mit Worten nicht ausdrücken.“

Johann Wolfgang von Goethe

INDEX

1 ABSTRACT

The present study proves that the mannose receptor (MR) bears beside its function as endocytic receptor a second responsibility namely the induction of tolerance.

The results of our experiments show that the decision, whether this immune-suppressive effect is carried out depends on the inflammatory status of the surrounding milieu. Whereas at steady-state conditions the MR has a tolerogenic effect during activation of $CD8^+$ T cells, this suppressive phenotype is overcome under inflammatory conditions. Thereby, the MR resembles a molecular switch between tolerance induction on the one hand and allowance or even mediating immunity by antigen-uptake on the other hand.

The investigations of this thesis shed light into the underlying molecular mechanism of the MR-mediated induction of tolerance. The MR on DCs can bind to the tyrosine phosphatase CD45 on the T cell surface. This interaction leads to inhibition of its phosphatase activity, which is responsible for a reduced cytotoxic capacity of activated $CD8^+$ T cells. The executive molecule in this process is the inhibitory protein cytotoxic T-lymphocyte antigen 4 (CTLA-4), being up-regulated upon inactivation of CD45.

After maturation of the DCs with the inflammatory molecule CpG, the immune suppressive effect of the MR is overcome and a robust immune response is initiated. The findings of this study pinpoint this effect to the abolished expression of CTLA-4. It is furthermore shown that signaling events via the co-stimulatory molecule CD28 are sufficient to suppress CTLA-4 up-regulation. Hence, a potent cytotoxic $CD8^+$ T cell response is induced.

Finally, it can be demonstrated that the tolerogenic effect of the MR as well as its molecular mechanism also holds true *in vivo*.

2 INTRODUCTION

2.1 The immune system

The immune system protects organisms from pathogens like bacteria, viruses, funghi and parasites. One discriminates between the faster but unspecific innate immune system and the time-consuming but very pathogen-specific adaptive immune system.

The innate immune system comprises of chemical, mechanical and microbiological barrier mechanisms in addition to neutrophils, monocytes, macrophages, complement, cytokines and acute phase proteins (1). This first line of defense prevents pathogen-spreading from the site of infection within the first 96 hours of infection. Afterwards the adaptive immune system is initiated (2).

Pathogenic composites which are absent in mammalian organisms, like bacterial wall compounds, unmethylated CpG motifs or double-stranded RNA are designated as pathogen-associated molecular patterns (PAMPs). These can be recognized by pattern recognition receptors (PRRs) expressed by cells of the immune system. The most prominent PRRs are the so-called Toll-like receptors (TLRs) whose encounter with pathogenic ligands leads to inflammation on the site of infection and induction of the adaptive immune response (3).

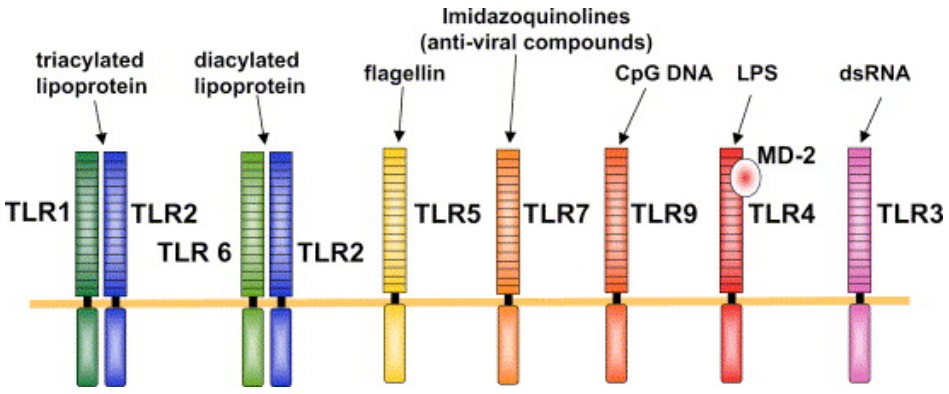

Fig. 2-1: Toll-like receptors and their ligands

TLR1-7 and TLR9 recognize microbial compounds not expressed by mammals. TLR2 senses microbial lipopeptides and is associated with TLR1 or TLR6 leading to a specific recognition of tri- or diacetylated lipoproteins respectively. Bacterial flagellins are recognized by TLR5, viral single stranded RNA by TLR7, CpG DNA by TLR9, LPS by TLR4 and viral double stranded RNA is sensed by TLR3. Thereby the immune system can discriminate different pathogenic patterns by a variety of TLRs. Adopted from Takeda K in Seminars in Immunology, 2006.

The adaptive immune system is a hallmark of higher animals (1) and besides its antigen-specificity one major peculiarity is the development of a immunological memory. The immunological memory ensures an accelerated immune response in case of a secondary infection (2). Activated B cells and T cells represent the effector cells of the adaptive immune system. B cells produce antibodies, whereas T cells are diverse in function with cytotoxic T cells, T helper cells and regulatory T cells as the main T cell subtypes.

2.2 Necessity of dendritic cell maturation for T cell activation

T cells have to be activated by professional antigen-presenting cells (APC) such as dendritic cells (DC), macrophages and B cells (2). However, DCs drastically render their phenotypic appearance upon pathogen-encounter, thus enabling them for T cell priming (4).

Under non-inflammatory steady state conditions, DCs reside in and patrol through peripheral tissue, blood, lymph and secondary lymphoid organs. Thereby they constantly take up, process and load antigens onto major histocompatibility complexes (MHC), a process called antigen presentation (3). However, this is quite ineffective and does not lead to potent induction of immunity.

Upon pathogen recognition by for example TLRs, DCs undergo a process of maturation. As consequence, migration capacities, expression of co-stimulatory molecules, antigen presentation on surface MHC molecules and secretion of cytokines are increased and hence a potent immune response is initiated (3, 4).

2.2.1 DC maturation enhances expression of co-stimulatory molecules

It is commonly accepted that up-regulation of co-stimulatory molecules like CD80, CD86 and CD40 is initiated upon DC maturation and hence they serve as markers for mature DCs (5). The binding of these molecules with their corresponding stimulatory counter-receptors CD28 (for both CD80 and CD86) and CD40 ligand (CD40L) on the T cell surface is necessary for prolonged T cell activation and survival (6).

2.2.2 DC maturation enhances antigen presentation

The process of antigen presentation can be subdivided into the acquisition of antigens, their degradation and their loading on MHC molecules. These MHC-peptide complexes are finally transported to the cell surface, where they are presented to T cells (7).

Depending on the source of antigens, they can be presented on different MHC molecules. Basically, intracellular antigenic peptides originating from viruses, intracellular bacteria or cellular transformation are processed by the proteasome and transported via the transporter associated with antigen processing (TAP) into the endoplasmic reticulum (ER), where they are loaded on MHC class I (MHC I) molecules (8) (see **Fig. 2-2)**.
On the other hand, peptides from extracellular antigens, like extracellular bacteria or parasites, plus endogenous antigens acquired by autophagy are taken up, degraded in lysosomal compartments and peptides are presented on MHC class II (MHC II) molecules (9) (see **Fig. 2-2**).

Corresponding to these different presentation pathways, distinct T cell subsets recognize the MHC-peptide complexes, as they are $CD4^+$ T cells for MHC II and $CD8^+$ T cells for MHC I. Activated $CD4^+$ T cells gain T helper function and assist in DC maturation by CD40/CD40L binding (10, 11). Furthermore, they support activation of B cells and macrophages, which leads to antibody production and destruction of extracellular antigens (9). In contrast to that, $CD8^+$ T cells achieve cytotoxic capacities, resulting in a specific elimination of target cells displaying the antigenic peptides on surface MHC I molecules (8).
A bypass of this strict discrimination exists in presentation of extracellular antigens on MHC I, a process called cross-presentation (12). This ensures immunity against viruses or tumor antigens that do not affect the DCs themselves and would otherwise escape annihilation by the immune system (see **Fig. 2-2**).

In the process of maturation, antigen capture is reduced. Thus, mainly antigens are presented on MHC molecules, which have been acquired during maturation (3). Furthermore, surface expression of antigen-loaded MHC molecules on immature DCs is rather transient and is enhanced and prolonged after DC maturation (13), leading to

increased antigen presentation after pathogen recognition. Besides the decision which kind of responder cell is activated, the characteristics of pathogens also induce the secretion of a specific set of cytokines (14).

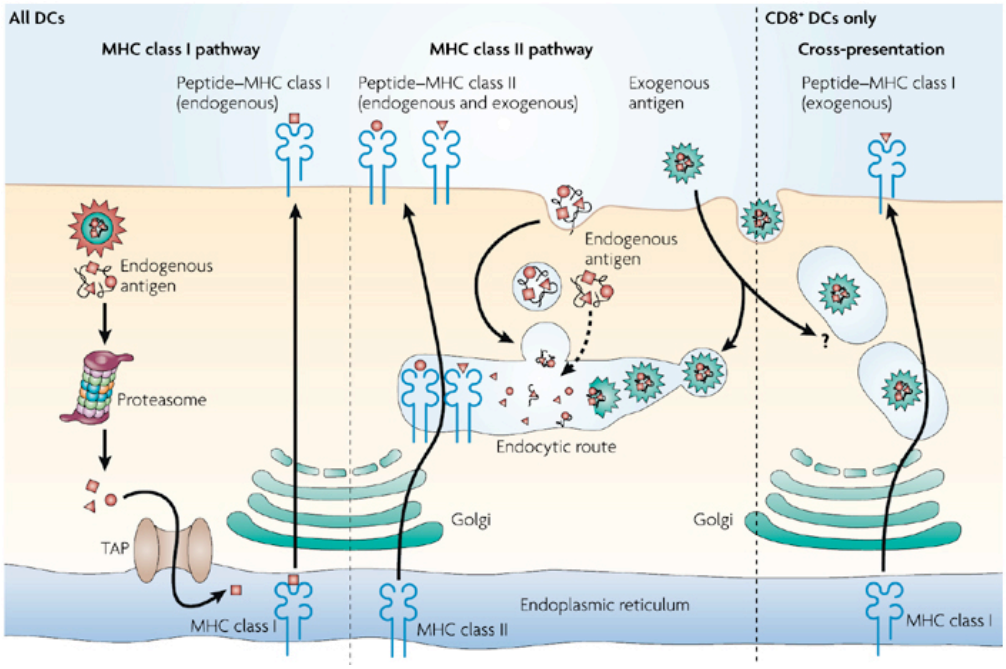

Fig. 2-2: Antigen presentation pathways

Endogenous antigens are degraded by the proteasome and resulting peptides are transported via the TAP transporter into the ER and loaded onto MHC I. Subsequently, they are presented on the cell surface towards $CD8^+$ T cells. In contrast to that, endocytosed exogenous antigens or endogenous antigens taken up by autophagy are lysed in endo-lysosomes, which fuse with MHC II-bearing vesicles. In these compartments the loading of antigens on MHC II takes place and after transfer to the cell surface presentation to $CD4^+$ T cells occurs. The third pathway of antigen presentation is the cross-presentation in which exogenous antigens are loaded on MHC I molecules and are presented towards $CD8^+$ T cells. Adopted from Villadangos JA in Nature Reviews Immunology, 2007.

2.2.3 DC maturation enhances and switches cytokine secretion

During DC maturation the profile of secreted cytokines is affected by the nature of the recognized pathogen. Intracellular pathogens trigger the DC to release interleukin 12 (IL-12) which in turn results in the differentiation of naive $CD4^+$ T helper cells towards a T_H1 phenotype accompanied with secretion of cytokines like IFN-γ, IL-2 and tumor necrosis factor (TNF) (15, 16) (see **Fig. 2-3**). T_H1 differentiated cells and the secreted cytokines act in concert to activate cytotoxic T cells and macrophages, resulting in a cell-mediated immune response against infected or transformed cells.

In contrast to that, identification of extracellular pathogens fails to induce IL-12 secretion, which leads to secretion of IL-4 and IL-10 by the DC instead. This results in differentiation

of naive $CD4^+$ T cells of a T_H2 phenotype with cytokine release of IL-4, IL-5, IL-6, IL-9, IL-10, IL-13 and transforming growth factor beta (TGF-β) (15, 16) (see **Fig. 2-3**). Hence, a humoral immune response against extracellular pathogens is initiated by activation of B cells accompanied with antibody production.

In addition to these paracrine cytokine effects on T cells, secreted cytokines also possess autocrine functions on the producing DCs themselves. IFN-γ for example enhances IL-12 secretion and the expression of co-stimulatory molecules (e.g. CD80, CD86 and CD40) (17), whereas secretion of IL-10 has the opposing effect (18, 19). The combination of increased expression of co-stimulatory molecules and surface MHC-peptide complexes plus the enhanced and altered cytokine secretion, qualify mature DCs for potent T cell activation.

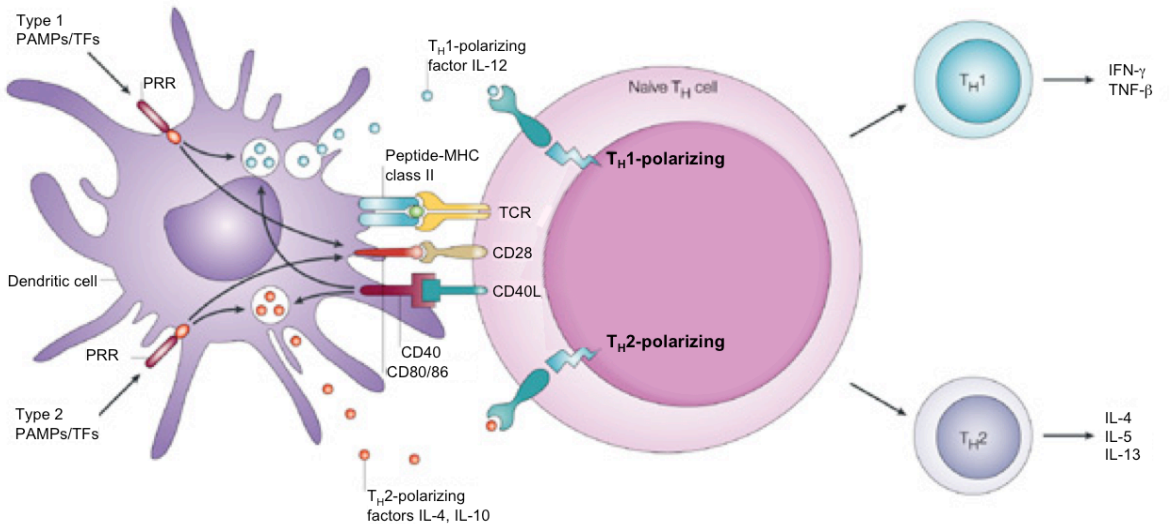

Fig. 2-3: T_H1 and T_H2-cell differentiation

Activated DCs present pathogenic antigens in combination with co-stimulatory molecules in the local cytokine milieu towards $CD4^+$ T cells which lead to their differentiation into either T_H1 or T_H2 helper T cells. Certain pathogens are sensed by the DC via PRRs which lead to IL-12 secretion. Thus, IL-12 promotes differentiation of $CD4^+$ T cells into IFN-γ- and TNF-secreting T_H1 cells. The inability of pathogens to induce IL-12 secretion in DCs results in IL-4 and IL-10 production. Hence, T_H2-cell differentiation accompanied with the secretion of interleukins 4 and 5 and 13 is induced. Modified from Kapsenberg ML in Nature Reviews Immunology, 2003.

2.3 Three signals required for T cell activation

Three signals are necessary for an efficient T cell activation. Signal one is the T cell-specific antigen presented on MHC molecules, signal two is provided by co-stimulatory molecules and the third signal is delivered by inflammatory cytokines.

The T cell receptor (TCR) recognizes the haplotype-matching MHC loaded with foreign antigenic peptides. Mismatching of either of the two components normally leads to T cell unresponsiveness (2). One particularity resembles the alloreaction in which the TCR either strongly interacts with a well fitting peptide even if it is presented on a nonself MHC molecule (peptide-dominant binding), or the TCR binds the nonself MHC molecule independent of the associated peptide (MHC-dominant binding) (2). The interaction of the TCR and MHC/peptide complexes is respectively stabilized by the TCR co-receptors CD4 and CD8. Especially when low-affinity ligands are bound, this stabilization takes place. Furthermore, the co-receptors recruit signaling molecules to the site of antigen recognition (2, 20).

Co-stimulatory molecules on DCs and their respective counter-receptors on T cells form complexes leading either to stimulatory or inhibitory T cell signaling. A multitude of such complexes exist such as CD80/CD86-CD28/CTLA-4, ICOSL-ICOS, PD-L1/PD-L2-PD1/PD2, CD40-CD40L and OX40L-OX40 just to state the major molecules (21). In the case of CD80/CD86-CD28/CTLA-4, the molecules CD80 and CD86 can either bind to the stimulatory receptor CD28 resulting in T cell activation or they can bind to the inhibitory receptor CTLA-4 with a ten-fold increased affinity (22), which induces T cell tolerance (23).

Whereas already signal one and two can trigger T cell proliferation and IL-2 secretion (24), only signal three causes development of full effector function of $CD8^+$ cytotoxic T cells (25). Inflammatory cytokines deliver a “danger” signal in case of an infection. $CD8^+$ T cells require IL-12 or Type I interferons (IFN-α/β) for increased survival, formation of a memory population and induction of optimal cytotoxic effector function along with IFN-γ secretion (26) (see **Fig. 2-4**).

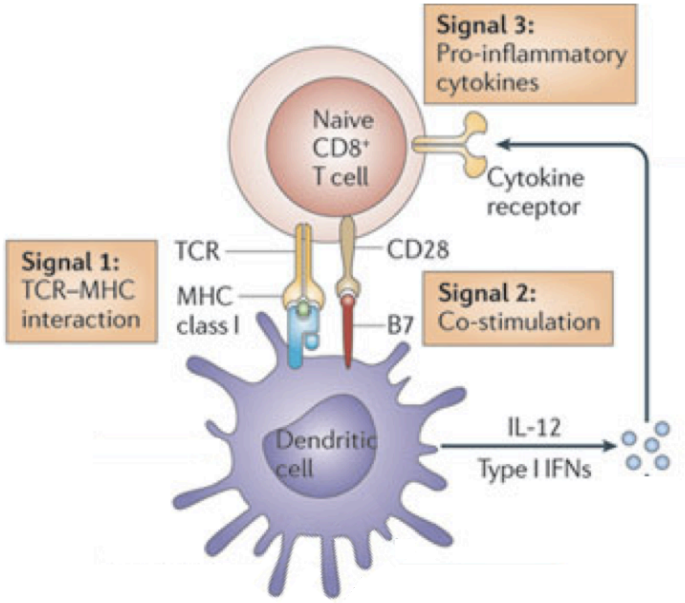

Fig. 2-4: The three signals for T cell activation

Signal one is the immunogenic antigen presented on MHC molecules on DCs, which are recognized by the antigen-specific TCR. Signal two is provided by the DC in form of co-stimulatory molecules with a binding molecule on the T cell side. To achieve $CD8^+$ cytotoxic T cell activation, the third signal is predominantly delivered by IL-12 and Type I IFNs. Modified from Sun JC in Nature Reviews Immunology, 2011.

2.4 Killing mechanisms of $CD8^+$ cytotoxic T lymphocytes

$CD8^+$ cytotoxic T lymphocytes (CTLs) and natural killer cells (NK) are the two main cytotoxic effector cells with common pathways to induce cell death. The triggering of apoptosis of condemned cells is preferred to necrosis since it is a non-inflammatory elimination (27).

Two main routes of apoptosis induction are used: the calcium-dependent exocytosis of granzyme and perforin containing granules and the calcium-independent FAS pathway. Both are conditional on direct contact with the target cell in which caspases are activated leading to the induction of apoptosis. Besides these two pathways, also cytokines like IFN-γ and TNF can mediate cytotoxicity by either increasing cytotoxic capacities of CTLs (28) or respectively by direct induction of apoptosis via cell surface receptors (29) (see **Fig. 2-5**).

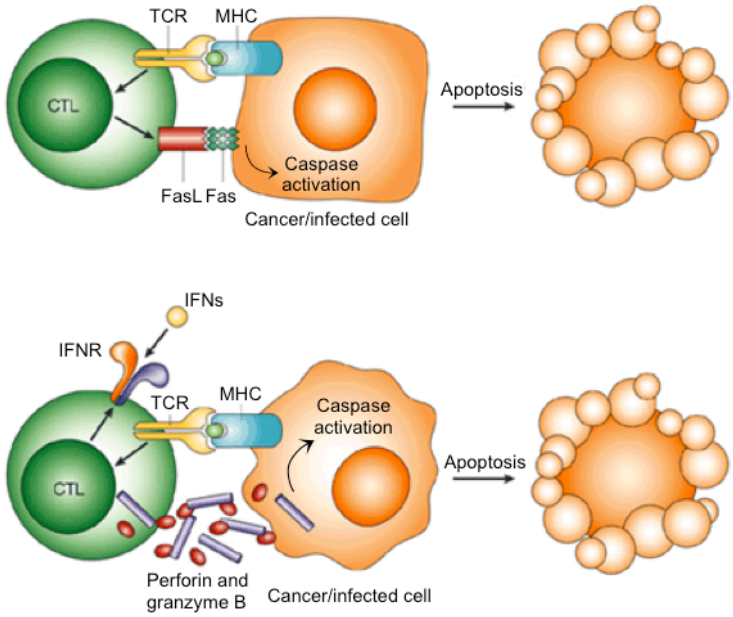

Fig. 2-5: Induction of apoptosis by cytotoxic T cells

The two main routes of inducing apoptosis in cancer cells or virally infected cells are via ligation of Fas with its ligand FasL and exocytosis of cytotoxic granules. Both pathways lead to activation of several caspases in the condemned cell, which in the end result in induction of apoptosis. Additionally, cytokines like interferons are able to increase the cytotoxic capacity of CTLs by binding to their receptor (IFNR). Modified from Trapani JA in Nature Reviews Immunology, 2002.

2.5 CD28 triggers the effector function of $CD8^+$ cytotoxic T cells

For a proper $CD8^+$ T cell activation accompanied with the obtainment of cytotoxic capacities, a series of signaling events are initiated within the T cell.

As already indicated, stimulation of the TCR alone leads to T cell irresponsiveness and anergy (see **Fig. 2-6**). Despite activation of signaling pathways like the Calcineurin/ Calmodulin pathway, no T cell effector function can be achieved. Although signaling molecules like the nuclear factor of activated T cells (NFAT) are activated and are able to translocate into the nucleus, lacking expression of the activator protein 1 (AP1) results in transcription of anergy inducing genes (see **Fig. 2-6**).

This anergic state can be circumvented by signals via co-stimulatory molecules, primarily by CD28 on DCs. CD28 interacts with CD80/86 on the T cell surface and promotes T cell proliferation, cytokine production, cell survival and cellular metabolism (30). This is due to the fact that additional signaling pathways (e.g. RAS-MAPK, IKK and PKC) are induced, leading to NF-κB and AP1 expression. These transcription factors can act in concert with

NFAT, as for AP1, or by themselves to target a set of genes whose expression results in effective T cell activation.

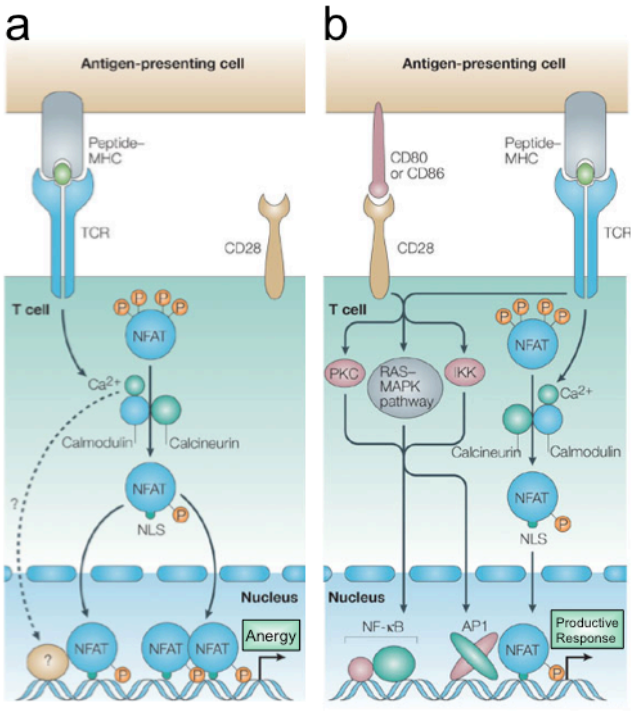

Fig. 2-6: TCR signaling in the absence and the presence of co-stimulatory molecules

Co-stimulatory molecules lead to the induction of signaling events, which are necessary for productive T cell activation and prevention of anergy. **a)** TCR stimulation in the absence of co-stimulation only activates NFAT which translocates into the nucleus and induces transcription of anergy-related genes. **b)** In contrast to that, the presence of co-stimulatory molecules triggers additional pathways like RAS-MAPK, PKC or IKK. These pathways result in synthesis of transcription factors like AP1 and NF-κB finally targeting T cell effector genes. Modified from Macian F in Nature Immunology Review, 2005.

2.6 T cell signaling in CD8$^+$ cytotoxic T cells

The molecular mechanism leading to the cytotoxic effector function of CD8$^+$ T cells comprises a cascade of protein interactions combined with their successive activation. This cascade delivers the signal coming from the surface TCR into the nucleus of the T cell. Here, the transcription of specific target genes mediates the differentiation into cytotoxic effector T cells.

The functional TCR is composed of two elements. The highly variable heterodimer of TCRα and TCRβ chains form the antigen-binding pocket whereas the invariant CD3 complex, consisting of CD3γ, δ and ε in association with the cytoplasmic ζ homodimer, is responsible for efficient TCR surface expression and intracellular signaling (2).

Located in close proximity, the CD8 co-receptor stabilizes the interaction of the TCR with MHC I-peptide complexes (2, 20) and recruits, bound to its cytoplasmic tail, the lymphocyte-specific protein tyrosine kinase (Lck) towards the TCR (31, 32). Each of the two CD3 ζ-chains harbor three ITAM (immunoreceptor tyrosine-based activation motif) tyrosines. Upon TCR ligation, they are substrates for phosphorylation by Lck (33) resulting in the recruitment of ZAP-70 (ζ-chain-associated protein kinase of 70kDa) (see **Fig. 2-7**).

Smith-Garvin reviewed in 2009 (34) the afterwards events of the TCR signaling. A multi-molecular complex, designated as proximal signaling complex, is formed. The core of this complex consists of the transmembrane adaptor molecule LAT (linker for the activation of T cells) and the cytosolic adapter SLP76 (Src homology 2 (SH2) domain-containing leukocyte phosphoprotein of 76kDa) arranging all later recruited molecules in the correct spatiotemporal manner (see **Fig. 2-7**).

This proximal signaling complex initiates a cascade of phosphorylation events and a recruitment of further molecules being mostly kinases. As a result, a series of phenotypic changes are initiated within the T cells including rearrangement of the Actin cytoskeleton, increased cell adhesion by enhanced surface expression of integrins and activation of transcription factors like NFAT, NF-κB and AP1.

The initiation of transcription factor expression is mediated via three main routes, all starting with the hydrolyzation of the membrane lipid PtdIns(4,5)P_2 (phosphatidylinositol-4,5-bisphosphate) into the second messengers $InsP_3$ (inositol-1,4,5-triphosphate) and DAG (diacyl glycerol). This hydrolyzation is performed by the phospholipase Cγ1 (PLCγ1), which is recruited to the proximal signaling complex after TCR-ligation.

$InsP_3$ induces the first pathway, comprising the calcium release via the molecules Calcineurin/Calmodulin which in turn results in NFAT activation accompanied with transcription of genes involved in T cell activation, amongst them IL-2 (34).

DAG activates two diverse signaling pathways, being the Ras and the protein kinase C (PKC) pathways.

Ras itself induces the MAPK (mitogen-associated protein kinase) signaling cascade which in turn initiates the synthesis of AP1 and thereby the transcription of IL-2 transcription, T cell proliferation, growth and differentiation (34).

The second pathway being initiated by DAG is the one including activation of PKC. At the end, active PKC triggers the NF-κB pathway leading to transcription of several genes important for survival, proliferation and effector function development (35) (see **Fig. 2-7**).

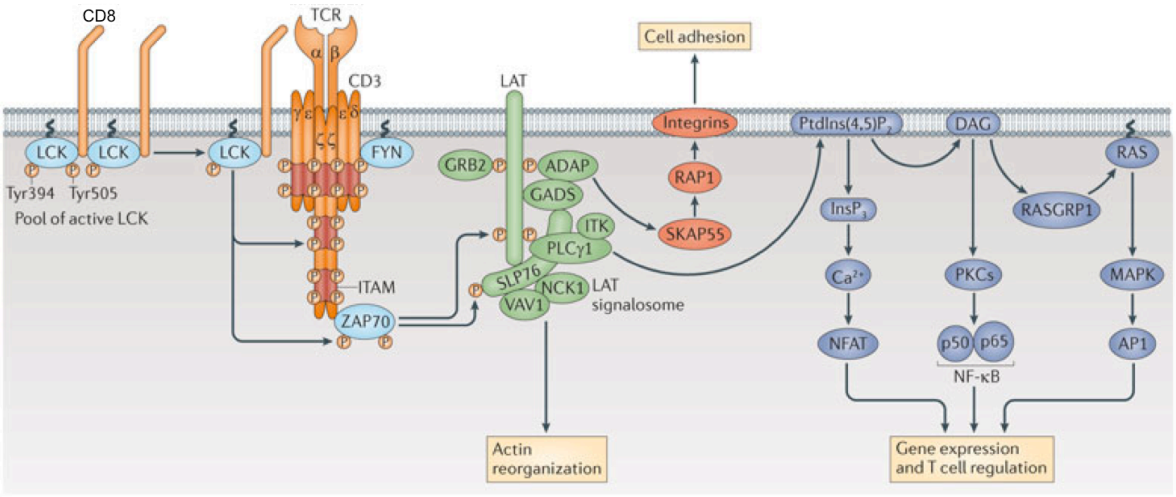

Fig. 2-7: TCR-induced signaling pathways

Upon TCR stimulation, the kinase Lck is recruited to the TCR and initiates the formation of the proximal signaling complex. This complex is the starting point for the induction of several signaling pathways. The second messengers DAG and IP3 are generated by activated PLC-γ1 and trigger the Ras-MAPK pathway, the NF-κB pathway and the NFAT pathway, all being essential for T cell activation and regulation. Modified from Brownlie RJ in Nature Immunology Review, 2013.

Besides these stimulatory signaling events, it is not less important to prevent overreaching or long-lasting T cell activation which could lead to T cell hyperproliferation, destruction of healthy tissue and increased susceptibility to autoimmune disease (36, 37).

One very important mediator in this shutdown process is the inhibitory molecule CTLA-4 whose expression is induced after T cell activation (38). CTLA-4 binds with increased affinity to CD80/86 compared to CD28, countering its signaling and results in prevention of IL-2 production and cell cycle arrest (39). Another very effective way in disabling TCR signaling events is to negatively regulate the proximal signaling complex.

The most prominently controlled protein in this regulation process is Lck. Lck bears both stimulatory (tyrosine Y394) and inhibitory tyrosine sites (tyrosine Y505), whose phosphorylation status determines the kinase activity of Lck (see **Fig. 2-8a**). To terminate the TCR signaling, the inhibitory Y505 is phosphorylated by the C-terminal Src kinase (Csk). Additionally, the phosphatase PTPN22 (Protein tyrosine phosphatase, non-receptor type

22) dephosphorylates the active site Y394. These two events render Lck in an inactive state accompanied with interrupted TCR signaling (see **Fig. 2-8b**). Davis et al. also ascribe a crucial role to CD45 during Y394 dephosphorylation in this shutdown process (40).

Interestingly, also for mediating the initial activation of the TCR signaling cascade, the phosphorylation status of Lck is regulated. In resting cells, CD45 predominantly dephosphorylates Y505, leading to basally active Lck. Upon TCR engagement, CD45 is excluded from the proximal signaling complex. Subsequently, Lck undergoes autophosphorylation at the catalytic tyrosine Y394 and becomes fully active. Just later, CD45 is recruited back to the TCR and can dephosphorylate the activating Y394 site in order to interrupt the TCR signaling cascade (see **Fig. 2-8b**). The dual function of CD45, being important both for the initiation as well as for the shutdown of the T cell signaling cascade, highlights CD45 as crucial regulator in T cell activation.

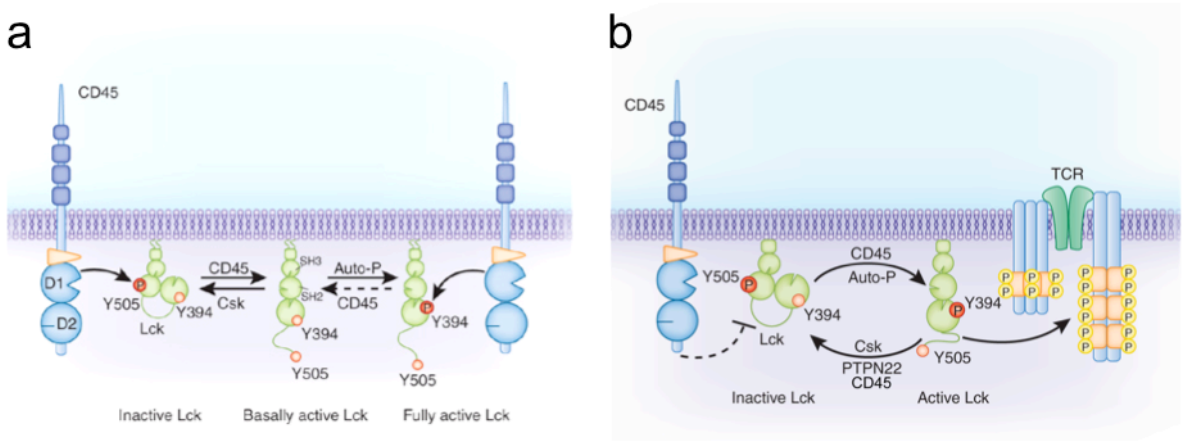

Fig. 2-8: CD45-mediated regulation of Lck

(a) CD45 preferentially dephosphorylates the inhibitory Y505 which results in a basally active or primed state of Lck. Autophosphorylation at the stimulatory Y394 results in fully active Lck. To a lesser extend, CD45 can dephoshorylate also the tyrosine Y394, rendering the active Lck into the basally active form. Finally, the kinase Csk can completely inactivate Lck by phosphorylation of the tyrosine Y505. **(b)** For induction of the TCR signaling cascade, the inactive Lck has to be activated by CD45-mediated dephosporylation of the tyrosine Y505 and autophosphorylation of the tyrosine Y394. To shutdown the TCR signaling cascade via Lck, the tyrosine Y505 is phosphorylated by Csk plus Y394 is dephosphorylated by the phosphatases PTPN22 and CD45. Besides the shown mono-phosphorylated forms of Lck, phosphorylation on both tyrosines is possible and leads to active Lck. Modified from Rhee I in Nature Immunology Review, 2012.

2.7 The phosphatase CD45

In 1989, Matthew L. Thomas first mentioned the prototypic receptor-like protein tyrosine phosphatase (PTP) CD45. CD45 bears an abundant expression on all nucleated hematopoietic cells of up to 10% of the cell surface area (41). The protein comprises an extracellular domain of variable length, a single transmembrane region and a constant cytoplasmic domain, which is 95% homologous in all mammals (42).

The variability in the extracellular domain is due to alternative splicing events of the exons four, five, six and seven resulting in five different isoforms being R0, RB, RAB, RBC and RABC. The expression and glycosylation pattern of the isoforms depend on the cell type, developmental stage and the activation status (see **Fig. 2-9**). These alternatively expressed parts are heavily O-glycosylated together with variable sialylation resulting in divergent molecular weights of about 180kDa (R0) and up to 230kDa (RABC) together with differences in shape and negative charge (42).

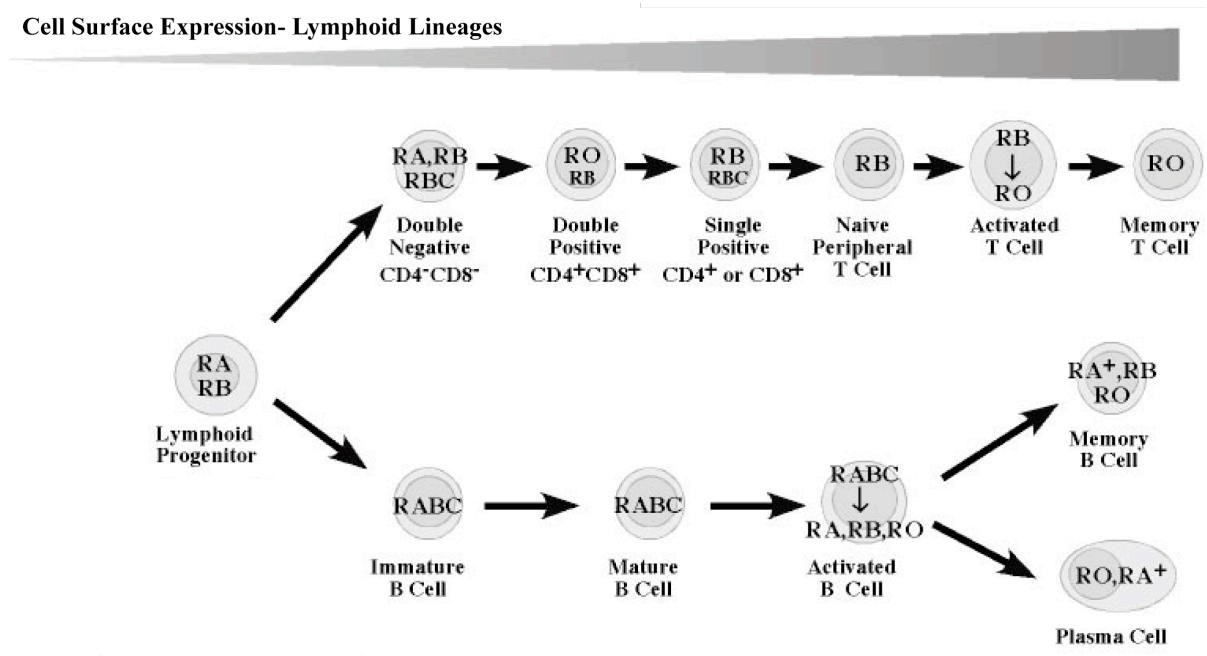

Fig. 2-9: CD45 isoform expression in lymphoid lineages

Depending on the cell type together with the status of differentiation and activation, divergent CD45 isoforms are expressed and isotype-switching occurs. Modified from Hermiston ML in Annual Reviews in Immunology, 2003.

Besides this inconstant part of the extracellular domain, the remaining extracellular part is heavily N-glycosylated and consists of three membrane-proximal type III fibronectin domains followed by a cystein-rich region (see **Fig. 2-10**).

The large intracellular part is composed of two tandemly duplicated PTPase homology domains, D1 and D2, separated by a spacer region. Whereas only D1 forms a substrate-binding wedge and bears phosphatase activity, the function of D2 is not yet fully understood. Even so, it seems to have regulatory capacities by binding Lck and thereby increasing its availableness for D1 (43).

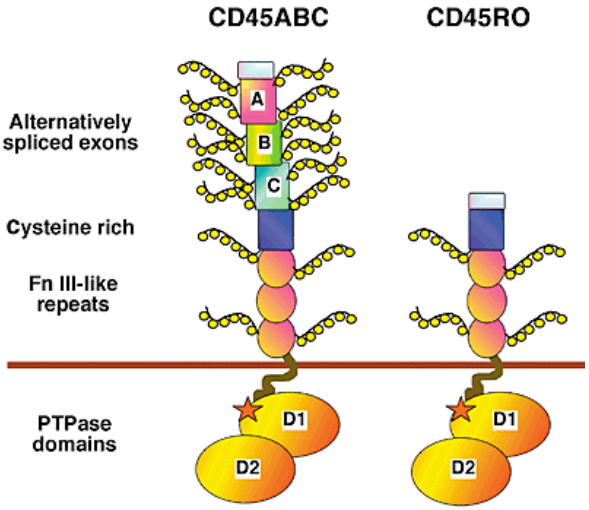

Fig. 2-10: Structure of CD45 isoforms

The extracellular domain of CD45 comprises three FN III-like repeats, a cystein-rich domain and, if expressed, a varying number of alternatively spliced exons, which are absent in CD45R0. Intracellularly one can find the tandemly repeated PTPase domains D1 and D2. Whereas only D1 posses phosphatase activity, the function of D2 is still unclear, although regulatory capacities are discussed. Adopted from Penninger JM In Nature Immunology, 2001.

Within three days after T cell stimulation, the expression of larger CD45 isoforms switches towards the isoform R0 (44, 45) depending on the activation of PKC and Ras (46). Defects in this isoform switch are linked with the development of multiple sclerosis (MS) (47) whereas CD45-deficient humans and mice develop severe-combined immunodeficiency (SCID) (48, 49). This is due to disordered positive and negative selection in the thymus resulting in far less thymocytes but bearing auto-reactive features (50, 51).

As already described in chapter 2.6, CD45 has a dual role in the regulation of TCR signaling events by dephosphorylation of either negative regulatory or catalytic tyrosine residues in

the kinase Lck. The regulation of the initiative T cell signaling molecule Lck is tightly and complexly regulated by interplay of the phosphatase CD45 and the kinases Csk and Lck itself.

In resting T cells, CD45 predominantly dephosphorylates the negative regulatory Y505 site resulting in a signaling-disposed unphosphorylated pool of Lck. Upon TCR stimulation, CD45 is segregated (52) from its substrate Lck which autophosphorylates its catalytic tyrosine motive Y394 and thereby becomes activated. To terminate TCR signaling, the kinase Csk phosphorylates the negative regulatory tyrosine residue Y505, with Lck still remaining active. Yet, the subsequent recruitment of CD45 (and PTPN22) leads to dephosphorylation of the tyrosine Y394 accompanied with intramolecular interactions of Lck and hence its inactivation (40). The favorable dephosphorylation of Y394 by CD45 after phosphorylation of Y505 by Csk might most likely be due to blocked accessibility of Y505 by Csk.

Shenoi et al. (53) and Roach et al. (54) could observe an increased Src kinase activity in CD45-deficient macrophages and T cells. This is warranted by an enhanced overall phosphorylation status of e.g. Lck. Additionally to the autocatalytic tyrosine motives, the negative regulatory tyrosines are also phosphorylated. Despite hyperphosphorylation of these negative regulatory tyrosines, the kinase activity is enhanced. Thereby, the bias towards kinase activity in the absence of CD45 activity is underlined.

The importance of CD45 in modulating the strength of TCR signaling requires strong regulation of CD45 activity. Dimerizing CD45 antibodies leads to inhibited phosphatase activity. Further investigations on related proteins reveal a blocking effect on the catalytic site of one molecule after interaction with a structural wedge in the membrane-proximal region of the second molecule (55). Comparative mechanisms for CD45 are likely due to structural similarities.

Dimerization of CD45 appears in a spontaneous and isoform-dependent manner. The tendency of the isoform R0 to form dimers exceeds the one of the larger isoforms. This is due to the fact that R0 lacks great amounts of O-glycosylation, whereas in larger isoforms the voluminous sugar side chains prevent dimerization and thereby CD45 shut-off (see

Fig. 2-11). Resting T cells preferentially express larger and therefore more active CD45 isoforms which lead to signaling-competent Lck. TCR signaling also induces enhanced splicing (46) and within three days after T cell stimulation, the expression of larger isoforms is augmented by R0 (44, 45) with increased tendencies for dimerization and reduced phosphatase activity.

The observation that dimerization-incompetent mice develop a lymphoproliferative syndrome and autoimmune nephritis co-occurring with early death (56), highlights the *in vivo* relevance for CD45 inactivation by dimerization.

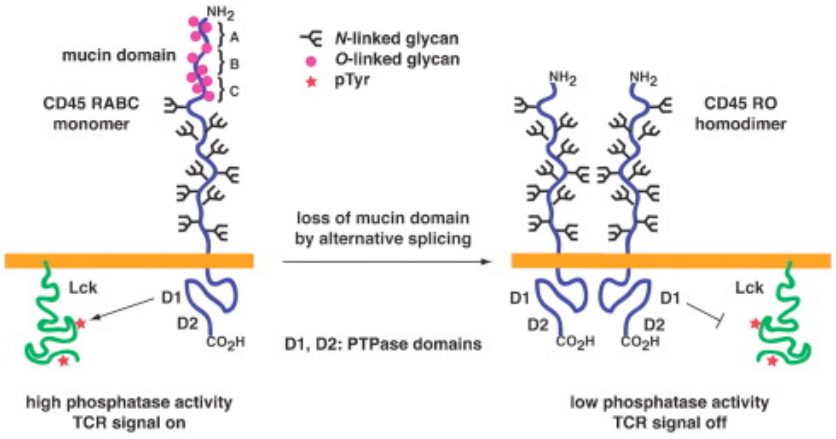

Fig. 2-11: Isoform-dependent dimerization of CD45

Larger CD45 isoforms bear voluminous sugar side chains, which prevent dimerization and lead to active phosphatase. The isoform R0 is less glycosylated and is prone to formation of dimers, which reduces CD45 activity. Adopted from Hang HC in Bioorganic and Medicinal Chemistry, 2005.

Besides spontaneous self-ligation, it was shown by van Vliet et al. (57) that the lectin MGL (macrophage galactose-type lectin) binds and inactivates CD45. This process is also possible for other lectins like the mannose receptor whose interaction with CD45 was reported by Martinez-Pomares et al. (58).

2.8 The Mannose Receptor

In the late 1970s, the MR was mentioned as being involved in clearance of endogenous proteins (59), which up to now was extended with further functions like promotion of antigen presentation and modulation of cellular activity and trafficking (60). It is expressed by some DCs and most murine tissue macrophages. Whereas the expression of the MR on steady-state splenic $CD8^+$ DCs in mice is controversially discussed (61-63), there is no question about its expression on inflammatory splenic DCs (61).

The MR is a carbohydrate-binding molecule of 180kDa belonging to the MR family of the C-type lectins. This family also comprises the molecules Endo180, the M-type PLA2R and DEC205.

The extracellular structure of the MR is a N-terminal cystein rich (CR) domain, a fibronectin type II (FNII) domain and eight C-type lectin-like carbohydrate recognition domains (CTLDs), also referred to as carbohydrate recognition domains (CRDs). In addition to this, there is a single membrane-spanning portion and a short intracellular tail (64) (see **Fig. 2-12**).

The most distal domain of the MR is the CR domain. Within the MR family, the mannose receptor is the only one bearing a functional CR domain (65). The CR domain binds calcium-independently to sulfated sugars, especially galactose or N-Acetylgalactosamine (GalNAc) sulfated in position 3 or 4 (65-68) (see **Fig. 2-12**).

C-terminally to the CR domain resides the collagen binding FNII domain. This is the most conserved domain among the MR family members (66). For the MR, there is strong affinity for the collagens I, II, III and IV and a weak binding of collagen V (69, 70) (see **Fig. 2-12**). Importantly, binding via the FNII domain is neither dependent on glycosylation nor on the lectin activity of the MR (71).

Being inherent in its name is the ability of the MR to bind mannosylated antigens. Besides these, also glycoconjugates terminated in fucose or GalNAc (67, 72, 73) are taken up by the MR in a calcium-dependent manner. Noteworthy, this uptake is mediated only by CTLD4 whereas the remaining CTLDs ensure the required conformational folding of the MR and thereby contribute to antigen binding (64, 72) (see

Fig. 2-12).

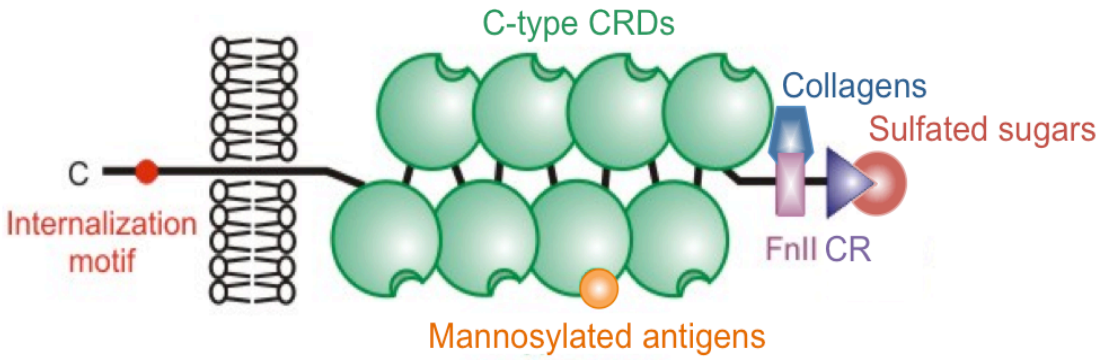

Fig. 2-12: Structure and antigen binding of the mannose receptor

The MR comprises a short C-terminal intracellular domain with an internalization motif, one transmembrane domain, eight C-type carbohydrate recognition domains (CRD) followed by a fibronectin type II (FnII) and a cystein-rich domain (CR). Mannosylated antigens can bind to the CRD, preferentially to CRD4. Collagens interact with the FNII domain and the CR domain recognizes sulfated sugars.
Modified from http://www.functionalglycomics.org/CFGparadigms/images/b/ba/Mannose_receptor.jpg

Though the very short intracellular domain of the MR lacks any signaling motives, it is responsible for receptor internalization and recycling (74). Only 10-30% of the total MR amount is expressed on the cell surface whereas 70-90% are located intracellularly in early endosomal compartments. Clathrin-coated vesicles mediate the continuous recycling of surficial MR to intracellular compartments. This process of endocytosis strongly depends on Actin polymerization (75) and is essential for MR recycling (76). Besides these cell-resident forms, also a shed variant of the MR exists. Herein, the whole extracellular region of the MR is proteolytically cleaved off by a metalloprotease and released into the surrounding (77). This soluble form of the MR is reported to be detectable in mouse serum (77). The shedding of the MR directly correlates with its expression (78) and due to the necessity of surface expression, Actin polymerization is needed for this process (75).

The function of the soluble MR is thought to be the delivery of pathogenic antigens under inflammatory conditions to cells that do not express the MR (60). Since mannosylated antigens are frequently found on pathogen surfaces (e.g. *Candida albicans* (77, 79), *Leishmania* (80), *Mycobacterium tuberculosis* (81), HIV (82), *Pneumocystis carnii* (83),

Dengue virus (84), *Klebsiella pneumoniae* (85), *Streptococcus pneumoniae* (85)) and the MR is designated as PRR (86), this potential function is feasible.

The immunogenic properties of the MR could further be confirmed by Burgdorf et al.. They reported that under inflammatory conditions, soluble antigens which have been taken up by the MR were transported into a specialized endocytic compartment, the stable early endosomes, and are exclusively loaded onto MHC I molecules for subsequent cross-presentation to $CD8^+$ T cells (87-89). Hence, many attempts at MR-targeting in vaccination strategies were ventured. Surprisingly, these trials resulted in tolerance instead of immunity (90-92). Yet, after the addition of endotoxins, a potent immune response could be induced (90, 93). These results raised the possibility that the MR might not solely have immunogenic functions.

Supportive to this is the fact that anti-inflammatory cytokines (e.g. IL-4, IL-10, IL-13) and the glycocorticoid dexamethasone increase MR expression (59, 78, 94, 95) whereas pro-inflammatory stimuli like IFN-γ and LPS have inhibitory functions (67, 96).
Furthermore it is known that several tolerance-inducing and immune-suppressive cells extensively express the MR. Examples are given for liver sinusoidal endothelia cells (97, 98), uterine mucosal macrophages (99), oral macrophages and macrophages in the lamina propria of the small intestine (100). In addition to this, the MR is found on M2-differentiated macrophages in reoccurring and vaccine-resistant tumors, whose resistance towards treatment could be pinpointed to these MR-bearing macrophages (101-103).
Finally, it is reported that expression of the MR is induced by the immunosuppressive transcription factor PPARγ *(*Peroxisome proliferator-activated receptor gamma) and is directly linked to the expression of the co-inhibitory molecule B7H1 (104).

All these hints lead to assumption that first of all, the MR is not only capable to impart immunity but also tolerance and second of all, the help of additional factors regulated by the MR might accomplish this tolerogenic effect.

2.9 Aims of the thesis

The question to be answered in my thesis was whether the mannose receptor (MR) has an additional role during T cell activation apart from leading to cross-presentation of antigens. This question arouse due to the divergent observations showing that on the one hand the MR is a potent mediator of cross-presentation under inflammatory conditions and on the other hand many tolerance-inducing cells bear a strong expression of the MR. Furthermore, there have been several attempts to target the MR in vaccination approaches which surprisingly led to anergy instead of immunity. Therefore, my task was to investigate a putative effect of the MR during $CD8^+$ T cell activation by DCs. Importantly, this was done in a system completely independent from antigen-uptake by the MR. Amendatory to a descriptive examination, the molecular mechanisms underlying the MR-mediated influence were investigated.

3 MATERIAL AND METHODS

3.1 Material

3.1.1 Equipment

DEVICE	COMPANY
0.75 Plan S Apo 20x objective	Olympus
ChemiDoc MP System	Bio Rad
Climate chamber	Evotec
FACS LSR II	BD Biosciences
HiScanSQ	Illumnia
Inverted Fluoview 1000 confocal miroscope	Olympus
Motorized xyz-stage	Märzhäuser
NanoDrop 2000 Spectrophotometer	Thermo Scientific
Thermo MultiskanEX Plate reader	Thermo Scientific

3.1.2 Software

SOFTWARE	COMPANY
Ascent Software	Thermo Scientific
Endnote 9	Thomson Reuters
FACS DIVA Software	BD Biosciences
FlowCytomixPro Software	Bender
FlowJo V8.8.4	Tree Star, Inc.
Fluoview 3.0	Olympus
GenomeStudio V2011.1	Illumnia
Illustrator CS4	Adobe
Image Lab™ Software	Bio Rad
ImageJ64	National Institute of Health
Mayday	Center for Bioinformatics Tuebingen (ZBIT), University of Tuebingen
Microsoft Office 2008	Microsoft

NanoDrop 2000 Software	Thermo Scientific
Partek® Genomics Suite V6.6 (PGS)	Partek Inc
Photoshop CS4	Adobe
Prism 4 for Macintosh	GraphPad Software, Inc.

3.1.3 Consumables

CONSUMABLE	COMPANY
∅ 10cm Petri dishes	Sarstedt
∅ 15cm tissue culture plates	Sarstedt
1000mL Bottle Top Vacuum Filter, 0.22µm pore	Corning®
24-well tissue culture plate	TPP
6-well tissue culture plate	TPP
96-well tissue culture plate	TPP
ELISA-Plate Microlon 96W, Flat-bottom, High binding	Greiner
FACS tubes, 5mL, ∅12mm, PP	Sarstedt
Falcon cell strainer, 40 µm	BD Biosciences
IBIDI chamber µ-Slide I	IBIDI®
Sterile syringe filter, 0,45µm, Cellulose acetate	VWR

3.1.4 Chemicals and reagents

All unlisted standard chemicals were purchased at the company Carl Roth.

COMPONENT	COMPANY
4-(2-hydroxyethyl)-1-piperazineethanesulfonic acid (HEPES)	PAA
4-Nitrophenolphosphate	Sigma-Aldrich
Adenovirus Luciferase OVA GFP (AdLOG)	Kindly provided by Dr. Andreas Limmer
Ammonium persulfate (APS)	Sigma-Aldrich
Ampicillin Sodiumsalt (Amp)	Sigma-Aldrich

Bovine serum albumin (BSA)	Roth
Bromphenolblue	Roth
Carboxyfluorescein succinimidyl ester (CFSE)	BD Biosciences
CD8a (Ly-2) MACS beads	Miltenyi Biotec
$CD8a^+$ T Cell Isolation Kit II	Miltenyi Biotec
Chloramphenicol	Sigma-Aldrich
Collagen (TypeI) R	Serva
ColorPlus™ Prestained Protein Ladder, Broad Range (10-230 kDa)	New England Biolabs
Complete EDTA-free Protease Inhibitor Cocktail Tablets	Roche
CpG ODN 1668	Invitrogen
CTLA-4-IgG Fusion Protein	BD Biosciences
Dephostatin	Santa Cruz Biotechnology, Inc.
Dithiothreitol (DTT)	Roth
DMEM, high glucose (4,5g/L), with L-Glutamine	PAA
EZ-Link Sulfo-NHS-Biotin	Thermo Scientific
FCS Clone	PAA
Ficoll-Paque™ Premium 1.084	GE Healthcare
FlowCytomix Th1/Th2 10plex Sample Kit	Bender MedSystems
Hoechst 33258 1mg/mL	Invitrogen
ICAM-1 Fc chimera	R&D Systems
IFN-γ recombinant protein as ELISA standard	eBioscience, Inc.
IL-2 recombinant protein as ELISA standard	eBioscience, Inc.
IMDM, with L-Glutamine	PAA
Kanamycinsulphate (Kana)	Roth
L-Glutamine, 200mM	PAA
Lipofectamine ™2000	Invitrogen
Low fat dry milk powder	Roth
Mouse serum	PAA
MouseWG-6 v2.0 Beadchips	Illumnia

N-(9,10-Dioxo-9,10-dihydro-phenanthren-2-yl)-2,2-dimethyl-propionamide (SF1670), CD45 Inhibitor	Calbiochem
NeutrAvidin™-Horseradish peroxidase	Thermo Scientific
NucleoBond® Xtra Midi Kit	Macherey-Nagel
OptiMEM	Invitrogen
OVA (257-264) SIINFEKL peptide	Tebu-Bio
Penicillin (10.000 Units/mL) / Streptomycin (10mg/mL), (Pen/Strep)	PAA
pFuse-hIgG1-Fc2 vector	Invitrogen
Phosphate buffered saline (PBS)	Sigma-Aldrich
Pierce Protein G Agarose	Thermo Scientific
pIgplus vectors including MR domains	Kindly provided by Dr. Luisa Martinez-Pomares
Protein G UltraLink Resin	Thermo Scientific
PVDF Blotting membrane	GE Healthcare
RNeasy Mini Kit	Qiagen
RPMI-1640, without L-Glutamine, with HEPES	PAA
Sodium Pyrovate, 100mM	PAA
Sulfo-NHS-LC-Biotin	Thermo Scientific
SuperSignal West Pico ECL Substrate	Thermo Scientific
TargetAmp™-Nano Labeling Kit for Illumina® Expression BeadChip®	Epicentre® Biotechnologies
TRIzol®	Invitrogen
Ultracomp™ *E.coli*	Invitrogen
Vivaspin 6 MWCO 30.000	GE Healthcare
X-ray films, CL-XPosure	Thermo Scientific
Zeocin™	Invitrogen

3.1.5 Buffers and solutions

Buffers were pH-adjusted with HCl respectively NaOH.

3.1.5.1 Common buffers

1x PBS

138mM NaCl, 2,7mM KCl, adjusted to pH 7,4, autoclaved. Storage at RT.

500mM EDTA

500mM EDTA in H_2O, adjusted to pH 7,6, sterile filtered. Stored at -20°C.

2mM EDTA

500mM EDTA diluted 1/250 in sterile PBS. Storage at 4°C.

FACS Buffer

0,1% [w/v] BSA, 0,1% [w/v] NaN_3 in 1x PBS. Storage at 4°C.

3.1.5.2 ELISA buffers

ELISA coating buffer

0,1M $NaHCO_3$ in H_2O adjusted to pH 8,2. Storage at 4°C.

ELISA washing buffer

0,05% Tween20 in PBS. Storage at RT.

ELISA coating buffer for chimeric MR constructs

154mM NaCl in H2O. Storage at RT.

ELISA washing and incubation buffer for chimeric MR constructs

10mM Tris-HCl, 10mM Ca^{2+} (as $CaCl_2$), 154mM NaCl, 0,05% Tween20. Storage at 4°C.

ABTS buffer

0,1M Citric acid, adjusted to pH 4,35. Storage at 4°C.

ABTS substrate solution

1mg/mL ABTS, 15µL H_2O_2 in 10mL ABTS buffer. Used freshly.

3.1.5.3 Protein lysis and Western blot buffers

Protein lysis buffer

10mM Tris-HCl (pH 8,2), 2% TritonX-100, 10mM NaN_3, 150mM NaCl, 2mM EDTA in H_2O. Storage at 4°C. Before usage 1x Proteinase Inhibitor was added.

Protein lysis buffer for CD45 detection by chimeric MR

10mM Triethanolamine (pH 8,2), 150mM NaCl, 1mM $MgCl_2$, 1mM $CaCl_2$, 1% (v/v) TritonX-100 in H_2O. Storage at 4°C. Before usage 1x Proteinase Inhibitor was added.

4x Laemmli buffer

240mM Tris (pH 6,8), 8% (w/v) SDS, 40% (v/v) Glycerol, 0,01% (w/v) Bromphenolblue in H_2O. Storage at -20°C.

10x SDS running buffer

250mM Tris, 1,92M Glycin, 1% SDS in H_2O. Storage at RT.

1x SDS running buffer

10x SDS running buffer diluted 1/10 in H_2O. Storage at RT.

10x Towbin transfer buffer

250mM Tris, 1,92M Glycin in H_2O, adjusted to pH 8,53. Storage at RT.

1x Towbin transfer buffer

10% (v/v) 10x Towbin transfer buffer, 20% (v/v) Methanol, 70% (v/v) H_2O. Used freshly.

Western blot blocking buffer

5% Milk in TBST. Storage at 4°C.

Western blot blocking buffer for WB with chimeric MR

5% Milk in PBST. Storage at 4°C.

10x TBS (Tris buffered saline) buffer

500mM Tris, 1,5M NaCl in H_2O, adjusted to pH 7,5. Storage at RT.

1x TBST buffer

10x TBS diluted 1/10 in H_2O. 0,1% Tween20 were added. Storage at RT.

1x PBST buffer

10x PBS diluted 1/10 in H_2O. 0,05% Tween20 were added. Storage at RT.

3.1.5.4 Buffers for Protein G agarose columns

Binding buffer Protein G columns

50mM Sodium acetate in H_2O, adjusted to pH 5,0. Storage at RT.

Elution buffer Protein G columns

0,1M Glycin in H_2O, adjusted to pH 2-3. Storage at RT.

Neutralization buffer Protein G columns

1M Tris in H_2O, adjusted to pH 8-9. Storage at RT.

3.1.5.5 Phosphatase assay buffers

Phosphatase assay lysis buffer

20mM HEPES, 2mM EDTA, 2mM Dithiothreitol, 1% (v/v) Glycerol in H_2O. Storage at 4°C.

Phosphatase assay buffer

100mM HEPES, 2mM EDTA in PBS. Storage at 4°C.

Complexation buffer for chimeric MR constructs

0,3% [w/v] BSA in 1x PBS. Storage at 4°C.

3.1.5.6 Cell culture buffers

Red cell lysis buffer (RCB)

155mM NH_4Cl, 12mM $NaHCO_3$, 0,1mM EDTA in H_2O, sterile filtered. Storage at -20°C.

MACS buffer

0,1% [w/v] BSA, 2mM EDTA in 1x sterile PBS. Storage at 4°C.

3.1.5.7 Solutions

Fetal calf serum (FCS)

500mL FCS were heat-inactivated at 56°C for 30 minutes and aliquots of 50mL were stored at -20°C.

25x Protease Inhibitor

One Proteinase Inhibitor Cocktail tablet in 2mL H_2O. Storage at 4°C.

3.1.6 Media

BMDC culture medium

IMDM, 10% FCS Clone, 100 Units/mL Penicillin, 0,1mg/mL Streptomycin, 50mM β-Mercaptoethanol, 2,5% R1 supernatant.

T cell medium

RPMI 1640, 10% FCS Clone, 100 Units/mL Penicillin, 0,1mg/mL Streptomycin, 50mM β-Mercaptoethanol, 2mM L-Glutamine.

HEK293T cell medium

DMEM, 10% FCS Clone, 1mM Sodium Pyrovate.

R1 cell medium

IMDM, 10% FCS Clone, 100 Units/mL Penicillin, 0,1mg/mL Streptomycin, 50mM β-Mercaptoethanol.

3.1.7 Antibodies

If not indicated otherwise, all antibodies were purchased from eBioscience. Antibodies against Actin were purchased form Sigma Aldrich, CD45 was purified form YBM42.2.2 hybridoma-supernatant, αMR was received from AbD Serotec, H2-Kb SIINFEKL dextramers were from Immudex and αpLcK was obtained from New England Biolabs.

ANTIGEN	CLONE	CONJUGATE	APPLICATION
Actin	AA20-33	Unconjugated	Western Blot
B7H1	MIH5	PE	Flow cytometry
CD11c	N418	PerCP/Cy5.5	Flow cytometry
CD28	37.51	Unconjugated	*In vitro* assays
CD3	145-2C11	Unconjugated	Restimulation
CD40	3/23	PE	Flow cytometry
CD45	YBM42.2.2	Unconjugated	Western blot
CD8	53-6.7	Pacific Blue	Flow cytometry
CD80	16-10A1	FITC	Flow cytometry
CD86	PO3	PE	Flow cytometry
CTLA-4	UC10-4B9	APC	Flow cytometry
H2-K^b SIINFEKL Dextramer		APC	Flow cytometry
IFN-γ	AN-18	Unconjugated	ELISA
IFN-γ	R4-6A2	Biotinylated	ELISA
IL-2	JES6-1A12	Unconjugated	ELISA
IL-2	JES6-5H4	Biotinylated	ELISA
MHC-II	M5/114.15.2	PerCP/Cy5.5	Flow cytometry
MR	MR5D3	APC	Flow cytometry
pLck	2751	Unconjugated	Western blot

3.1.8 Mouse strains

STRAIN	DESCRIPTION	BACKGROUND	HAPLOTYPE
C57/BL6J	Wildtype strain	C57/BL6J	H-$2K^b$
DesTCR	Transgenic expression of a K^b-specific T cell receptor (KB5.C20 TCR) in $CD8^+$ thymocytes (105).	B10.BR	H-$2K^k$
$MR^{-/-}$	Stop-codon inserted at the Mannose receptor start codon of Exon 1, preventing its expression (106).	C57/BL6J	H-$2K^b$

3.1.9 Cell lines

CELL LINE	DESCRIPTION
HEK293T	Human embryonic kidney cells
HEK293T-MR	Human embryonic kidney cells, transduced with murine MR (107)
R1 cells	NIH3T3 cells stably transfected with GM-CSF gene
RMA	Murine T cell tumor
RMA-S	Mutagenized RMA, reduced surface MHC-I (108)
YBM42.2.2	Rat Hybridoma, production of CD45 antibody, (109), kindly provided by Prof. Stephen Cobbold and Prof. Hermann Waldmann

3.2 Methods

3.2.1 Generation and handling of BMDCs

3.2.1.1 Cell culture conditions

Standard cell culture conditions were at 37°C at levels of 5% CO_2 and a relative humidity of 90%. Cell lines and BMDCs were spun at 290xg for five minutes, whereas splenocytes were centrifuged at 300xg for ten minutes.

3.2.1.2 Generation of GM-CSF-containing R1 cell supernatant

GM-CSF-containing supernatant was produced by R1 cells. $1*10^6$ R1 cells were plated in 30mL R1 cell medium in ∅ 15cm tissue culture plates and incubated for four days. Afterwards, cell supernatant was collected, sterile filtered and stored in 50mL aliquots at -20°C.

3.2.1.3 Differentiation of bone-marrow derived dendritic cells (BMDC)

Hind limbs were isolated from one mouse and bone marrow was flushed out with 1x PBS. Cell clusters were dissociated by pipetting, cell suspension was filtered through a 40µm cell strainer and centrifuged. Afterwards, cells were resuspended in 30mL BMDC culture medium, distributed to three Petri dishes (∅ 10cm) and cultured under standard conditions. Three days later, cell supernatant was collected, cells were harvested (3.2.1.4),

resuspended in 60mL BMDC culture medium and distributed to six Petri dishes (∅ 10cm). By default, at day seven of culture, experiments were performed.

3.2.1.4 Harvesting of BMDCs

Cell supernatant was collected, 2mM EDTA was added and incubated for five minutes at RT. Adherent cells were detached by pipetting, added to the collected supernatant and spun. Cell pellet was resuspended assay-dependent in appropriate medium and volume.

3.2.1.5 CpG activation of BMDCs

On day six of BMDC differentiation, cell supernatant was collected, spun, cell pellet was resuspended in BMDC culture medium supplemented with 5µg/mL CpG and returned to original plate. BMDC activation took place for 18 hours.

3.2.2 *In vitro* proliferation assay

3.2.2.1 Isolation of splenocytes

Spleens were isolated, smashed into 1x cold PBS with a syringe plunger through a metal cell strainer, cell aggregates were dissolved by pipetting and cells were centrifuged. Supernatant was discarded, cell pellet resuspended by flicking the tube and 2mL RCB was applied for five minutes at RT. Afterwards, erythrocyte lysis was stopped by addition of 8mL cold T cell medium, cell suspension was filtered through a 40µm cell strainer and centrifuged.

3.2.2.2 CFSE-staining of cells

Cells were washed once with 1x PBS and spun at their respective G forces and durations, resuspended in 1x PBS and CFSE was added. For T cell proliferation assays, 1µM CFSE were used. For cytotoxicity assays, target cells received 1µM and non-target cells were stained with 0,1µM CFSE. For live cell imaging, T cells were stained with 0,1µM CFSE. Incubation was performed for 15 minutes at 37°C, staining was stopped by addition of 30mL T cell medium and cells were spun down. Washing took place twice with 10mL T cell medium.

3.2.2.3 *In vitro* proliferation assay of $CD8^+$ T cells

$5*10^4$ wildtype or $MR^{-/-}$ BMDCs were plated in a 96-well tissue culture plate and let adhere for one hour. In the meantime, splenocytes form DesTCR mice were isolated and labeled with CFSE (see 3.2.2.1 and 3.2.2.2). T cells were resuspended in 10mL T cell medium, counted in a Neubauer chamber and adjusted to $5*10^5$ cells/mL. Finally, supernatant from plated BMDCs was removed, $1*10^5$ total T cells in 200µL T cell medium added per well and incubated for three days. After 24 hours, 50µL supernatant was removed for IL-2 ELISA. On day three, T cells were resuspended and CD8 FACS staining was performed as described in 3.2.2.4.

3.2.2.4 Flow cytometry

Harvested cells were transferred into FACS tubes, washed once with 4mL FACS buffer and spun. Supernatant was decanted and staining solution was added. If not indicated otherwise, all stainings were performed in FACS buffer supplemented with 1/100 diluted mouse serum and 1µg/mL antibodies. Staining was performed at 4°C under dark conditions, followed by washing and final resuspension in FACS buffer. Staining of SIINFEKL-dextramers was performed in 1/50 dilution in 1x PBS for 15 minutes at room temperature, followed by default FACS staining procedures for further surface markers.

3.2.3 *In vitro* cytotoxicity assay and re-stimulation

3.2.3.1 *In vitro* cytotoxicity assay

$4*10^5$ CpG-activated (3.2.1.5) or untreated wildtype or $MR^{-/-}$ BMDCs were plated in a 24-well tissue culture plate and let adhere for one hour. In the meantime, splenocytes form DesTCR mice were isolated (see 3.2.2.1). T cells were resuspended in 10mL T cell medium, counted in a Neubauer chamber and adjusted to $1*10^6$ cells/mL. Finally, supernatant from plated BMDCs was removed, $5*10^5$ total T cells in 500µL T cell medium added per well and incubated for four days. 24 hours later another 2mL T cell medium were added. After four days T cells were purified by density gradient centrifugation (see 3.2.3.2). Target cells (RMA) and non-target cells (RMA-S) were stained with CFSE as described in 3.2.2.2, counted, adjusted to $4*10^4$ cells/mL and mixed equally. 100µL cell mixture ($2*10^3$ total cells each) was co-cultured for four hours with different ratios of T cells, added in 100µL.

Afterwards, cells were resuspended, transferred into FACS tubes and stained immediately before analysis with 10µg/mL Hoechst 33258. Cells were analyzed by Flow cytometry and specific cytotoxicity was calculated with the following formula:

$$\%Cytotoxicity = 100 - \left(100 * \left(\frac{RMA(target)}{RMA - S(target)}\right) \Big/ \left(\frac{(RMA(control)}{RMA - S(control)}\right)\right)$$

For cytotoxicity assays in the presence of chimeric MR protein, during BMDC and T cell co-culture, 10µg/mL indicated chimeric protein was added, non-supplemented 2mL medium was appended 24 hours later. CD45 inhibitor N-(9,10-Dioxo-9,10-dihydro-phenanthren-2-yl)-2,2-dimethyl-propionamide (SF1670) was added during the four days lasting T cell priming phase with a constant concentration of 40mM. Soluble CTLA-4 fusion protein and inhibitory αCTLA-4 antibody were applied with a concentration of 1µg/mL.

3.2.3.2 T cell purification by density gradient centrifugation

Activated T cells that were co-cultured with BMDCs were resuspended and spun down. Afterwards, T cells were resuspended in 5mL T cell medium, underlaid with 2mL Ficoll and centrifuged at 805xg, acceleration 7 and break 0 for ten minutes. The T cell-containing interphase was collected, washed with 1x PBS and resuspended in 1mL T cell medium.

3.2.3.3 Re-stimulation of primed DesTCR T cells

A 96-well tissue culture plate was coated with 10µg/mL αCD3 antibody diluted in 100µL 1x PBS for one hour at 37°C. Wells were washed twice with excess of PBS, purified (see 3.2.3.2) activated T cells were adjusted to $5*10^5$ cells/mL and 200µL were applied to the coated plate. After 18 hours, the plate was spun at 300xg for five minutes, 150µL supernatant was fetched and the IFN-γ concentration determined by ELISA (see 3.2.4).

3.2.4 Enzyme-linked immuno sorbent assay (ELISA)

ELISA plates were coated with 0,5µg/mL purified capture antibody in 50µL coating buffer for one hour at 37°C, followed by three washing steps with 150µL washing buffer. Blocking took place with 100µL blocking buffer for 30 minutes at RT, followed by three washing steps. IL-2 standard protein was 1/4 serially diluted in the corresponding cell medium, standard protein and samples were applied to ELISA plates and incubated o.n. at 4°C.

Afterwards, three washing steps took place and 50µL biotinylated detection antibody (0,5µg/mL) in blocking solution were added for one hour at 37°C. After three-fold washing, 1µg/mL horseradish peroxidase-coupled Neutravidin was diluted in 1x PBS, applied and incubated for 30 minutes at RT. Finally, three washing steps were performed and 50µL ABTS substrate solution added. Colorimetric changes were analyzed with an ELISA reader at 450nm.

3.2.5 Cell surface molecules and cytokine secretion of BMDCs

3.2.5.1 Staining of cell surface molecules

$4*10^5$ BMDCs were plated in a 24-well tissue culture plate and let adhere for about one hour. Isolated DesTCR splenocytes (see 3.2.2.1) were counted and adjusted to $1*10^6$ cells/mL. Supernatant was removed from BMDCs, $5*10^5$ DesTCR T cells were added and incubated for 18 hours. Afterwards, cell supernatants were collected and secreted cytokines and chemokines were determined by Fluorescent bead immuno assay (see 3.2.5.2). Adherent BMDCs were scraped off with a rubber scraper and stained for CD11c plus either other marker like CD86, CD80, CD40, MHC II or B7H1 as described in 3.2.2.4. CD11c was used as marker for BMDCs.

3.2.5.2 Fluorescent bead immuno assay

A Fluorescent bead immuno 10plex assay allows quantification of ten different cytokines and chemokines simultaneously in a FACS-based method. Cell supernatant was treated as described in the manufacturers manual. Briefly, a mixture of beads, which were coupled with ten different capture antibodies against cytokines, was added to the collected cell BMDCs supernatant. Afterwards, biotinylated detection antibodies were added, followed by Streptavidin-PE. The read-out was performed by flow cytometry. Beads can be distinguished from each other, firstly, by two different sizes and, secondly, by different fluorescent intensities for the channel Far Red. The amount of detected antigen is analyzed by measurement of the intensity in the PE channel. Internal standard curves for all examined cytokines and chemokines allow quantification with the FlowCytomixPro Software.

3.2.6 MACS sorting of $CD8^+$ T cells

T cell isolation was performed as described in the manufacturers manual. Briefly, splenocytes were incubated with αCD8a (Ly-2)-coupled magnetic beads and loaded onto separation columns within a magnetic field. Contaminating, unlabeled cells were washed away and magnetically labeled cells of interest were eluted from column beyond the magnetic field, washed and resuspended in an appropriate volume of T cell medium.

For gene array samples, the T cell isolation kit was used in which all other cell types in the spleen were isolated and untouched T cells were collected in the flow-through.

3.2.7 Live cell imaging

3.2.7.1 ICAM-coating of IBIDI chambers

Plastic channel µ-slides were coated with 5µg/mL ICAM-1 chimeric protein which is coupled to the F_C part of human IgG_1. To block lumen-directed F_C parts, 12µg/mL goat αhuman IgG antibody (Dianova) were added.

3.2.7.2 Live-cell imaging

DesTCR splenocytes were isolated as described above (see 3.2.2.1), $CD8^+$ T cells MACS sorted (see 3.2.6) and stained with CFSE (see 3.2.2.2). $1{,}6*10^5$ T cells were mixed with $4*10^5$ wildtype or $MR^{-/-}$ BMDCs in a total volume of 110µL T cell medium. 100µL cell mixture was loaded in ITAM-coated (see 3.2.7.1) plastic channel µ-slides. In cooperation with Thomas Quast, time-lapse microscopy was performed in a climate chamber (Evotec; 37°C and 5% CO_2 with humidity) with an inverted Olympus Fluoview 1000 confocal microscope, equipped with an automated motorized xyz-stage (Märzhäuser). Every two minutes, the green fluorescence and differential interference was recorded with a 0.75 Plan S Apo 20x objective over a period of 12 hours. Subsequently, the duration of interaction between BMDCs and T cells was analyzed with the Fluoview Software.

3.2.8 Generation of chimeric MR proteins

3.2.8.1 Vectors encoding for chimeric MR constructs

The vector pFuse-hIgG1-Fc2 bears a Zeocin™ resistance and encodes the isotype control protein. The chimeric MR proteins MR-FN (consisting of CR-domain, FN-domain and CTLD 1-3) and MR-CTLD (consisting of CTLD 4-7) were encoded on plasmids of the pIgplus backbone.

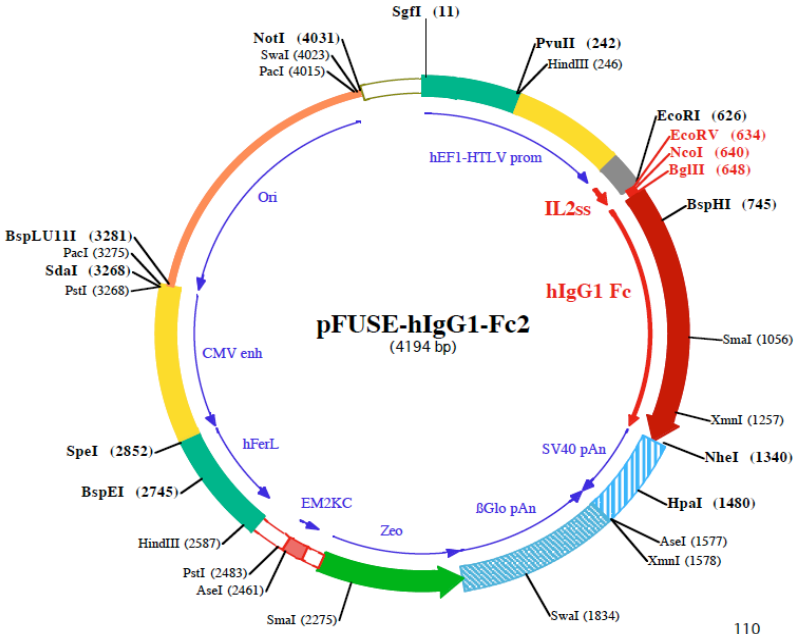

http://www.invivogen.com/PDF/pFUSE_hIgG1_Fc2_TDS.pdf

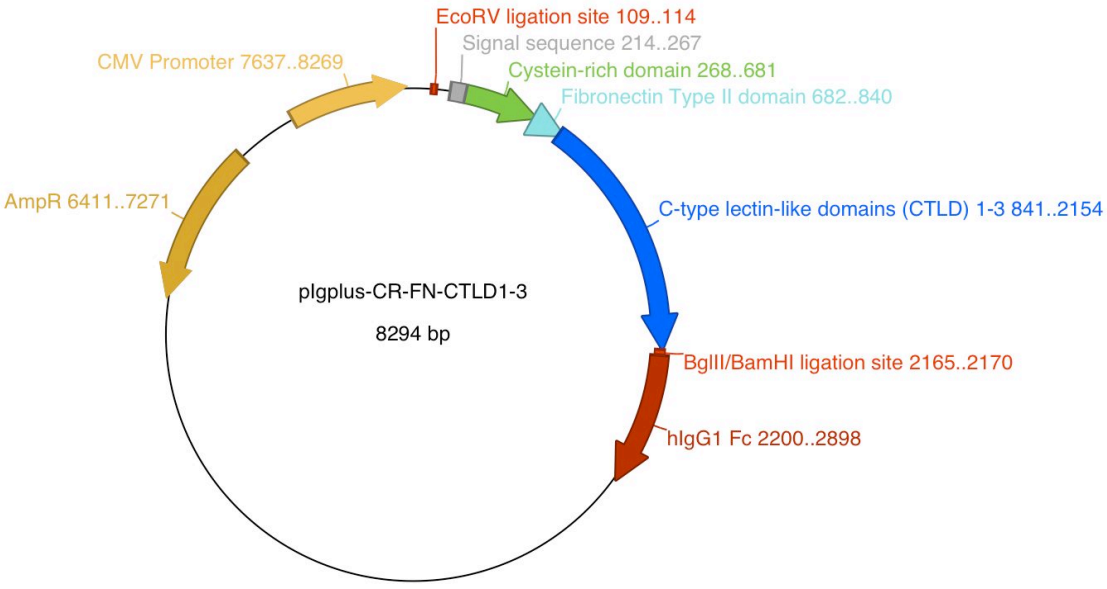

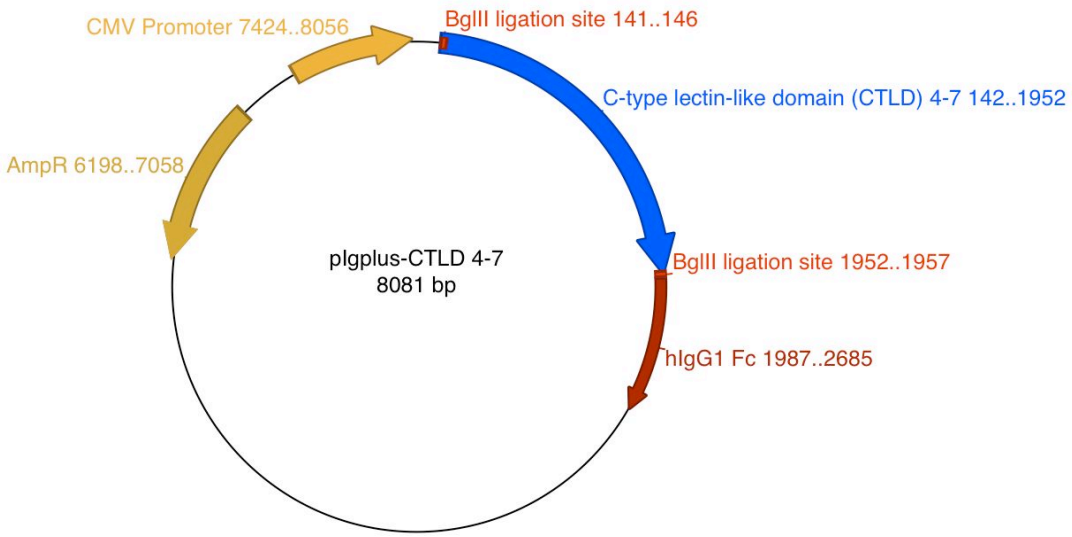

Fig. 3-1: Maps of vectors encoding for the control protein or two different chimeric MR constructs

The control protein is encoded on the vector pFuse-hIgG1-Fc2 containing the gene for the human F_c2 part of IgG1. The vector pIgplus contains besides the human F_c part of IgG1 also the FN, CR and CTLD1-3 domains (pIgplus-CR-FN-CTLD1-3) or the domains CTLD1-4 (pIgplus-CTLD1-4) of the murine MR.

3.2.8.2 Transformation of Ultracomp™ *E.coli* with vector DNA

Transformation was performed by standard methods (110). Cells were plated afterwards on antibiotics-supplemented LB agar. 25µg/mL Zeocin™ were used for transformation of the pFuse-hIgG1-Fc2 vector and a combination of 40µg/mL Ampicillin and 50µg/mL Kanamycin were used for pIgplus vectors.

3.2.8.3 Midi cultures of E.coli

Over night cultures were performed under standard conditions. *E.coli* cells that had been transformed with the low-copy vector pIgplus received 200µg/mL Chloramphenicol for four hours to inhibit cell division and increase DNA yield. Plasmid DNA was isolated as describes in 3.2.8.4.

3.2.8.4 Plasmid DNA isolation

Plasmid DNA was isolated referring to the manufacturers manual of the NucloeBond® Xtra Midi Kit. The concentration and purity (A_{260}/A_{280}) of isolated DNA was determined with a Nanodrop spectral photometer.

3.2.8.5 Transfection of HEK293T cells

For production of chimeric MR constructs, cells were transfected with vectors encoding either only the human IgG_1 F_C (Isotype control) or the F_C part which was coupled to the Cystein-rich (CR) domain, the Fibronectin-like (FN) domain and the C-type lectin-like domains 1-3 (CTLD) (MR-FN) or with vectors whose F_C part was coupled to the CTLDs 4-7 of the murine MR (MR-CTLD) (69) (see vector cards 3.2.8.1; **Fig. 3-1**). 24 hours before transfection, $4*10^6$ HEK293T cells were plated in 10mL HEK cell medium in $75cm^2$ flasks. On the day of transfection, medium was replaced by 10mL fresh HEK293T cell medium. For Lipofectamine™ 2000 transfection, 10µg DNA were mixed with 2mL Opti-MEM® as well as 25µL Lipofectamine™ 2000 were mixed with 2mL Opti-MEM®. Afterwards, mixtures were combined and incubated at RT for five minutes and added to the plated HEK293T cells. After 24 hours of culture, the medium containing the transfection solution was carefully replaced by 20mL Opti-MEM and protein production and secretion took place for four days under standard cell culture conditions.

3.2.8.6 Isolation of chimeric MR proteins by Protein G column

For protein purification with Protein G columns, the manufacturers manual was followed and a constant fluidic flow of 1ml/minute was ensured by using a peristaltic pump. Briefly, cell supernatants from transfected HEK293T cells (see 3.2.8.5) were mixed with binding buffer, loaded on the Protein G column, washed and captured proteins were eluted in eight fractions of 900µL in 100µL neutralization buffer. To concentrate and wash the protein, plus performing a buffer-exchange to 1x PBS, eluted fractions were pooled and applied to 30kDa Vivaspin ultrafiltration columns. Centrifugation took place at 4000xg for 20 minutes, two times 6mL 1x PBS were added and centrifuged as before. The last centrifugation resulted in about 1mL final volume of concentrated protein dissolved in 1x PBS. The protein concentration was determined by spectral photometry at 280nm.

3.2.8.7 Complexation of chimeric MR protein

The indicated amount of chimeric MR protein or isotype control protein was incubated with 1µg/mL horseradish peroxidase-coupled αhuman antibody in 0,3%BSA/PBS in the presence of 1x proteinase inhibitor for one hour at RT.

3.2.9 Co-Immunoprecipitation and analysis of pLck

3.2.9.1 Surface biotinylation of T cells

Isolated splenocytes (see 3.2.2.1) were washed with 1x PBS, adjusted to $25*10^6$ cells/ml in PBS, 2mM biotin reagent was added and incubated for 30 minutes at RT. Afterwards, cells were washed twice with T cell medium and finally with 1x PBS.

3.2.9.2 Generation of protein lysates

$1*10^7$ PBS-washed cells were incubated with 1mL appropriate cold cell lysis buffer and incubated on ice for 30 minutes. Cell debris was removed by centrifugation at 14000xg for ten minutes. Supernatant was collected and further assays performed.

3.2.9.3 Co-Immunoprecipitation

Surface biotinylated DesTCR splenocytes (3.2.9.1) were lysed (3.2.9.2) and incubated for one hour on ice with 10µg/mL complexed (3.2.8.7) chimeric MR or isotype control protein. Protein G agarose beads were washed twice with 1x PBS, 20µL bead solution was added to lysates, incubated under inverting conditions at 4°C for one hour. Afterwards, beads were spun down at 5900xg for 30 seconds, washed once with lysis buffer, and bound proteins were eluted by addition of 50µL Laemmli buffer and incubation at 50°C for five minutes. Beads were spun for one minute at 16.100xg, supernatant collected and Western blot performed.

3.2.9.4 Analysis of pLck

$4*10^5$ wildtype or $MR^{-/-}$ BMDCs were plated in a 24-well tissue culture plate. One hour later, supernatant was removed, $1{,}35*10^6$ $CD8^+$ MACSed (3.2.6) DesTCR T cells were added in 200µL T cell medium and incubated for the indicated time points. Afterwards, T cells were resuspended, lysed (3.2.9.2) and Western blot performed as described in 3.2.10. In case of addition of chimeric MR protein, $MR^{-/-}$ BMDCs were plated and T cells were added in the presence of 10µg/mL complexed (3.2.8.7) chimeric proteins.

3.2.10 Western blotting

20µL sample and 5µL protein ladder were loaded onto an 8% SDS gel and electrophoresis was conducted at 30mA const., 120V and 100W for 60 minutes in 1x SDS running buffer. Semi-dry transfer to methanol-equilibrated PVDF-membrane was done at 200mA const., 25V and 300W for 75 minutes with blotting paper soaked in 1x Towbin transfer buffer.

Membranes were blocked o.n. at 4°C under rocking conditions in the appropriate blocking solution and primary antibodies were added in TBST for one hour at RT. Washing took place three times for 10 minutes with TBST, followed by incubation of the horseradish-coupled secondary antibodies diluted in TBST. Finally, another three washing steps were carried out, ECL substrate was added and chemiluminescence was analyzed either by X-array films or ChemiDoc™ Systems. For Western blotting, 0,2µg/mL horseradish peroxidase-coupled Neutravidin, 1µg/mL αCD45, 1/1000 αActin, 1/1000 αpLck and 1/5000 diluted secondary antibodies were used. For stainings with chimeric MR proteins, 100µL 10µg/mL complexed protein (3.2.8.7) were added to 900µL blocking solution and applied to the membrane. PBST was used instead of TBST.

3.2.11 CD45 Phosphatase assay

$1{,}5*10^6$ HEK or HEK-MR respectively wildtype or $MR^{-/-}$ BMDCs were plated in a 6-well tissue culture plate. 24 respectively four hours later, supernatant was removed, $CD8^+$ MACSed (see 3.2.6) DesTCR T cells were added in 1,5mL T cell medium and incubated for one hour. Afterwards, cells were lysed as described above (3.2.9.2) in 600µL phosphatase lysis buffer, separated into triplicates, 50ng/mL αCD45 antibody was added and incubated for one hour at 4°C. 20µL Protein G agarose beads were washed twice with 1x PBS and coupled with 50ng/mL αrat antibody in 200µL 1x PBS for one hour at 4°C. Subsequently, beads were spun at 5900xg for 30 seconds and cell lysates were added for another hour under inverting conditions at 4°C. Samples were washed twice with 100mM HEPES, split into two and 70µL phosphatase assay buffer with 2mM 4-Nitrophenylphosphate (4-NPP) was added in the presence or absence of 1µM CD45 inhibitor SF1670. The substrate was incubated over night at 37°C in the dark, beads were spun down, 35µL supernatant were transferred into ELISA plates and absorption at 405nm was determined.

3.2.12 Gene array of activated DesTCR T cells

3.2.12.1 RNA isolation and microarray analysis

$4*10^5$ wildtype or $MR^{-/-}$ BMDCs were plated in a 24-well tissue culture plate. $CD8^+$ DesTCR T cells from three different mice (natural replicates) were MACS isolated using the T cell isolation kit (see 3.2.6). $5*10^5$ DesTCR T cells and BMDCs were co-cultured for four, 18 or 48 hours in the presence of 10µg/mL either Fc-MR or isotype control protein. Afterwards, T cells were resuspended and FACS stained with αCD8 as described in 3.2.2.4. $CD8^+$ T cells were FACS sorted in TRIzol® and kept at -80°C until RNA was isolated following the manufacturers instructions in the Qiagen RNeasy kit. By reverse transcription, cDNA was generated and biotinylated using the TargetAmp™-Nano Labeling Kit for Illumina® Expression BeadChip®. 1,5µg biotinylated cDNA was hybridized to MouseWG-6 v2.0 Beadchips (Illumina) and scanned on an Illumina HiScanSQ system. The department of Genomics and Immunoregulation, LIMES institute performed RNA isolation and microarray analysis.

3.2.12.2 Bioinformatical analysis

With the program GenomeStudio V2011.1 (Illumina), raw intensity microarray data were processed followed by bioinformatical analysis with Partek® Genomics Suite V6.6 (PGS). Data were normalized and application of a two-way ANOVA model, variable transcripts and significantly differentially expressed transcripts were determined. The definition of variable and significantly differentially transcripts was set as a false discovery rate (FDR) with a corrected p-value <0,05 and a fold change ±2. By PGS hierarchical clustering among the variable genes, similarities or differences in gene expression depending on the different conditions were highlighted. Literature research revealed 49 tolerance- and anergy-associated genes, whose differential expression was visualized in heat-maps of the z-transformed log2 expression profiles (Mayday open source software). The microarray data have been deposited on GEO under accession number GSE45805 (http://www.ncbi.nlm.nih.gov/geo/query/acc.cgi?acc=GSE45805).

Dr. Astrid M. Draffehn performed the bioinformatical analysis (Department of Genomics and Immunoregulation, LIMES institute).

3.2.13 CTLA-4 expression

$5*10^4$ CpG-activated (3.2.1.5) or untreated wildtype or $MR^{-/-}$ BMDCs were incubated with isolated DesTCR splenocytes (3.2.2.1) in 200µL T cell medium for three days in the presence or absence of 40mM CD45 specific inhibitor SF1670 or 1µg/mL αCD28 antibody. On day three, 1µg/mL fluorescently labeled αCTLA-4 antibody or isotype control was added for four hours. Afterwards, T cells were resuspended and FACS stained with αCD8 antibody as described in 3.2.2.4.

3.2.14 Surface expression on BMDCs

$4*10^5$ CpG-activated (3.2.1.5) or untreated wildtype or $MR^{-/-}$ BMDCs were plated in a 24-well plate and let adhere for one hour or directly FACS stained for CD11c, CD80 and CD86 (3.2.2.4). Supernatant was replaced by medium supplemented with 250ng/mL fluorescently labeled OVA and incubated for 15 minutes. Cells were scraped off with a rubber-scraper and stained for CD11c.

3.2.15 *In vivo* experiments

3.2.15.1 *In vivo* CTLA-4 expression

Wildtype or $MR^{-/-}$ BMDCs were transduced with an Adenovirus encoding for Luciferase, OVA and GFP (AdLOG) with a MOI of 20 for three hours under cell culture conditions or left untransduced. $0,75*10^6$ washed cells were injected i.v. into C57/BL6 mice and priming of endogenous T cells took place for six days. Afterwards, C57/BL6 splenocytes were isolated (3.2.2.1) and $5*10^6$ cells were incubated with 2µg/mL fluorescently labeled αCTLA-4 antibody or isotype control for four hours. Afterwards splenocytes were resuspended and FACS stained with SIINFEKL-dextramers and αCD8 antibody as described in 3.2.2.4.

3.2.15.2 *In vivo* cytotoxicity

Wildtype or $MR^{-/-}$ BMDCs were transduced with an Adenovirus encoding for Luciferase, OVA and GFP (AdLOG) with a MOI of 20 for three hours under cell culture conditions or left untransduced. $1*10^6$ washed cells were injected i.v. into C57/BL6J mice and priming of endogenous T cells took place for four days. Afterwards, C57/BL6J splenocytes were

isolated (3.2.2.1) and loaded with 2µM OVA minimal peptide SIINFEKL for 30 minutes or left untreated. Loaded target cells and unloaded non-target cells were labeled with CFSE (3.2.2.2), mixed at equal ratios and $1*10^7$ total cells were injected i.v. per mouse. After four hours, splenocytes were isolated (3.2.2.1) and specific cytotoxicity determined as described in 3.2.3.1.

4 RESULTS

4.1 The Mannose receptor affected T cell activation under steady-state conditions

4.1.1 The MR had no influence on T cell proliferation or IL-2 secretion

In the present study, the effect of the MR on T cell activation was investigated. To prevent influences of the MR during antigen uptake or presentation, use was made of DesTCR T cells (105). The haplotype of Des TCR transgenic mice is H-2K^{K}. The T cell receptor of CD8^{+} DesTCR T cells recognizes in an alloreaction three endogenous peptides, pKB1, 2, and 3 (111) presented on MHC-I molecules of the haplotype H-2K^{b} which is expressed on cells with C57/BL6J background.

First, the influence of the MR on T cell proliferation was investigated. To this end, CFSE-labeled DesTCR T cells were co-cultured for three days in the presence of wildtype (wt) respectively MR-deficient (MR$^{-/-}$) BMDCs. Afterwards, the proliferation profile was analyzed by flow cytometry. No difference could be observed in the proliferation behavior of DesTCR T cells being activated by wildtype or MR$^{-/-}$ BMDCs (**Fig. 4-1a**). This was also confirmed by measuring the secreted IL-2 amount in supernatants of co-cultures of DesTCR T cells with either wildtype or MR$^{-/-}$ BMDCs by ELISA (**Fig. 4-1b**).

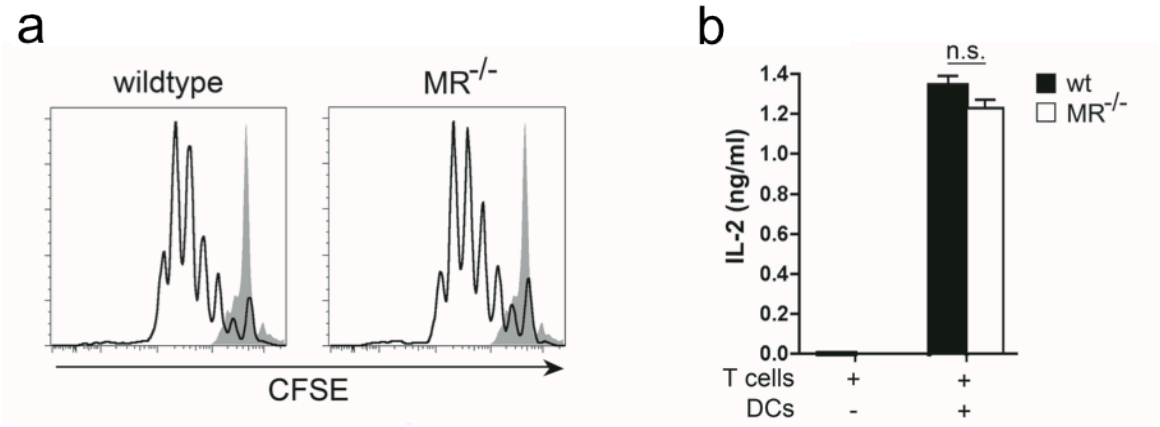

Fig. 4-1: The MR had no influence on T cell proliferation or IL-2 secretion.

a) Wildtype or MR$^{-/-}$ BMDCs were co-cultured for three days with CFSE-labeled DesTCR T cells. CFSE-dilution profile of CD8^{+} T cells was determined by flow cytometry. **b)** DesTCR T cells were co-cultured for 24 hours with or without wildtype or MR$^{-/-}$ BMDCs. IL-2 concentration in the supernatant was determined by ELISA. n.s.: not significant.

4.1.2 The MR on BMDCs decreased T cell cytotoxicity and IFN-γ secretion

Since T cell proliferation is just the first step during T cell activation, further studies dealt with the cytotoxic capacities of DesTCR T cells activated by wildtype or $MR^{-/-}$ BMDCs in an *in vitro* cytotoxicity assay. On that account, DesTCR T cells were primed for three days by either type of BMDCs. Afterwards, T cells were isolated and separated from BMDCs by density gradient centrifugation. Purified T cells were cultured for four hours with differentially CFSE-labeled antigen-bearing RMA target cells ($CFSE^{high}$) and RMA-S control cells lacking cell surface antigens (TAP2 deficient mutant of RMA; $CFSE^{low}$). Finally, the cells were analyzed by Flow cytometry and the specific cytotoxic T cell activity was determined.

Figure 4-2a shows a strongly decreased cytotoxic capacity of T cells which were primed by wildtype BMDCs compared to T cells after activation with $MR^{-/-}$ BMDCs. In addition to this, re-stimulation of activated T cells with an αCD3 antibody revealed a significantly lower IFN-γ secretion of T cells that were activated in the presence of the MR compared to T cells activated in the absence of the MR (**Fig. 4-2b**). This indicated that the presence of the MR on DCs during T cell activation results in T cell development into a more tolerogenic state represented by suppressed cytotoxicity and IFN-γ secretion.

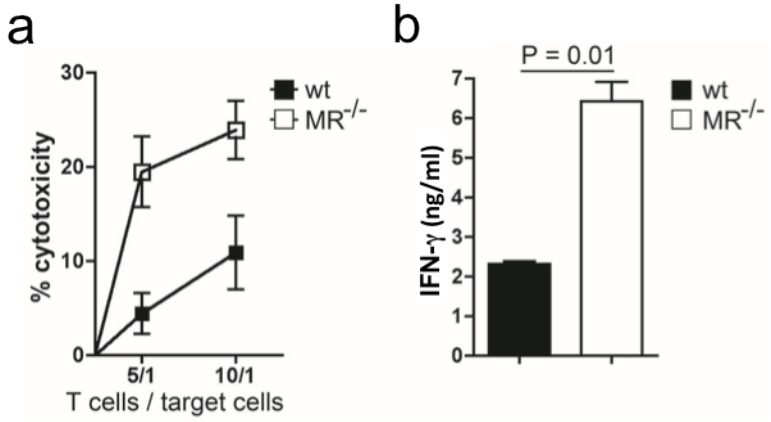

Fig. 4-2: The MR on BMDCs decreased cytotoxic capacities of DesTCR T cells.

a) Wildtype or $MR^{-/-}$ BMDCs were co-cultured for three days with DesTCR T cells. T cells were purified by density gradient centrifugation and distinctly CFSE-labeled target or control cells were added in different ratios to the T cells. After four hours, the ratio of target cells to control cells was analyzed by flow cytometry and the specific cytotoxicity was calculated. **b)** Purified T cells from a) were re-stimulated for 24 hours with an αCD3 antibody and the IFN-γ concentration in the supernatant was determined by ELISA.

4.1.3 Wildtype and MR$^{-/-}$ BMDCs were phenotypically equivalent

This inhibitory effect of the MR on cytotoxicity might be due to two reasons. First, upon binding of an interaction partner, the MR might alter the immunogenic properties of the DCs themselves. Alternatively, the MR might recognize an interaction partner located on the T cell surface, altering the immunogenic properties of the T cells directly.

To discriminate between these two possibilities, the phenotype of either wildtype or MR$^{-/-}$ CD11c^{+} BMDCs after co-culture for 18 hours with DesTCR T cells was analyzed. On that account, the surface expression of co-stimulatory molecules like CD86, CD86 and CD40, the expression of MHC II, the co-inhibitory molecule B7H1 and the secretion of the cytokines IL-6 and IL-10 were determined. Controls were either unstained cells or, in case of cytokine secretion, BMDCs in the absence of T cells.

No significant differences between wildtype and MR$^{-/-}$ BMDCs were detectable (**Fig. 4-3a** and **b**), indicating that influences of the MR onto the immunogenic properties of the DCs were unlikely.

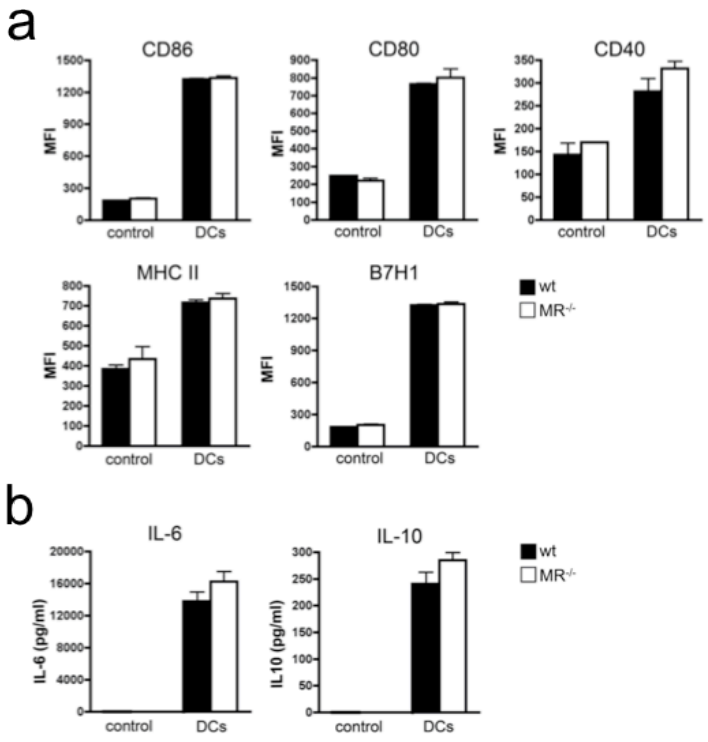

Fig. 4-3: Wildtype and MR$^{-/-}$ BMDCs were phenotypically equivalent.

(a) Wildtype or MR$^{-/-}$ BMDCs were co-cultured for 18 hours with DesTCR T cells. Surface expression of indicated molecules on BMDCs was determined by flow cytometry. Unstained cells served as control. All cells were gated on CD11c^{+} cells as marker for BMDCs. (**b)** IL-6 and IL-10 concentration was analyzed in the supernatant of (a) by BD™ Cytometric Bead Array (CBA).

4.1.4 The MR on BMDCs resulted in prolonged interaction with T cells

Since the MR did not seem to alter the immunogenic properties of DCs, it was then investigated whether the influence of MR might be due to an interaction with proteins on the T cell surface. To this end, analysis considering the contact duration of wildtype or $MR^{-/-}$ DCs with T cells were performed by time-lapse microscopy (in close cooperation with Prof. Waldemar Kolanus and Dr. Thomas Quast).

Figure 4-4 shows that the presence of the MR on DCs led to a significantly prolonged interaction with T cells compared to BMDCs lacking the MR. These results emphasized a possible interplay of the MR with T cell surface molecules.

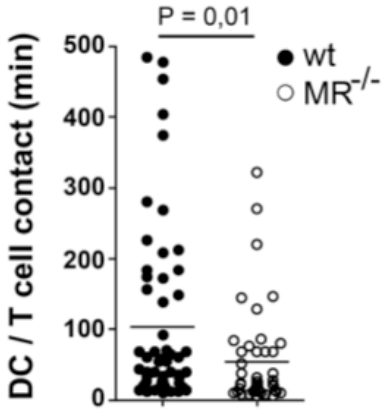

Fig. 4-4: The MR on BMDCs resulted in prolonged interaction with T cells.

Wildtype or $MR^{-/-}$ BMDCs were co-cultured with CFSE-labeled $CD8^+$ MACS-isolated DesTCR T cells in a plastic channel µ-slide for 12 hours. Every two minutes, the green fluorescence and differential interference was recorded at 20-fold magnification. At least 40 randomly chosen interaction events were analyzed considering their contact duration.

4.1.5 Chimeric MR constructs displayed distinct binding characteristics

To irrevocably test whether the MR-mediated decrease in cytotoxicity in deed was due to interactions with T cell surface molecules, chimeric MR proteins were used. These consisted of the human IgG_1 F_c portion (Isotype control) coupled either to the Cystein-rich (CR) domain, the Fibronectin-like (FN) domain and the C-type lectin-like domains 1-3 (CTLD) (MR-FN) or coupled to the CTLDs 4-7 (MR-CTLD) (69). Whereas the isotype control lacks domains which are capable of binding to antigens, the FN domain is able to bind to Collagens and the CTLDs 4-7 possess binding capacities for glycosylated proteins, as for example the model antigen ovalbumin (OVA).

First of all, these binding properties of the chimeric proteins were tested. On this account, the constructs were applied to an either OVA- or Collagen-coated ELISA plate, washed and detected by conversion of ABTS via colorimetry at 450nm. As isotype control served the human IgG_1 F_c portion.

There was a significant binding of the chimeric protein comprising the CTLDs 4-7 to OVA-coated plates, lacking any binding capacity towards Collagen (**Fig. 4-5**). In contrast to that, the chimeric protein consisting of the CR and FN domain, strongly bound to Collagen without any binding towards OVA (**Fig. 4-5**). This approved the functional binding capacities of the chimeric proteins.

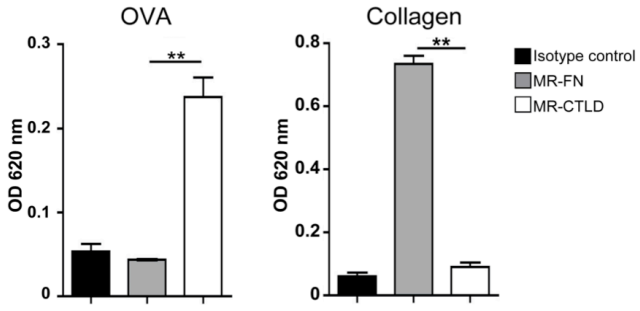

Fig. 4-5: Chimeric MR constructs displayed distinct binding characteristics.

10µg/mL chimeric MR constructs comprising the human IgG_1 F_c part plus either the CR domain, the FN domain and the CTLDs 1-3 (MR-FN) or comprising the CTLDs 4-7 (MR-CTLD) were complexed using an αhuman antibody coupled to horseradish peroxidase. Complexed constructs were then applied to either OVA-coated (0,5mg/mL) or Collagen-coated (0,1mg/mL) ELISA plates, washed and detected by conversion of ABTS via colorimetry at 450nm. As isotype control served the human IgG_1 F_c part only.

4.1.6 Addition of soluble MR suppressed cytotoxicity and IFN-γ secretion

With the soluble, chimeric MR it is possible to discriminate in an *in vitro* cytotoxicity experiment whether the MR has any direct influence on the BMDCs or on the DesTCR T cells. In case the MR renders the properties of the BMDCs, this would only be possible if the MR were attached to the BMDCs leading to intracellular signaling events via its cytoplasmic domain. Hence, addition of the soluble MR should have no effect on the outcome of experiments.
In contrast to that, if the MR binds an interaction partner on the T cell surface and thereby alters their phenotype, no contact to the BMDCs would be necessary. Hence, the addition of the soluble form of the MR should still lead to decreasing cytotoxic capacities of T cells.

Therefore, an *in vitro* cytotoxicity assay was carried out. To this end, DesTCR T cells were activated with wildtype or $MR^{-/-}$ BMDCs in the presence of either a soluble form of the MR protein comprising the CR-domain, the FN-domain and the CTLD1-3 (FcMR) or a control protein.

Addition of neither the control protein nor of FcMR, had any effect on the cytotoxicity of T cells being primed by wildtype BMDCs (**Fig. 4-6a**). Furthermore, in the presence of control protein the cytotoxicity of T cells primed by $MR^{-/-}$ was still higher compared to T cells that were primed by wildtype BMDCs (**Fig. 4-6a**). In contrast to that, addition of FcMR to T cells that were activated by $MR^{-/-}$ BMDCs strongly diminished the cytotoxic capacity (**Fig. 4-6a**). This cytotoxic capacity was comparable to T cells activated by wildtype BMDCs (**Fig. 4-6a**). No such effect could be detected by addition of the chimeric protein consisting of the CTLDs4-7 (data not shown).
Restimulation of T cells with an αCD3 antibody revealed decreased IFN-γ amounts in the supernatant when T cells were primed by $MR^{-/-}$ BMDCs in the presence of FcMR compared to control protein (**Fig. 4-6b**). These results evidence that the decreased cytotoxicity and secretion of IFN-γ in the presence of the MR indeed was due to an interaction with proteins on the T cell surface.

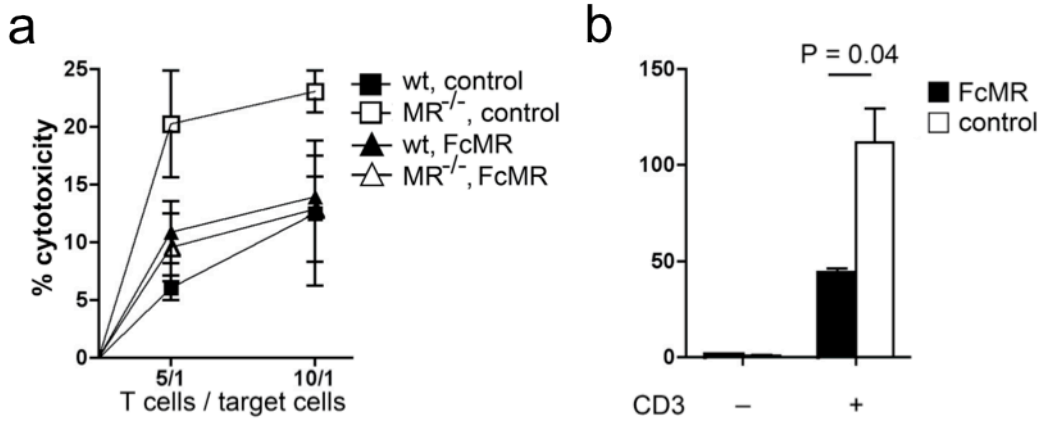

Fig. 4-6: Addition of the MR suppressed cytotoxicity and IFN-γ secretion.

(a) Wildtype or $MR^{-/-}$ BMDCs were co-cultured for three days with DesTCR T cells in the presence of 10µg/mL complexed FcMR or control protein consisting of the human IgG_1 F_c part only. T cells were purified by density gradient centrifugation and distinctly CFSE-labeled target cells or control cells were added in different ratios to the T cells. After four hours, the ratio of target cells to control cells was analyzed by flow cytometry and the specific cytotoxicity was calculated. **(b)** Purified T cells from (a) were re-stimulated for 24 hours with an αCD3 antibody and the IFN-γ concentration in the supernatant was determined by ELISA.

4.2 The influence of the Mannose Receptor on CD45

4.2.1 CD45 was one interaction partner of the MR

As a matter of course, it was of interest to find out which molecule on the T cell interacted with the MR on BMDCs. To answer this question, co-immunoprecipitation experiments were performed with FcMR or control protein as bait in lysates of surface-biotinylated DesTCR cell. The subsequent Western blot was detected with horseradish peroxidase-coupled NeutrAvidin (NA).

No signal could be achieved using the control protein as bait (**Fig. 4-7a**). In contrast to that, when FcMR was used as bait, there was a double band visible of about 180-230kDa and a double band between 70-80kDa (**Fig. 4-7a**).

Since it has been published that the MR and a related lectin called Macrophage galactose lectin (MGL) are capable to bind CD45 (57, 58), whose isotype-dependent molecular weight is between 180kDa and 230kDa, it was specifically stained for CD45. Indeed, a CD45-specific signal could be detected after co-immunoprecipitation with FcMR (**Fig. 4-7b**).

To further validate the interaction between the MR and CD45, a different approach was followed together with Maria Embgenbroich. Herein, CD45 was immunoprecipitated from DesTCR T cell lysates and loaded onto a Western blot. As detection reagent either FcMR

was applied to the Western blot or an αCD45 antibody. CD45 led to four bands between 180kDa and 230kDa resembling different isoforms of CD45 (**Fig. 4-7c**). FcMR revealed a single signal at about 200kDa corresponding to one of the CD45 isoform bands (**Fig. 4-7c**). This effectively proved that CD45 on T cells was actually an interaction partner of the MR.

Fig. 4-7: CD45 was one interaction partner of the MR.

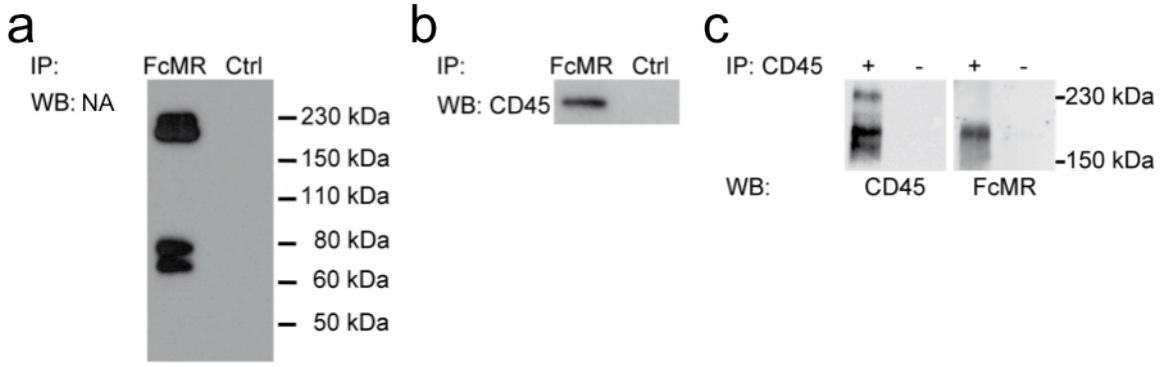

(a) FcMR or huIgG$_1$-control protein were complexed with an αhuman antibody. 10µg/mL complexed constructs were added to lysates of surface-biotinylated DesTCR T cells, incubated for one hour, Protein G agarose beads were added and incubated for one hour, washed and bead bound proteins were eluted. Western blot was performed and detection occurred with HRP-coupled NeutrAvidin (NA). **(b)** Samples from (a) were stained with an αCD45 antibody followed by HRP-coupled secondary antibody. **(c)** Lysates of DesTCR T cells were incubated for one hour with Protein G agarose beads which were either coupled with αCD45 or left untreated, washed and bead bound proteins were eluted. Western blot was performed and detection occurred either with an αCD45 antibody followed by HRP-coupled secondary antibody or with 10µg/mL FcMR constructs which had been complexed with an αhuman-HRP antibody.

4.2.2 Impairment of CD45 activity led to decreased T cell cytotoxicity and was induced by the MR

To investigate whether CD45 was responsible for the reduced T cell effector functions in ther presence of the MR, we performed *in vitro* cytotoxicity assay in the presence or absence of the CD45 specific phosphatase inhibitor N-(9,10-Dioxo-9,10-dihydro-phenanthren-2-yl)-2,2-dimethyl-propionamide (SF1670) (112) during the priming phase.

In the absence of the CD45 inhibitor, there was an increased cytotoxic capacity of T cells that were primed with MR$^{-/-}$ BMDCs compared to T cells primed by wildtype BMDCs (**Fig. 4-8a**). This effect was completely abolished in the presence of CD45 inhibitor, indicating that inactivation of CD45 led to the reduction in T cell cytotoxicity (**Fig. 4-8a**).

To investigate whether binding of the MR altered CD45 activity, a phosphatase activity assay was established together with the master student Jessica König. To this end, $CD8^+$ DesTCR T cells were incubated with either wildtype or $MR^{-/-}$ BMDCs, T cells were isolated, lysed and CD45 was immunoprecipitated. The phosphatase activity was determined in the presence or absence of the CD45 inhibitor SF1670 by addition of the CD45-specific substrate 4-nitrophenyl phosphate (4-NPP) (57) whose turnover could be measured by colorimetry at 405nm.

The CD45 inhibitor SF1670 reduced the signal to background levels similar to control samples, in which no CD45 was immunoprecipitated (**Fig. 4-8b**). The CD45 phosphatase activity of T cells that were cultured with wildtype BMDCs was decent compared to the CD45 phosphatase activity of T cells that were primed by $MR^{-/-}$ BMDCs which was significantly higher (**Fig. 4-8b**).

Similar results were obtained with HEK293T cells bearing (HEK-MR) or lacking the MR (HEK). Together with the diploma student Melanie Nehring, a phosphatase assay was performed with T cells that have been incubated with HEK-MR or HEK cells. Again, it could be shown that in the presence of the MR the CD45 phosphatase activity was significantly diminished compared to samples lacking the MR (**Fig. 4-8c**).

It was further investigated whether the above-described inactivation of CD45 also had down-stream effects on Lck as a direct substrate of CD45. Together with Maria Embgenbroich, $CD8^+$ DesTCR T cells were incubated with either wildtype or $MR^{-/-}$ BMDCs. Thereafter, we analyzed the phosphorylation of Lck at the tyrosine Y505. At this tyrosine residue, CD45 is able to remove an inhibitory phosphate.

The Western blot in **figure 4-8d** shows a drastic reduction of phosphorylated Lck in the absence of the MR on BMDCs compared to T cells that were incubated with MR-bearing wildtype BMDCs. The quantification of the ratio between pLck to Actin revealed an approximately 2,5-fold decrease of Y505 pLck in the knock-out treated T cells compared to wildtype primed T cells (**Fig. 4-8d**).

To attest that this effect was really due to the influence of the MR, the experiment was additionally performed together with Annegret Zweynert with only $MR^{-/-}$ BMDC in the presence of FcMR or control protein. Also in these experiments, an increase in Lck phosphorylation in the presence of the MR could be observed (**Fig. 4-8e**). These outcomes

verify that the MR inhibits CD45 phosphatase activity upon binding and inhibition of CD45 results in a tolerogenic state of the T cells accompanied with decreased cytotoxicity.

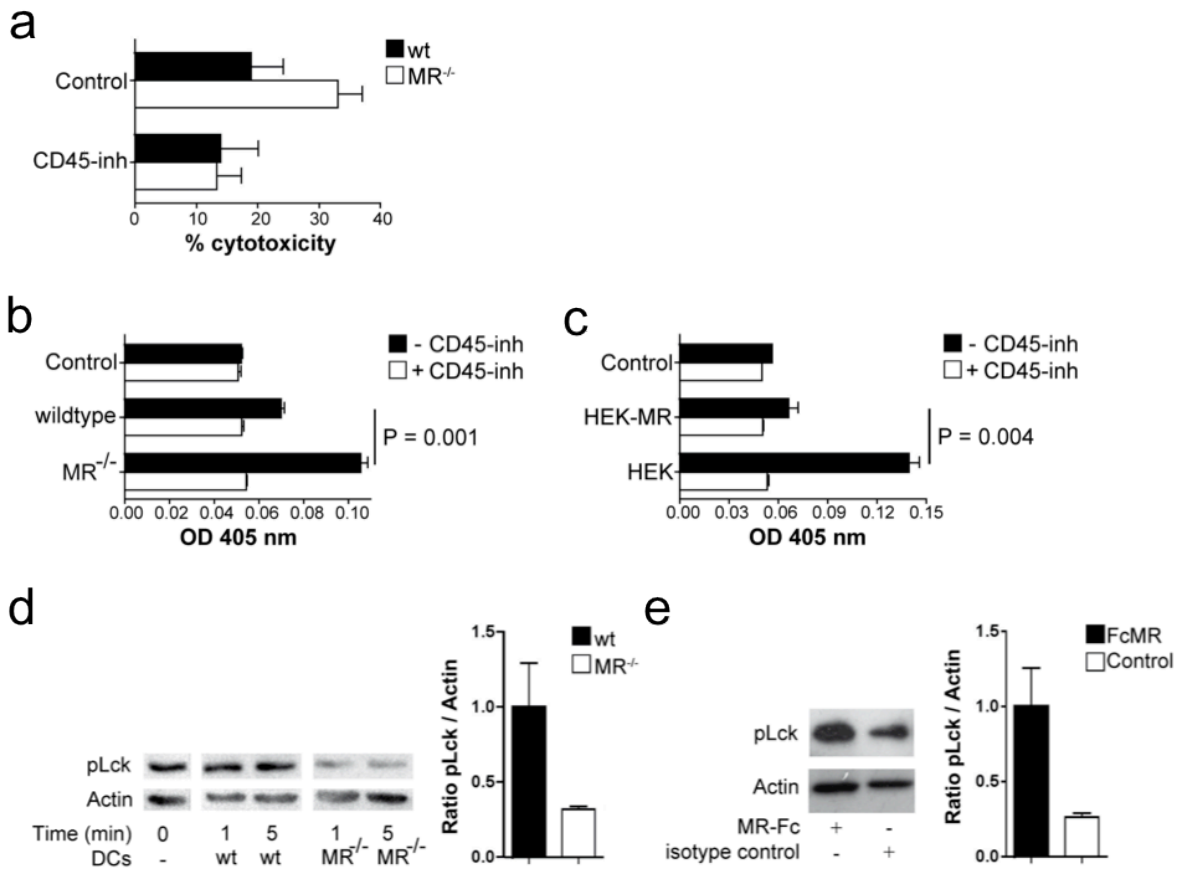

Fig. 4-8: Impairment of CD45 activity led to decreased T cell cytotoxicity and could be induced by the MR.

(a) Wildtype or $MR^{-/-}$ BMDCs were co-cultured for three days with DesTCR T cells in the presence or absence of 40mM CD45 specific inhibitor SF1670. T cells were purified by density gradient centrifugation and distinctly CFSE-labeled target cells or control cells were added in different ratios to the T cells. After four hours, the ratio of target cells to control cells was analyzed by flow cytometry and the specific cytotoxicity was calculated. **(b)** DesTCR T cells were incubated for one hour with wildtype or $MR^{-/-}$ BMDCs, T cells were lysed and Protein G agarose beads which were either coupled with an αCD45 or left untreated (control) were added for one hour. Beads were washed and incubated over night with 2mM CD45-specific substrate 4-nitrophenyl phosphate (4-NPP) in the presence or absence of 1µM CD45 inhibitor SF1670. Turnover of the substrate was analyzed by colorimetry at 405nm. **(c)** See (b), but instead of wildtype and $MR^{-/-}$ BMDCs, MR-bearing HEK293T (HEK-MR) cells or MR-lacking HEK293T (HEK) cells were used. **(d)** DesTCR T cells were incubated for the indicated time points with wildtype or $MR^{-/-}$ BMDCs, T cells were lysed and Western blotting was performed. Membranes were stained with either antibodies against Y505 phosphorylated Lck (pLck) or Actin as loading control. The ratio between pLck and Actin was quantified using ImageJ software. **(e)** FcMR or $huIgG_1$-control protein were complexed with an αhuman antibody. 10µg/mL complexed constructs were added to a co-culture of $MR^{-/-}$ BMDCs and DesTCR T cells and incubated for five minutes. T cells were lysed and Western blotting was performed. Membranes were stained with either antibodies against Y505 phosphorylated Lck (pLck) or Actin as loading control. The ratio between pLck and Actin was quantified using ImageJ software.

4.3 The Mannose Receptor led to a differential gene expression profile in T cells

Since the MR obviously influenced the signaling cascade of activated T cells, the impact of the MR on gene expression modifications was examined adopting a cDNA microarray. For this purpose, $CD8^+$ DesTCR T cells were incubated for zero, four, 18 and 48 hours with $MR^{-/-}$ BMDCs in the presence of either FcMR or control protein. Afterwards, $CD8^+$ T cells were FACS sorted, RNA isolated, reverse-transcribed into cDNA and the samples were applied to gene array analysis (in close cooperation with Prof. Joachim Schultze and Dr. Astrid Draffehn).

Bioinformatics revealed clustering of replicates within the same samples plus rough clustering among the different incubation durations. The gene expression heat map in **Figure 4-9a** shows a clear distinction of samples that were incubated in the presence of the MR and of the ones incubated in the absence of the MR throughout all time points.

To elicit potential key-players in this re-programming process, literature research was performed by Dr. Astrid Draffehn, screening for differentially expressed genes associated with T cell tolerance and/or anergy. 49 candidate genes were found, whereof 34 were expressed in all tested conditions and 16 showed a differential expression compared to naive T cells during the exercised time course. These 16 genes were depicted in a heat map in **figure 4-9b**, indicating their log2 expression levels for all three conditions (naive, isotype control and FcMR) and time points (t= 4h, 18h and 48h). Additionally, the fold change (FC) of isotype control- or FcMR-treated cells relative to naive cells plus the FC ratio between both treatments was calculated.

Candidate genes showing a strong regulation were further visualized in their time course, comparing T cells under the influence of the isotype control protein or the FcMR protein relative to naive T cells (**Fig. 4-9c**). Amongst them were Ctla-4 (Cytotoxic T-lymphocyte Antigen 4), Egr1, 2 and 3 (Early growth response protein 1, 2 and 3) and Jmjd3 (Jumonji domain containing 3).

Egr1, 2 and 3 were up-regulated at the early time point (4h) relative to naive T cells (**Fig. 4-9b, c**) and showed an increased transcription under the influence of FcMR compared to control-treated samples (**Fig. 4-9c**). For all three genes there was a sharp drop in their transcription for the intermediate (18h) and late (48h) time points. For the 18 hours time point, the transcription levels were quite diverse, for Egr1 having been higher in the FcMR-treated sample, for Egr2 having been slightly higher in the control sample and having been equal for Egr3 (**Fig. 4-9c**). However, the late time point, again showed a clear picture with all genes having been transcribed weaker in the FcMR-treated samples compared to control sample (**Fig. 4-9c**).

The transcription level of Jmjd3 could also be determined to be strongly enhanced upon T cell activation relative to naive cells (**Fig. 4-9b, c**). Moreover, the expression is elevated in FcMR treated samples compared to the control samples for all time points, emphasizing Jmjd3 as a putative candidate to be further investigated (**Fig. 4-9c**).

However, Ctla-4 showed the most prominent differences during the time course with strong up-regulation upon T cell activation relative to naive cells. In the presence of FcMR, the transcription of Ctla-4 was robustly increased compared to samples treated with the control protein. This was especially the case for the intermediate (18h) and late (48h) time points (**Fig. 4-9**). Amongst the selected genes Egr1, 2 and 3, Jmjd3 and Ctla-4, CTLA-4 was the only effector protein, whereas the others were involved in transcriptional regulation. Furthermore, ligation of CD45 had been demonstrated to up-regulate CTLA-4 and induce tolerance against allografts (113). Therefore, we decided to investigate whether impaired T cell effector function in the presence of the MR might be due to up-regulation of CTLA-4 after MR-induced inactivation of CD45.

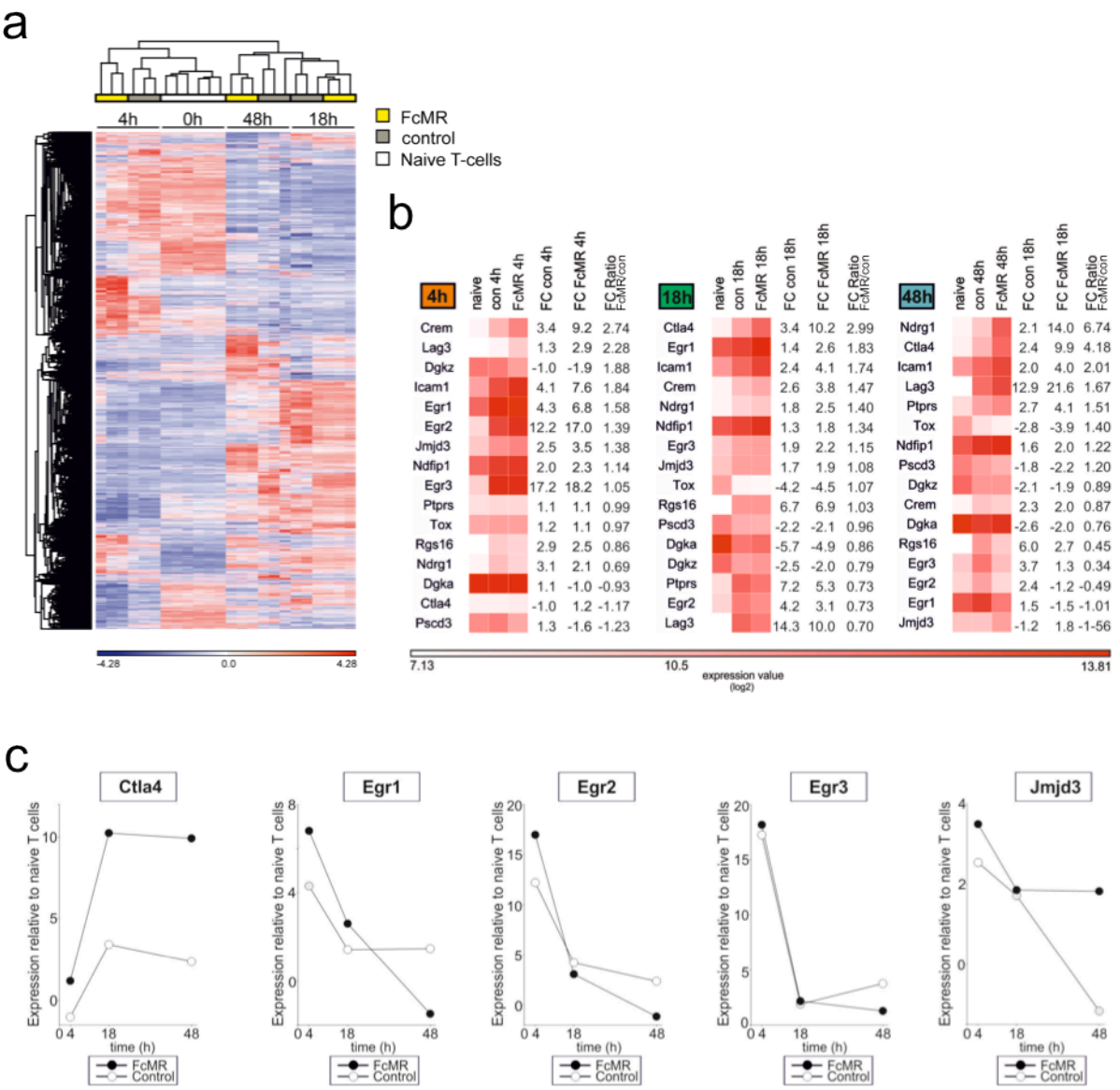

Fig. 4-9: The MR lead to differential gene expression profile in T cells.

DesTCR T cells were incubated for 4h, 18h or 48h with $MR^{-/-}$ BMDCs in the presence of 10µg/mL either complexed isotype control protein or FcMR. Naïve T cells were not co-cultured with BMDCs. RNA was isolated from $CD8^{+}$ sorted T cells, reverse transcribed into cDNA and applied to micro array analysis. **(a)** Heat map of hierarchical clustering of significantly variable transcripts. **(b)** Z-transformed log2 expression profiles of differentially expressed genes during the time course, associated with T cell tolerance and/or anergy. Fold change (FC) ratio of isotype control/FcMR protein treated samples was calculated. **(c)** Selected candidate genes form b) were shown. Time course of relative expression levels of isotype control respectively FcMR treated T cells compared to naïve T cells.

4.4 The influence of the Mannose Receptor on T cells depended on CD45 and was mediated by CTLA-4 up-regulation

4.4.1 CTLA-4 up-regulation was detectable in the presence of the MR and by inhibition of CD45

To additionally confirm the up-regulated expression of CTLA-4 in the presence of the MR on protein level, DesTCR T cells were co-cultured with wildtype or $MR^{-/-}$ BMDCs for three days and CTLA-4 expression on $CD8^+$ T cells was analyzed by flow cytometry.

First of all, an enhanced number of CTLA-4 expressing $CD8^+$ T cells could be detected when having been cultured in the presence of MR-bearing wildtype BMDCs compared to $MR^{-/-}$ BMDCs (**Fig. 4-10a**). Quantification revealed a significantly higher percentage of CTLA-4 expressing cells (**Fig. 4-10b**) plus a significantly increased CTLA-4 mean fluorescence intensity (MFI) of $CD8^+$ T cells (**Fig. 4-10c**).

To investigate whether this increased expression was associated with CD45 activity, which was decreased in the presence of the MR (see **Fig. 4-8a**), CTLA-4 expression of $MR^{-/-}$ primed T cells was examined in the presence of the CD45-specific inhibitor SF1670. In **figure 4-10d** one can see a clear increase of CTLA-4 expressing T cells in the presence of the CD45 inhibitor compared to T cells whose priming was performed without inhibitor. Again, quantification resulted in significantly increased percentages of $CTLA\text{-}4^+$ cells and MFI of CTLA-4 on T cells in the presence of the CD45 inhibitor (**Fig. 4-10e, f**). Thus, the presence of the MR or the inhibition of CD45 led to up-regulation of CTLA-4.

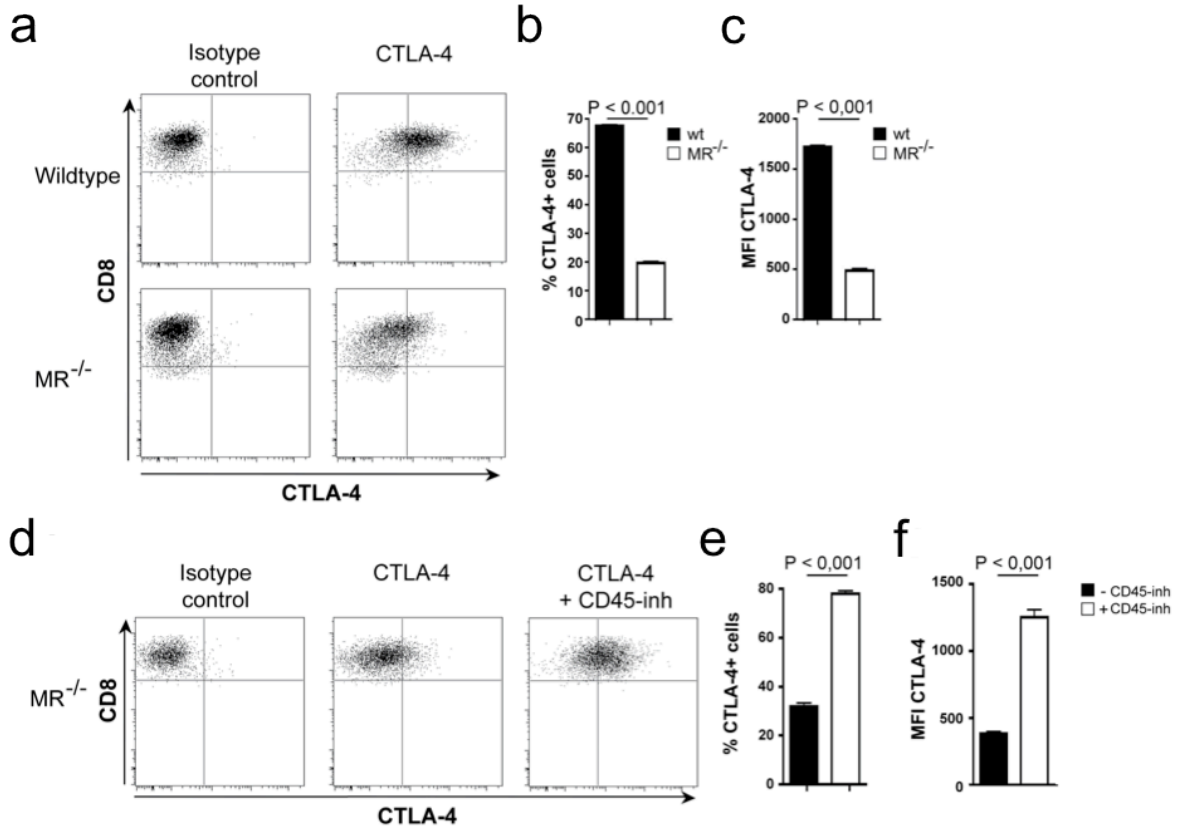

Fig. 4-10: CTLA-4 up-regulation was detectable in the presence of the MR and by inhibition of CD45.

(a) DesTCR T cells were incubated for three days with wildtype or $MR^{-/-}$ BMDCs, 1µg/mL fluorescent-coupled αCTLA-4 or isotype control antibody were added to the supernatant for four hours. Cells were harvested, stained for CD8 and analyzed by flow cytometry. **(b)** Quantification of (a). **(c)** MFI of CTLA-4 of (a). **(d)** DesTCR T cells were incubated for three days with $MR^{-/-}$ BMDCs in the presence or absence of 40mM CD45 inhibitor SF1670, 1µg/mL fluorescent-coupled αCTLA-4 or isotype control antibody were added to the supernatant for four hours. Cells were harvested, stained for CD8 and analyzed by flow cytometry. **(e)** Quantification of (d). **(f)** MFI of CTLA-4 of (d). % $CTLA\text{-}4^{+}$ cells and MFI of CTLA-4 were determined after gating on $CD8^{+}$ cells.

4.4.2 MR-mediated suppression of cytotoxicity depended on CTLA-4

To explore whether the diminishing effect of the MR on the cytotoxic capacity of $CD8^{+}$ T cells was due to induced expression of CTLA-4 during T cell activation, further *in vitro* cytotoxicity assays were performed.

First, DesTCR T cells were activated by either wildtype or $MR^{-/-}$ BMDCs in the presence or absence of soluble CTLA-4 (sCTLA-4). Since CTLA-4 binds to the co-stimulatory molecules CD80/86 with higher affinity than CD28 does, it was possible to block these co-stimulatory molecules by addition of surplus sCTLA-4. **Figure 4-11a** shows a clearly diminished cytotoxicity of T cells which were primed by $MR^{-/-}$ BMDCs in the presence of sCTLA-4. Their cytotoxic capacities were diminished to levels comparable to wildtype primed T cells. The

same results could be observed when T cells were activated by $MR^{-/-}$ BMDCs in the presence or absence of FcMR with or without sCTLA-4 (**Fig. 4-11b**, together with Katharina Koch).

This indicated that the reduced cytotoxic capacity of T cells that had been primed in the presence of the MR might have been due to increased levels of the inhibitory protein CTLA-4.

To further verify this hypothesis, we performed *in vitro* cytotoxicity assays in the presence of an αCTLA-4 blocking antibody (a-CTLA-4). Addition of αCTLA-4 antibody had no effect on T cells that were primed by $MR^{-/-}$ BMDCs alone or in the presence of control protein (**Fig. 4-11c, d**). Noteworthy, in case of T cell priming by wildtype BMDCs, or by $MR^{-/-}$ BMDCs in the presence of FcMR, the cytotoxic capacity was increased to levels comparable to the knock-out situation (**Fig. 4-11c, d**).

This showed that the MR-mediated suppression of T cell cytotoxicity was indeed based on increased expression levels of the inhibitory molecule CTLA-4.

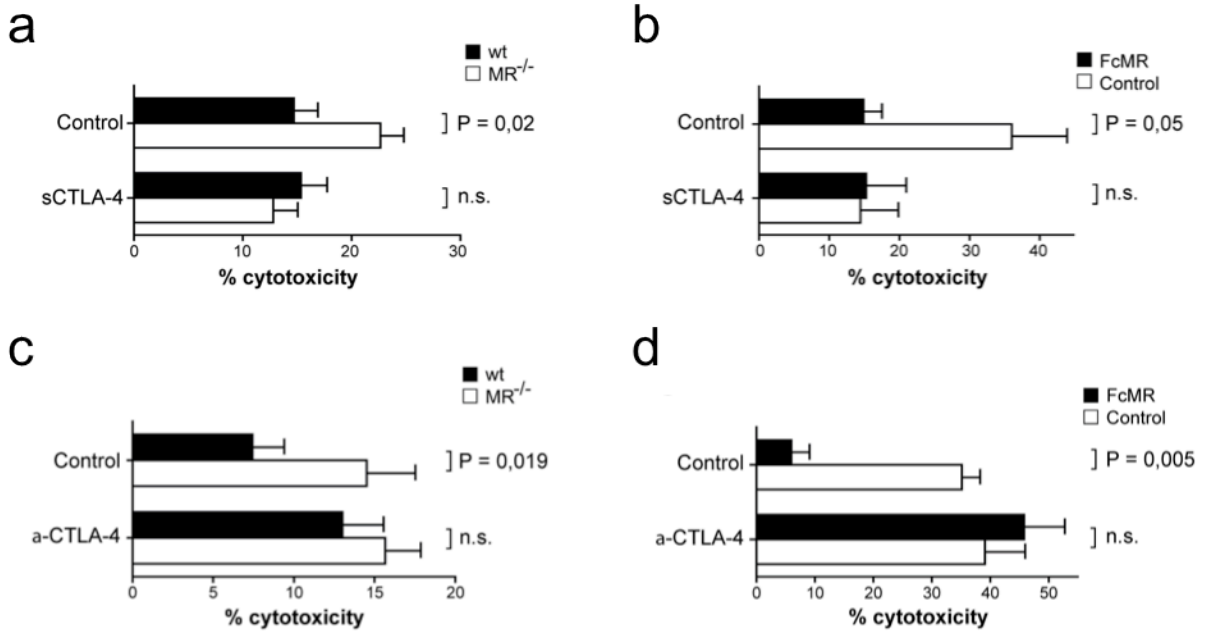

Fig. 4-11: MR-mediated suppression of cytotoxicity depended on CTLA-4.

(a) Wildtype or $MR^{-/-}$ BMDCs were co-cultured for three days with DesTCR T cells in the presence or absence of 1µg/mL soluble CTLA-4 protein (sCTLA-4). T cells were purified by density gradient centrifugation and distinctly CFSE-labeled target cells or control cells were added to the T cells. After four hours, the ratio of target to control cells was analyzed by flow cytometry and the specific cytotoxicity was calculated. **(b)** FcMR or huIgG_1-control protein was complexed with an αhuman antibody. 10µg/mL complexed constructs were added to co-cultures of DesTCR T cells with $MR^{-/-}$ BMDCs and incubated for three days. The following assay was performed as in (a). **(c)** See (a) instead of sCTLA-4, 1µg/mL inhibitory αCTLA-4 antibody (a-CTLA-4) was added. **(d)** See (b) instead of sCTLA-4, 1µg/mL inhibitory αCTLA-4 antibody was added.

4.5 MR-mediated CTLA-4 up-regulation and cytotoxicity suppression was circumvented under inflammatory conditions

The induction of tolerogenic effects obviously has to be reversible in case of infection. For that reason, the MR-mediated up-regulation of the inhibitory molecule CTLA-4 was investigated in the presence of inflammatory stimuli like CpG.

To this end, DesTCR T cells were incubated for three days with either naive or CpG-stimulated wildtype cells and CTLA-4 staining was performed as described above. Interestingly, the percentage of CTLA-4-expressing cells was distinctly diminished on T cells that were activated by CpG-stimulated BMDCs compared to activation by naive BMDCs (**Fig. 4-12a**). Again, quantification of the percentage of CTLA-4 positive cells and the verification of the MFI proved a significant decrease under the influence of CpG (**Fig. 4-12b, c**). These results indicated that the enhancing effect of the MR on CTLA-4 expression might be overruled under inflammatory conditions.

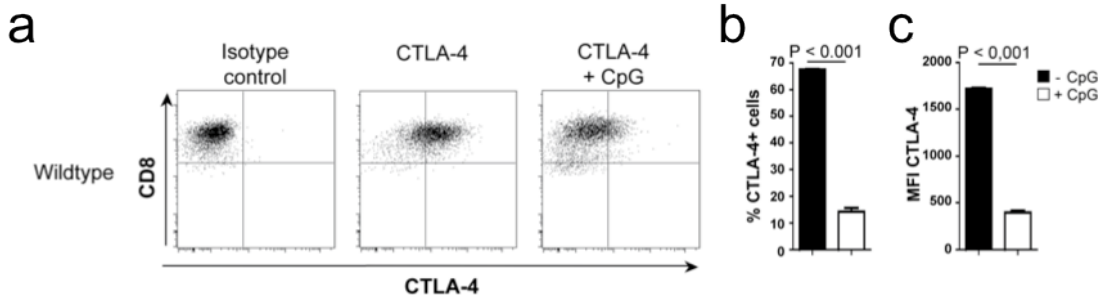

Fig. 4-12: MR-mediated CTLA-4 up-regulation could be circumvented under inflammatory conditions.

(a) Wildtype BMDCs were activated over night with 5µg/mL CpG or left untreated. DesTCR T cells were incubated for three days with activated or untreated BMDCs, 1µg/mL fluorescent-coupled αCTLA-4 or isotype control antibody was added to the supernatant for four hours. Cells were harvested, stained for CD8 and analyzed by flow cytometry. **(b)** Quantification of (a). **(c)** MFI of CTLA-4 of (a).

Yet, it had to be excluded that this effect might have been due to the fact that the MR was invaginated upon CpG-stimulation or due to differential expression of co-stimulatory molecules between CpG-treated wildtype and $MR^{-/-}$ BMDCs.

According to this, the surface expression of the co-stimulatory molecules CD80 and CD86 was stained and surface MR expression on untreated and CpG-activated wildtype and $MR^{-/-}$ BMDCs was analyzed.

An equally increased CD80 and CD86 expression was detectable on wildtype and $MR^{-/-}$ BMDCs after CpG-treatment compared to unstimulated BMDCs (**Fig. 4-13**). Furthermore, even after CpG-treatment, a considerable percentage of wildtype BMDCs still expressed the MR on their surface and took up MR specific antibodies (**Fig. 4-13**). The reduced antibody-uptake capacity upon CpG activation of BMDCs may not necessarily go along with decreased MR expression on the cell surface but might be due to an impaired antigen-uptake-machinery (114, 115).

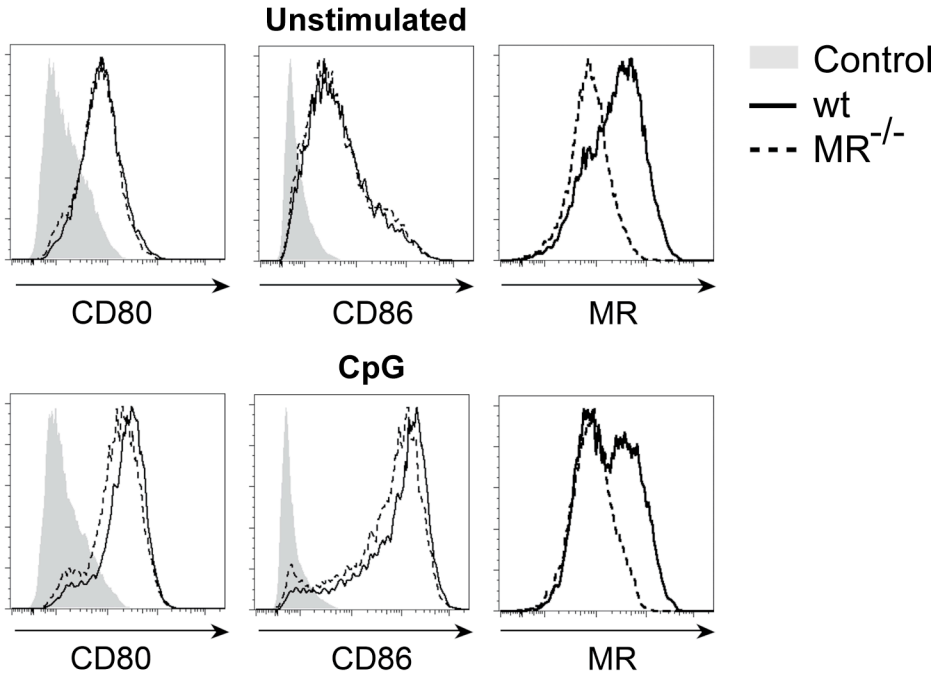

Fig. 4-13: Neither differential expression of co-stimulatory molecules on wildtype and $MR^{-/-}$ BMDCs nor MR-loss could be detected upon CpG treatment.

Wildtype or $MR^{-/-}$ BMDCs were activated over night with 5µg/mL CpG or left untreated. The following day, BMDCs were either harvested and stained for CD80 and CD86 or received 1µg/mL fluorescently labeled αMR antibody for 15 minutes. Finally, cells were analyzed by flow cytometry. Control cells were left unstained.

As described above, CTLA-4 up-regulation could be achieved in the presence of the MR and by inhibition of the CD45 phosphatase activity. Then, the hypothesis was tested whether inhibition of CD45 also affected the CpG-mediated suppression of CTLA-4.

Therefore, DesTCR T cells were incubated with naive $MR^{-/-}$ BMDCs in the presence or absence of a CD45 inhibitor. Alternatively, co-culture took place with CpG-stimulated BMDCs plus CD45 inhibitor. Stimulation of DesTCR T cells with $MR^{-/-}$ BMDCs led to only a weak expression of CTLA-4, though being strongly induced in the presence of CD45

inhibitor (**Fig. 4-14a**). Noteworthy, after CpG treatment of the BMDCs, the expression of the inhibitory molecule CTLA-4 on T cells was suppressed (**Fig. 4-14a**). Significant changes of % CTLA-4^+ cells and MFI of CTLA-4 on $CD8^+$ cells were proven by quantification in **figure 4-14b** and **c**.

To investigate whether the suppressed CTLA-4 expression under inflammatory conditions was due to signaling via co-stimulatory molecules like CD80/86 on BMDCs with its counter-receptor CD28 on T cells, inflammation was mimicked by application of a stimulating αCD28 antibody. If that assumption were true, the same effect on CTLA-4 expression had to be seen in the presence of the αCD28 antibody as under CpG influence.
In fact, T cells that were activated by $MR^{-/-}$ BMDCs in the presence of a αCD28 antibody showed a significantly reduced percentage of CTLA-4 expressing cells (**Fig. 4-14d, e**) plus decreased amounts of CTLA-4 (**Fig. 4-14f**).

Finally, it was examined whether inflammatory stimuli also have an impact on cytotoxic capacities of $CD8^+$ T cells. Therefore, DesTCR T cells were primed either by naive or by CpG-stimulated wildtype or $MR^{-/-}$ BMDCs and the *in vitro* cytotoxicity was analyzed.

Under steady-state conditions, $MR^{-/-}$-primed T cells showed an increased cytotoxicity compared to wildtype BMDC-primed DesTCR T cells (**Fig. 4-14g**). Importantly, the cytotoxic capacity of DesTCR T cells that were primed by wildtype BMDCs substantially increased under the influence of inflammatory stimuli (**Fig. 4-14g**). The cytotoxicity was elevated to an extent similar to T cells that were activated by $MR^{-/-}$ BMDCs (**Fig. 4-14g**). Plus, both wildtype- and $MR^{-/-}$ BMDC-primed T cells showed an increased cytotoxic capacity under inflammatory conditions compared to the steady-state conditions (**Fig. 4-14g**). These data highlight that the suppressive function of the MR on cytotoxicity under steady state conditions can be circumvented in case of inflammation.

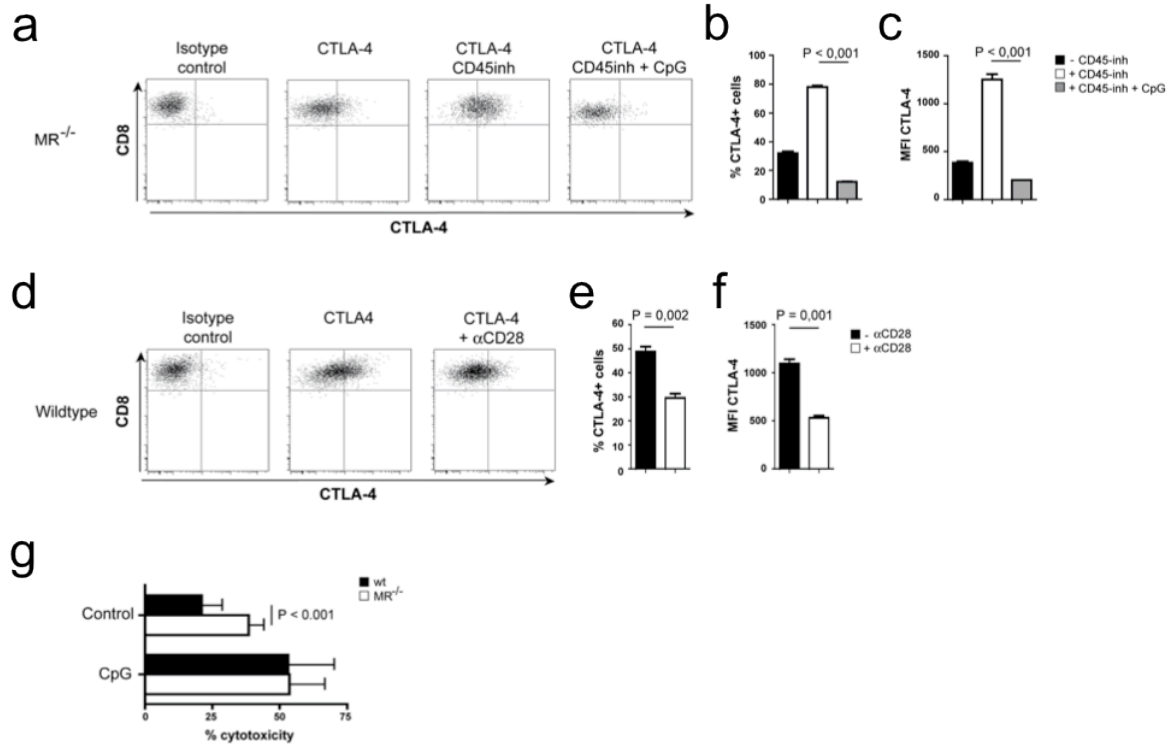

Fig. 4-14: Inflammatory stimuli could prevent MR-mediated up-regulation of CTLA-4 and suppression of T cell cytotoxicity.

(a) $MR^{-/-}$ BMDCs were activated over night with 5µg/mL CpG or left untreated. DesTCR T cells were incubated for three days with activated or untreated BMDCs in the presence or absence of 50 mM of the CD45-specific inhibitor methyl-3,4-dephostatin. After three days, 1µg/mL fluorescent-coupled αCTLA-4 or isotype control antibody was added to the supernatant for four hours. Cells were harvested, stained for CD8 and analyzed by flow cytometry. **(b)** Quantification of (a). **(c)** MFI of CTLA-4 of (a). **(d)** DesTCR T cells were incubated for three days with wildtype BMDCs in the presence or absence of a stimulatory αCD28 antibody. 1µg/mL fluorescent-coupled αCTLA-4 or isotype control antibody was added to the supernatant for four hours. Cells were harvested, stained for CD8 and analyzed by flow cytometry. **(e)** Quantification of (d). **(f)** MFI of CTLA-4 of (d). **(g)** Wildtype BMDCs were activated over night with 5µg/mL CpG or left untreated (Control). DesTCR T cells were incubated for three days with activated or untreated BMDCs. T cells were purified by density gradient centrifugation and distinctly CFSE-labeled target cells or control cells were added in different ratios to the T cells. After four hours the ratio of target to control cells was analyzed by flow cytometry and the specific cytotoxicity was calculated. % $CTLA\text{-}4^+$ cells and MFI of CTLA-4 were determined after gating on $CD8^+$ cells. % $CTLA\text{-}4^+$ cells and MFI of CTLA-4 were determined after gating on $CD8^+$ cells.

4.6 *In vivo,* the MR increased the expression of CTLA-4 accompanied with a decreased cytotoxicity

After having investigated the tolerogenic effect of the MR *in vitro*, further analysis should determine whether this effect also held true in the *in vivo* situation.

First, the CTLA-4 expression on T cells was examined after activation with wildtype respectively $MR^{-/-}$ BMDCs *in vivo*. On this account, wildtype or $MR^{-/-}$ BMDCs were transduced with an adenovirus encoding for Luciferase, OVA and GFP (AdLOG) or left untreated (Control). To ensure that the transduction efficiency of wildtype and $MR^{-/-}$ BMDCs was the same, the GFP expression of transduced BMDCs was determined 48 hours after transduction by flow cytometry. **Figure 4-15** shows an equal transduction efficiency of wildtype and $MR^{-/-}$ BMDCs.

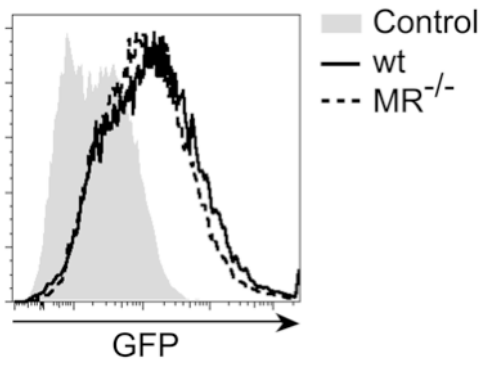

Fig. 4-15: Equal transduction efficiencies were detected for wt and $MR^{-/-}$ BMDCs.

Wildtype or $MR^{-/-}$ BMDCs were transduced for three hours with an adenovirus encoding Luciferase, OVA and GFP (AdLOG) with an MOI of 20 or left non-transduced (Control). After 48h, transduction efficiency was determined by flow cytometric analysis of GFP expression.

Transduced BMDCs were injected i.v. into C57/Bl6J recipient mice. After six days, splenocytes were isolated and stained for CTLA-4, CD8 and with SIINFEKL-dextramers for the MHC-I OVA epitope. CTLA-4 expression on endogenous antigen-specific (Dextramer+) and antigen-unspecific (Dextramer-) $CD8^+$ T cells was monitored by flow cytometry.

Despite similar transduction efficiencies, antigen-specific endogenous $CD8^+$ T cells that were primed by wildtype BMDCs revealed a significantly increased CTLA-4 expression compared to T cells activated by $MR^{-/-}$ BMDCs (**Fig. 4-16a**). In contrast, antigen-unspecific $CD8^+$ T cells did not show any CTLA-4 up-regulation, indicating that the up-regulation of

CTLA-4 indeed resulted from antigen-specific T cell activation in the presence of the MR. These results confirmed the findings of *in vitro* experiments (**Fig. 4-10a**) and emphasized the hypothesis that the regulatory effect of the MR is a mechanism being relevant also *in vivo*.

Finally, it was investigated whether also *in vivo* the MR displayed the same tolerogenic effect on T cell cytotoxicity which had been observed *in vitro* (**Fig. 4-2**). To this end, wildtype or $MR^{-/-}$ BMDCs were transduced with AdLOG and injected into C57/BL6J as described above. Control mice received non-transduced BMDCs lacking the capacity for T cell priming against OVA. Afterwards, C57/BL6 splenocytes were isolated and target cells were loaded with the OVA T cell peptide SIINFEKL ($CFSE^{high}$). Control cells were not loaded with peptide ($CFSE^{low}$) and both cell types were injected into the mice. Four hours later, spleens were isolated and the ratio between target and control cells was determined by flow cytometry.

Importantly, also *in vivo* it could be observed that T cells that were primed in the presence of the MR showed a significantly reduced cytotoxic capacity compared to T cells that were activated by $MR^{-/-}$ BMDCs (**Fig. 4-16b, c**). Thereby, the data from the shown *in vitro* studies above could be confirmed and the influence of the MR on limiting the cytotoxic capacity of endogenous T cells *in vivo* could be proved.

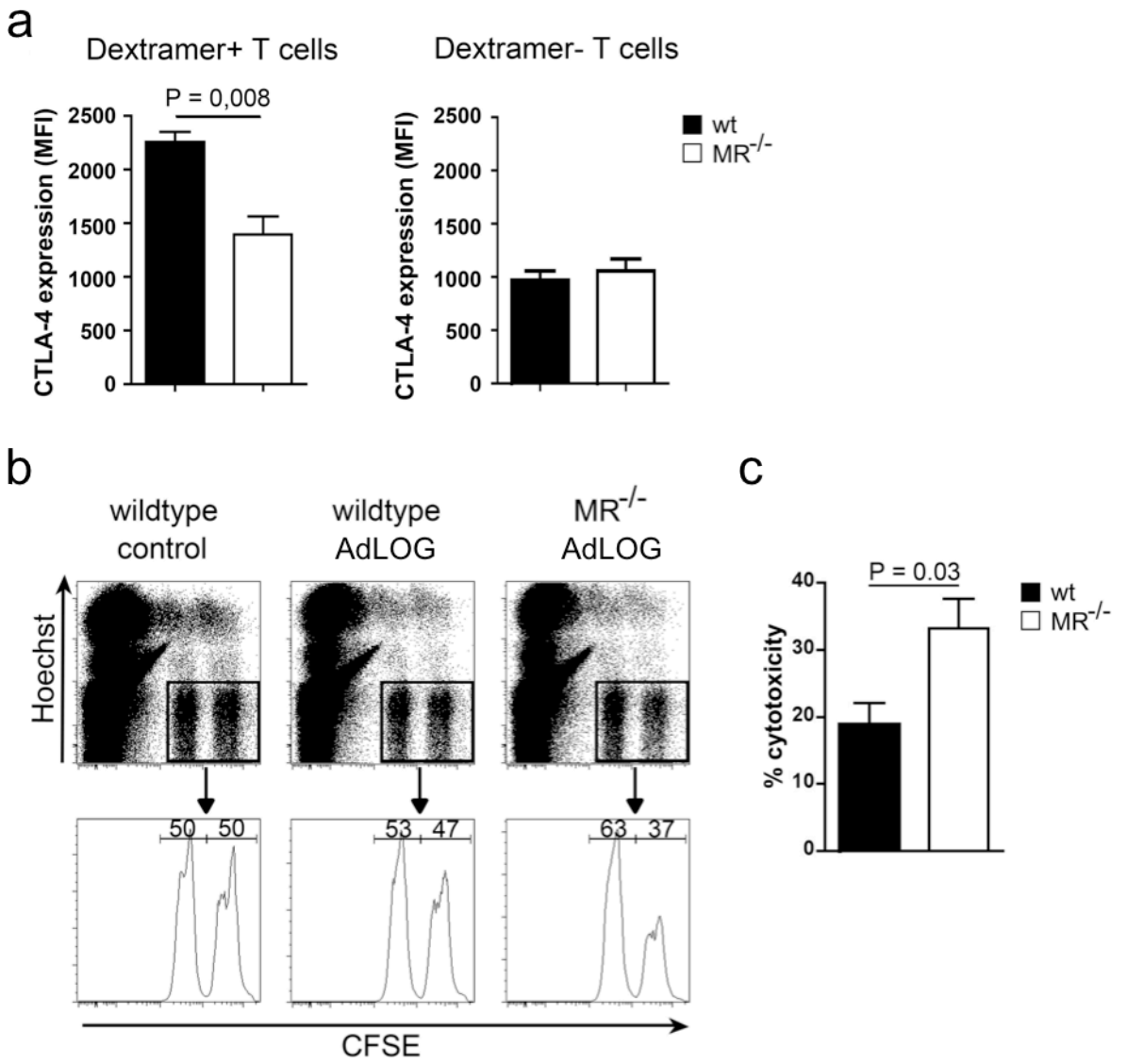

Fig. 4-16: Also i*n vivo,* the MR increased the expression of CTLA-4 accompanied with a decreased cytotoxicity.

(a) Wildtype or $MR^{-/-}$ BMDCs were transduced for three hours with an adenovirus encoding Luciferase, OVA and GFP (AdLOG) with an MOI of 20. $0{,}75*10^6$ adenovirally transduced or control BMDCs were injected i.v. into C57/Bl6J mice. After 6 days, splenocytes were isolated and $5*10^6$ cells were incubated for four hours with 2µg/mL fluorescently labeled αCTLA-4 or isotype control antibody. Cells were harvested, stained with fluorescently labeled SIINFEKL-dextramers and CD8 antibody and analyzed by flow cytometry. CTLA-4 expression of $CD8^+$ SIINFEKL-$dextramer^+$ and SIINFEKL-$dextramer^-$ T cells was determined. **(b)** Wildtype or $MR^{-/-}$ BMDCs were transduced for three hours with an adenovirus encoding Luciferase, OVA and GFP (AdLOG) with an MOI of 20 or left non-transduced (Control). $1*10^6$ BMDCs were injected i.v. into C57/Bl6J mice. After 5 days, splenocytes from C57/BL6 mice were isolated, target cells were loaded with 2µM OVA minimal peptide SIINFEKL (stained $CFSE^{high}$), non-target cells were left untreated (stained $CFSE^{low}$). Target cells and non-target cells were mixed equally and a total of $10*10^6$ cells per mouse were injected i.v.. Four hours later, spleens were isolated and analyzed by flow cytometry. The ratio between target cells and non-target cells was determined. **(c)** Calculation of the specific cytotoxicity of (b).

5 Discussion

The MR was so far known in the context of two immunogenic properties: inducing immunity (87) and being induced under immune suppressive conditions (94, 116, 117). This opposing behavior could until now neither be explained nor unified. Former studies demonstrated that the MR is only capable to induce a potent immune response under inflammatory conditions. However, in the absence of endotoxins, a tolerogenic state is achieved (89, 90). In the present study it is demonstrated that the MR represents a molecular switch between induction of immunity and tolerance in $CD8^+$ T cells. The decision towards the one or the other depends on the inflammatory condition of the surrounding milieu. Furthermore, it was discovered that the MR mediates its tolerogenic function by restricting the activity of CD45 and up-regulation of the inhibitory molecule CTLA-4.

5.1 The Mannose Receptor in tolerance induction and maintenance

The MR is expressed on a variety of cells that mediate tolerance and immune suppression. Several reports describe extensive MR expression on M2-differentiated macrophages in the immunosuppressive environment of re-occurring and vaccine-resistant tumors (101-103, 118).

Other tolerance-mediating cells expressing the MR are liver sinusoidal endothelia cells (97, 119), uterine mucosal macrophages (99), oral macrophages and macrophages in the lamina propria of the small intestine (100).

In the present study a tolerogenic effect of the MR on $CD8^+$ T cells under steady state conditions can be shown. Therefore it is conceivable that the above-mentioned cells might exert their suppressive function via the MR as well. Strengthening these observations, it was proven that tumor-associated macrophages (TAMs), being high in MR expression, can be selectively eliminated by application of the chemotherapeutic agent docetaxel (103). This deletion of MR-bearing TAMs, results in a potent CTL response against tumor

antigens. Therefore it is possible that also the immune-suppressive function of TAMs might be mediated via the MR.

Furthermore it is published that anti-inflammatory cytokines and agents like IL-10, IL-1RA, IL-4, dexamethasone and macrophage colony-stimulating factor (M-CSF) stimulate the expression of the MR and support the differentiation of MR-bearing immunregulatory macrophages (94, 99, 116, 117).

5.2 The Mannose Receptor as molecular switch for tolerance versus immunity

Quite contrary to the expression of the MR on tolerogenic cells, the MR has so far mainly been known as a crucial player in the induction of immunity. Uptake of glycosylated antigens by the MR leads to subsequent cross-presentation towards $CD8^+$ T cells and a potent immune response (60, 87-89). Noteworthy, this is only the case in the presence of inflammatory stimuli (89). These observations go along with the presented data of this study, proving that the tolerogenic effect of the MR under steady-state conditions is overcome after DC maturation. Comparable to Burgdorf et al. (89), the study at hand also detects a strong induction of immunity in the presence of the MR under inflammatory conditions.

Combination of the facts that the MR expression is reduced by pro-inflammatory stimuli but increased by immune suppressive agents, indicates a favorably tolerogenic function of the MR (67, 94, 96, 99, 116, 117). Supportive to that is the observation that the immune suppressive transcription factor PPARγ inhibits $CD8^+$ T cell activation by increased expression of the MR and up-regulation of the inhibitory molecule B7H1 (104).
In line with that, it is shown in this work that the MR on DCs leads to increased expression of the inhibitory molecule CTLA-4 on $CD8^+$ T cells and hence to T cell tolerance.

5.3 CD45 as crucial mediator for tolerance

The up-regulation of CTLA-4 was reported to be mediated by CD45 ligation (113). Application of an anti-CD45 antibody in transplantation experiments and allergic asthma yielded in allograft acceptance and decreased allergic responses (113, 120). The ligation of CD45 could thereby be linked with up-regulation of CTLA-4 and tolerance induction. However, the impact of the applied antibody on CD45 was not described.

In this thesis, the interaction of the MR and CD45 (58) is confirmed but additionally a restraining effect of the MR on CD45 activity is demonstrated. In the work at hand, it is shown that the presence of the MR and inhibition of CD45 are responsible for up-regulation of the inhibitory molecule CTLA-4 on the T cell surface. Accompanied with CTLA-4 expression, there is a decreased cytotoxic capacity. Such a reduced cytotoxic capacity of $CD8^+$ T cells might also be the reason for the enhanced allograft acceptance in the studies of Fecteau et al. (113). It is thinkable that the CD45 antibody used in their study, likewise as the MR in the present study, could result in an inhibition of the CD45 activity. Since the results of this work show that a reduced CD45 phosphatase activity leads to an enhanced CTLA-4 expression, this might also be the modus operandi of the CD45 antibody. This assumption is supported by the fact that an anti-CD45 antibody is used, which targets the isoform CD45RB. It could be shown by the work of Martinez-Pomares et al. and additionally in this study that the MR neither binds to the full-length version CD45RABC (230kDa) nor to the minimal form CD45R0 (180kDa). This was verified by Western blotting (see **Fig. 4-7**), where binding of the MR to CD45 of intermediate molecular weight (approx. 200kDa) could be shown. It is under current investigation to determine the isoform being bound by the MR but CD45RB is most likely, since only this isoform is expressed on naive CD8 T cells (see **Fig. 2-9**). Yet, as CD45RB is conceivable, the observed effect of Fecteau et al. might also be accomplishable by application of the MR (113).

As expected, the MR-mediated inhibition of CD45 also results in changes of the CD45 down-stream target Lck in the TCR signaling cascade. It could be verified that in the presence of the MR the phoshporylation status of the kinase Lck on the tyrosine Y505 is increased.

As outlined in the introduction (see chapter 2.6), the activity of Lck is complexly regulated. Different combinations of phosphorylations on the inhibitory (Y505) or the catalytic tyrosine Y394 result in divergent signaling competence. In $CD45^{-/-}$ thymocytes and cell lines, Lck is hyperphosporylated at its negative regulatory Y505, hence uncoupling the TCR from intracellular signaling (121, 122). This would result in a predominantly positive regulatory function of CD45 in T cell signaling (42). Surprisingly, the kinase activity of Lck in $CD45^{-/-}$ cell lines is increased (123, 124). This leads to two conclusions: Firstly, that CD45 can also target the catalytic tyrosine Y394 and secondly, that despite phosphorylation of the inhibitory Y505 the kinase is still active due to the additional phosphorylation of Y394. Hence, CD45 obviously has additional negative regulatory functions on the activity of Lck (125).

Which effect is dominating seems to be dependent on the availability of Lck for CD45 as a substrate. Hermiston et al. (42) discussed that in resting T cells, CD45 is in close proximity to Lck and dephosphorylates predominantly the negative regulatory Y505 and to a lesser extend Y394. This leads to a signaling-competent, mostly unphosphorylated pool of Lck. Upon TCR engagement, CD45 is excluded from the forming immunological synapse (42, 52) and thereby retrieved from Lck. As a result, autophoshorylation of Y394 leads to an active form of Lck which might still be phosphorylated at Y505.

A state of dual phosphorylation might also be the case for Lck in T cells that were activated in the presence of the MR. In the depicted Western blot (see **Fig. 4-8**), only the phosphorylation status of Y505 is shown, lacking the correspondent analysis for Y394. This issue, plus the analysis of the resulting kinase activity of Lck after MR-mediated CD45-inhibition, are under current investigation.

The importance of regulating the activity of CD45 becomes obvious by the phenotype of two different CD45 mutants. CD45-deficient mice (49, 50, 126) and humans (48, 127) develop a severe-combined immunodeficiency. In contrast to that, mutant mice unable to shut-off CD45 activity (CD45E613R) (56) suffer from profound lymphoproliferative syndrome combined with severe autoimmune nephritis due to autoantibody production, which results in early death. The present study shows a direct connection between CD45

activity and CTLA-4 expression. The necessity of the inhibitory molecule CTLA-4 is underlined by the phenotype of CTLA-4-deficient mice, which die within less than four weeks after birth due to diffuse lymphoproliferative disease (36, 128). These three mutants ($CD45^{-/-}$, CD45E613R and $CTLA\text{-}4^{-/-}$) clearly show the outcome of malregulation of the molecules CD45 and CTLA-4.

Interestingly, the immunosuppressive function of CD45 antibodies via CTLA-4 induction is decreased under the influence of the Calcineurin-inhibitor cyclosporine (129). Since Calcineurin activates NFAT and its inhibition prohibits CD45-mediated immunosuppression, it is reasonable that the observed CTLA-4 up-regulation upon CD45 ligation is due to NFAT signaling.

5.4 Tolerance induction mediated by NFAT

Fehr et al. (130) could show that the Calcineurin-dependent tolerance induction only is the case for $CD8^+$ and not for $CD4^+$ T cells. Furthermore, they could prove that the Calcineurin/NFAT pathway mediates mounting and maintenance only of the peripheral and not of the central tolerance.

The expression of NFAT itself is triggered by TCR stimulation, whereas co-stimulatory signals induce the expression of the interaction partner AP1. Under inflammatory conditions, NFAT1 interacts with the AP1 and leads to expression of genes typical for activated T cells (131). However, in the absence of AP1, other interaction partners for NFAT come into play resulting in T cell activation and/or tolerance induction (132).

Transcription factors of the EGR family (131) are alternative collaborators of NFAT. EGR1 is associated with T cell activation (133) and is elevated in its expression in the presence of the MR compared to control samples in the present study (see **Fig. 4-9c**). Notably, this is only the case for the early (4h) and intermediate (18h) time points. Later, between 18h and 48h, there is a steep decrease in its expression in the presence of the MR. In contrast to that, the level of EGR1 remains stable for the intermediate and late time points in the absence of the MR. This leads to a decreased expression of EGR1 under the influence of the MR.

However, EGR2 and EGR3 are known for induction of T cell anergy by down-regulation of EGR1 (134). In here, the presence of the MR during T cell activation leads to marginally higher expression levels of EGR2 and EGR3 at an early time point (4h).

It is possible that this increased expression of EGR2 and EGR3 at early time points is responsible for the subsequent down-regulation of EGR1 at the later time points. Yet, the time frame of EGR2/3 up-regulation and subsequent EGR1 down-regulation appears quite long for processes normally occurring within minutes or a few hours as common in transcription regulation (134). Since EGR genes are described as important regulators in T cell activation or induction of tolerance (133, 134), we investigated whether they can directly target the Ctla-4 promoter. However, bioinformatical approaches could not predict direct binding capacities of EGR1, 2 or 3 to the Ctla-4 promoter.

5.5 The role of CTLA-4 in tolerance induction

Besides the regulation of the EGR genes, NFAT also mediates the expression of another very important gene in tolerance induction, namely Ctla-4. Gibson et al. (135) showed the binding of NFAT to the proximal promoter of Ctla-4 in $CD3^+$ human peripheral blood mononuclear cells (PBMC). This promoter binding was accompanied with increased CTLA-4 expression. A possible scenario of how the MR leads to tolerance is that upon MR-mediated inhibition of CD45 the kinase Lck is hyperphosphorylated and thereby enhanced in its activity. This enhancement might result to increased Ca^{2+} release via the Calcineurin/Calmodulin pathway and in turn to increased NFAT expression. Additionally to the expression level of NFAT, also the retention time within the nucleus might be prolonged under the influence of the MR. As a consequence, enriched nuclear NFAT possibly binds to the CTLA-4 promoter resulting in its increased transcription accompanied with induction of tolerance.

The importance of NFAT-mediated tolerance induction becomes obvious by the fact that NFAT is able to induce forkhead box P3 (Foxp3) expression, which is a marker for $CD4^+$ regulatory T cells (T_{reg}) (136). Foxp3 can in turn interact with NFAT and up-regulates CTLA-4 expression in $CD4^+$ $CD25^+$ T_{reg} (137, 138). Wing et al. (139) reported that only lacking expression of CTLA-4 on T_{reg} is sufficient to cause autoimmune disease, allergies and tumor

growth. Interestingly, additional defects in CTLA-4 expression in T effector cells even pronounce the pathology. This highlights the importance in CTLA-4 regulation in T_{reg} as well as in T effector cells.

The significance of CTLA-4 is further stressed by the various therapeutic approaches targeting CTLA-4 (140). Anti-CTLA-4 antibodies are however antagonistic rather than agonistic and worsen autoimmune disease like EAE (141). They were therefore used in many different tumor-treatments (e.g. brain, breast, ovaries, colon), either applied solely or in combination with e.g. radiation therapy (142).
For autoimmune disease therapies, a soluble form of CTLA-4 (sCTLA-4) is used instead. This is a widely investigated co-stimulatory therapy, applied for murine models of systemic lupus erythematosus (SLE) (143), experimental allergic encephalo-myelitis (EAE) (144-146), allergic contact dermatitis (147), rheumatoid arthritis (RA) (148) and type 1 diabetes (T1D) (149). Furthermore sCTLA-4 is able to promote long-term graft survival (147, 148, 150). Approaches using sCTLA-4 are favorable compared to systemic immune suppression, since only T cells - and not all immune cells - are targeted.

Due to its capacity to induce CTLA-4 expression, also the application of the soluble form of the MR might lead to the same immune suppressive effect and might be an alternative in treatment of the above-mentioned autoimmune disease. This and the still unanswered question whether the MR-mediated induction of CTLA-4 is, as speculated, due to enhanced NFAT-binding to the Ctla-4 promoter, has to be experimentally tested in the future.

5.6 Influence of the Mannose Receptor on DC-T cell interactions

Marangoni et al. (151) showed via multiphoton intravital microscopy that tolerance induction is connected with delayed nuclear export of NFAT. Whether the MR also leads to prolonged transcriptional activity in the nucleus, remains to be investigated. Yet, the study of Maragoni et al. connected this tolerance induction with a predominance of unstable interactions between APCs and T cells. Divergent to this, the present data indicate prolonged interactions between tolerance inducing MR-bearing DCs and T cells compared to MR-lacking DCs.

At the first glance, the observation of prolonged DC-T cell contact in tolerance induction might sound contradictory to the general agreement that long-lasting contact durations between APCs and T cells result in efficient T cell priming, whereas short interactions lead to tolerance induction (152-155). Mostly, these long-lasting interactions accompanied with T cell priming were seen under inflammatory conditions whereas tolerance induction was reported under non-inflammatory conditions (154, 156, 157).

This study indicates that the MR also influences contact durations of DC-T cell interactions under non-inflammatory conditions. These findings are supported by Van Vliet et al. (57), proving the contribution of the lectin MGL in DC-T cell contacts. They detected an increased retention of Jurkat cells and peripheral blood lymphocytes by an MGL-transfected cell line compared to untransfected cells. A further supportive fact for the prolonged DC-T cell interaction in the presence of the MR, despite tolerance induction, are reports about increased integrin expression in CD45-deficient cells (53, 54). This increased integrin expression in macrophages and T cells is due to enhanced Src family kinase activity, to which also Lck belongs. As already highlighted, the MR is able to inhibit the phosphatase CD45 in T cells. Thereby, CD45 is disabled to dephosphorylate Lck neither on its catalytic tyrosine Y394, nor on its inhibitory tyrosine Y505, which may result in increased Lck activity. In turn, T cells which get into contact with MR-bearing DCs might also up-regulate integrins and thereby increase the contact duration.

It is nevertheless reported that not only the contact duration alone, but also cytokines and chemokines in concert determine the fate of T cells towards immunity or tolerance (153). The data from van Vliet et al. and my own work furthermore indicate that besides these, other factors, like lectins, play an important role during the interaction of APCs and T cells. Finally, it was proven that the contribution of the MR to the DC-T cell interaction not only influences its duration but also results in tolerance induction in $CD8^+$ T cells.

5.7 The Mannose Receptor as target for dampening the immune response

The ability of the MR to cross-present antigens led to the possibility to induce a potent immune response by targeting the MR for vaccination strategies. As a matter of fact, many attempts were in vain and resulted in T cell tolerance (90, 91). In these studies, immunity could only be induced by co-application of endotoxins (90, 93). Chieppa et al. (92) further stated that it also strongly depends on the kind of MR-targeting whether anergy or immunity is caused. This is supported by the detection that the specific MR-targeting via 3-sulfo-Lewis^A and tri-GlcNAc (N-acetylglucosamine) is able to induce potent $CD8^+$ response even in the absence of inflammatory agents (158).

These observations further strengthen the fact that one has to consider the dual function of the MR being either induction of immunity or tolerance when antigens were targeted towards the MR. Either a strong adjuvant has to be co-administered or only certain antigens-conjugates can be used to induce a strong immune response which would be desirable for example for tumor-vaccinations.

Otherwise, MR-targeting will lead to immune-suppression which however could be beneficial for targeting assays aiming at dampening the immune response as in autoimmune diseases like EAE, (159, 160).
A different approach in the treatment of autoimmune diseases, apart from antigen targeting towards the MR, could be to systemically facilitate the quantity of the MR. This may be achieved by the application of agents known to induce the MR expression.

Adorini et al. described an enhanced MR expression upon treatment of human myeloid dendritic cells with $1,25(OH)_2D_3$ (active vitamine D) and the preventive effect of VitD in mouse models of autoimmune disease like SLE, EAE, RA and T1D (161). Although these effects were not pinpointed to be due to the MR, it would be worth repeating it in MR-deficient mice. Thereby, one could investigate whether and to which extend the improving capacity of VitD is mediated by increased MR expression.

The expression of the MR might also be triggered *in vivo* by application of VitD. It was shown by Munger et al. (162) that intake of VitD and incidence of multiple sclerosis (MS) is inversely correlated. Furthermore, in the northern hemispheres with less sunlight and hence lower VitD levels the severity of MS is increased (163). VitD supplementation also had preventive effects on development of rheumatoid arthritis (164).

A systemic application of IL-10, which might also lead to enhanced MR expression, is controversially discussed. Not in all application models did IL-10 reveal immune-suppressive functions; immune-stimulatory effects could also be observed. Thus, it has to be carefully investigated which disorder at which developmental stage can be treated with which concentration of systemically administered IL-10 (165). For IL-4, another MR-inducing cytokine, Ghoreschi et al. (166) could achieve positive effects in treatment of psoriasis patients. Whether systemic administration of IL-10 or IL-4, besides many other effects, also leads to enhanced expression of the MR and thus might decrease the pathology of autoimmune disease remains to be investigated.

Since the expression of the MR directly correlates with its shedding, the above mentioned treatments may not only enhance surface MR-expression on cells, but the shed variant might be able to provide a humoral tolerogenic stimuli.
A soluble form of the mannose receptor could already be detected in serum of mice (77) indicating its natural appearance *in vivo.* After shedding, the MR still retains its binding capabilities as proven by Martinez-Pomares et al. (77) and in the present study. In this work, it was furthermore outlined that also the tolerogenic effect of the MR is still existent when applied as soluble protein. Hence, the application of the soluble mannose receptor might be a therapeutic tool in the treatment of $CD8^+$ T cell-mediated autoimmune diseases like MS, T1D and RA (167, 168, 169).

5.8 Concluding remarks

The results of the study at hand could deliver an explanation as to the question why many tolerance-inducing cells express the MR, why MR-targeting often led to anergy instead of immunity and why co-administration of strong adjuvants is necessary in these targeting-strategies. Additionally, it might be of help in further approaches of treating autoimmune diseases. Still, there are many open questions to be answered. Is the tolerogenic effect of the MR mediated via nuclear retention of NFAT? And would that be responsible for the up-regulation of CTLA-4? Which other factors, if any, are involved? Is it possible to prevent or improve pathological courses by application of the soluble MR? Does the MR also influences CD4+ T cells for example in their differentiation towards T_H1 or T_H2 T helper cells? Hopefully, others and myself are able to shed more light into this topic and give further insights into the function and regulation of the immune system.

6 REFERENCES

1. Parkin J & Cohen B (2001) An overview of the immune system. *Lancet* 357(9270):1777-1789.
2. Janeway CAT, Paul; Walport, Mark; Shlomchik, Mark J (2005) *Immuno Biology* (Garland Science Publishing) 6th Ed.
3. Guermonprez P, Valladeau J, Zitvogel L, Thery C, & Amigorena S (2002) Antigen presentation and T cell stimulation by dendritic cells. *Annu Rev Immunol* 20:621-667.
4. Reis e Sousa C (2004) Toll-like receptors and dendritic cells: for whom the bug tolls. *Semin Immunol* 16(1):27-34.
5. Bluml S*, et al.* (2005) Oxidized phospholipids negatively regulate dendritic cell maturation induced by TLRs and CD40. *J Immunol* 175(1):501-508.
6. Van Gool SW, Vandenberghe P, de Boer M, & Ceuppens JL (1996) CD80, CD86 and CD40 provide accessory signals in a multiple-step T-cell activation model. *Immunol Rev* 153:47-83.
7. Vyas JM, Van der Veen AG, & Ploegh HL (2008) The known unknowns of antigen processing and presentation. *Nat Rev Immunol* 8(8):607-618.
8. Purcell AW & Elliott T (2008) Molecular machinations of the MHC-I peptide loading complex. *Curr Opin Immunol* 20(1):75-81.
9. Rocha N & Neefjes J (2008) MHC class II molecules on the move for successful antigen presentation. *Embo J* 27(1):1-5.
10. Schuurhuis DH*, et al.* (2000) Immature dendritic cells acquire CD8(+) cytotoxic T lymphocyte priming capacity upon activation by T helper cell-independent or -dependent stimuli. *J Exp Med* 192(1):145-150.
11. Caux C*, et al.* (1994) Activation of human dendritic cells through CD40 cross-linking. *J Exp Med* 180(4):1263-1272.
12. Bevan MJ (1976) Cross-priming for a secondary cytotoxic response to minor H antigens with H-2 congenic cells which do not cross-react in the cytotoxic assay. *J Exp Med* 143(5):1283-1288.
13. Rescigno M*, et al.* (1998) Bacteria-induced neo-biosynthesis, stabilization, and surface expression of functional class I molecules in mouse dendritic cells. *Proc Natl Acad Sci U S A* 95(9):5229-5234.

14. Kapsenberg ML (2003) Dendritic-cell control of pathogen-driven T-cell polarization. *Nat Rev Immunol* 3(12):984-993.
15. Sacks D & Noben-Trauth N (2002) The immunology of susceptibility and resistance to Leishmania major in mice. *Nat Rev Immunol* 2(11):845-858.
16. Knutson KL & Disis ML (2005) Tumor antigen-specific T helper cells in cancer immunity and immunotherapy. *Cancer Immunol Immunother* 54(8):721-728.
17. Pan J*, et al.* (2004) Interferon-gamma is an autocrine mediator for dendritic cell maturation. *Immunol Lett* 94(1-2):141-151.
18. Corinti S, Albanesi C, la Sala A, Pastore S, & Girolomoni G (2001) Regulatory activity of autocrine IL-10 on dendritic cell functions. *J Immunol* 166(7):4312-4318.
19. Chan A, Baird M, Mercer AA, & Fleming SB (2006) Maturation and function of human dendritic cells are inhibited by orf virus-encoded interleukin-10. *J Gen Virol* 87(Pt 11):3177-3181.
20. Wooldridge L*, et al.* (2005) Interaction between the CD8 coreceptor and major histocompatibility complex class I stabilizes T cell receptor-antigen complexes at the cell surface. *J Biol Chem* 280(30):27491-27501.
21. Gerdes N & Zirlik A (2011) Co-stimulatory molecules in and beyond co-stimulation - tipping the balance in atherosclerosis? *Thromb Haemost* 106(5):804-813.
22. van der Merwe PA, Bodian DL, Daenke S, Linsley P, & Davis SJ (1997) CD80 (B7-1) binds both CD28 and CTLA-4 with a low affinity and very fast kinetics. *J Exp Med* 185(3):393-403.
23. Chikuma S & Bluestone JA (2003) CTLA-4 and tolerance: the biochemical point of view. *Immunol Res* 28(3):241-253.
24. Chambers CA & Allison JP (1999) Costimulatory regulation of T cell function. *Curr Opin Cell Biol* 11(2):203-210.
25. Curtsinger JM*, et al.* (1999) Inflammatory cytokines provide a third signal for activation of naive CD4+ and CD8+ T cells. *J Immunol* 162(6):3256-3262.
26. Curtsinger JM & Mescher MF (2010) Inflammatory cytokines as a third signal for T cell activation. *Curr Opin Immunol* 22(3):333-340.
27. Barry M & Bleackley RC (2002) Cytotoxic T lymphocytes: all roads lead to death. *Nat Rev Immunol* 2(6):401-409.

28. Curtsinger JM, Agarwal P, Lins DC, & Mescher MF (2012) Autocrine IFN-gamma promotes naive CD8 T cell differentiation and synergizes with IFN-alpha to stimulate strong function. *J Immunol* 189(2):659-668.

29. Rahman MM & McFadden G (2006) Modulation of tumor necrosis factor by microbial pathogens. *PLoS Pathog* 2(2):e4.

30. Acuto O, Mise-Omata S, Mangino G, & Michel F (2003) Molecular modifiers of T cell antigen receptor triggering threshold: the mechanism of CD28 costimulatory receptor. *Immunol Rev* 192:21-31.

31. Veillette A, Bookman MA, Horak EM, & Bolen JB (1988) The CD4 and CD8 T cell surface antigens are associated with the internal membrane tyrosine-protein kinase p56lck. *Cell* 55(2):301-308.

32. Barber EK, Dasgupta JD, Schlossman SF, Trevillyan JM, & Rudd CE (1989) The CD4 and CD8 antigens are coupled to a protein-tyrosine kinase (p56lck) that phosphorylates the CD3 complex. *Proc Natl Acad Sci U S A* 86(9):3277-3281.

33. Samelson LE, Phillips AF, Luong ET, & Klausner RD (1990) Association of the fyn protein-tyrosine kinase with the T-cell antigen receptor. *Proc Natl Acad Sci U S A* 87(11):4358-4362.

34. Smith-Garvin JE, Koretzky GA, & Jordan MS (2009) T cell activation. *Annu Rev Immunol* 27:591-619.

35. Schulze-Luehrmann J & Ghosh S (2006) Antigen-receptor signaling to nuclear factor kappa B. *Immunity* 25(5):701-715.

36. Waterhouse P*, et al.* (1995) Lymphoproliferative disorders with early lethality in mice deficient in Ctla-4. *Science* 270(5238):985-988.

37. Nishimura H*, et al.* (2001) Autoimmune dilated cardiomyopathy in PD-1 receptor-deficient mice. *Science* 291(5502):319-322.

38. Jago CB, Yates J, Camara NO, Lechler RI, & Lombardi G (2004) Differential expression of CTLA-4 among T cell subsets. *Clin Exp Immunol* 136(3):463-471.

39. Mukherjee S, Ahmed A, & Nandi D (2005) CTLA4-CD80/CD86 interactions on primary mouse CD4+ T cells integrate signal-strength information to modulate activation with Concanavalin A. *J Leukoc Biol* 78(1):144-157.

40. Davis SJ & van der Merwe PA (2011) Lck and the nature of the T cell receptor trigger. *Trends Immunol* 32(1):1-5.

41. Thomas ML (1989) The leukocyte common antigen family. *Annu Rev Immunol* 7:339-369.

42. Hermiston ML, Xu Z, & Weiss A (2003) CD45: a critical regulator of signaling thresholds in immune cells. *Annu Rev Immunol* 21:107-137.

43. Wang Y*, et al.* (2005) Visualizing the mechanical activation of Src. *Nature* 434(7036):1040-1045.

44. Birkeland ML, Johnson P, Trowbridge IS, & Pure E (1989) Changes in CD45 isoform expression accompany antigen-induced murine T-cell activation. *Proc Natl Acad Sci U S A* 86(17):6734-6738.

45. Deans JP, Boyd AW, & Pilarski LM (1989) Transitions from high to low molecular weight isoforms of CD45 (T200) involve rapid activation of alternate mRNA splicing and slow turnover of surface CD45R. *J Immunol* 143(4):1233-1238.

46. Lynch KW & Weiss A (2000) A model system for activation-induced alternative splicing of CD45 pre-mRNA in T cells implicates protein kinase C and Ras. *Mol Cell Biol* 20(1):70-80.

47. Jacobsen M*, et al.* (2000) A point mutation in PTPRC is associated with the development of multiple sclerosis. *Nat Genet* 26(4):495-499.

48. Kung C*, et al.* (2000) Mutations in the tyrosine phosphatase CD45 gene in a child with severe combined immunodeficiency disease. *Nat Med* 6(3):343-345.

49. Kishihara K*, et al.* (1993) Normal B lymphocyte development but impaired T cell maturation in CD45-exon6 protein tyrosine phosphatase-deficient mice. *Cell* 74(1):143-156.

50. Mee PJ*, et al.* (1999) Greatly reduced efficiency of both positive and negative selection of thymocytes in CD45 tyrosine phosphatase-deficient mice. *Eur J Immunol* 29(9):2923-2933.

51. Trop S, Charron J, Arguin C, Lesage S, & Hugo P (2000) Thymic selection generates T cells expressing self-reactive TCRs in the absence of CD45. *J Immunol* 165(6):3073-3079.

52. Cordoba SP*, et al.* (2013) The large ectodomains of CD45 and CD148 regulate their segregation from and Inhibition of ligated T-cell receptor. *Blood* .

53. Shenoi H, Seavitt J, Zheleznyak A, Thomas ML, & Brown EJ (1999) Regulation of integrin-mediated T cell adhesion by the transmembrane protein tyrosine phosphatase CD45. *J Immunol* 162(12):7120-7127.

54. Roach T*, et al.* (1997) CD45 regulates Src family member kinase activity associated with macrophage integrin-mediated adhesion. *Curr Biol* 7(6):408-417.

55. Bilwes AM, den Hertog J, Hunter T, & Noel JP (1996) Structural basis for inhibition of receptor protein-tyrosine phosphatase-alpha by dimerization. *Nature* 382(6591):555-559.

56. Majeti R*, et al.* (2000) An inactivating point mutation in the inhibitory wedge of CD45 causes lymphoproliferation and autoimmunity. *Cell* 103(7):1059-1070.

57. van Vliet SJ, Gringhuis SI, Geijtenbeek TB, & van Kooyk Y (2006) Regulation of effector T cells by antigen-presenting cells via interaction of the C-type lectin MGL with CD45. *Nat Immunol* 7(11):1200-1208.

58. Martinez-Pomares L*, et al.* (1999) Cell-specific glycoforms of sialoadhesin and CD45 are counter-receptors for the cysteine-rich domain of the mannose receptor. *The Journal of biological chemistry* 274(49):35211-35218.

59. Pontow SE, Kery V, & Stahl PD (1992) Mannose receptor. *Int Rev Cytol* 137B:221-244.

60. Martinez-Pomares L (2012) The mannose receptor. *J Leukoc Biol* 92(6):1177-1186.

61. Segura E, Albiston AL, Wicks IP, Chai SY, & Villadangos JA (2009) Different cross-presentation pathways in steady-state and inflammatory dendritic cells. *Proc Natl Acad Sci U S A* 106(48):20377-20381.

62. Burgdorf S*, et al.* (2010) Steady-state cross-presentation of OVA is mannose receptor-dependent but inhibitable by collagen fragments. *Proc Natl Acad Sci U S A* 107(13):E48-49; author reply E50-41.

63. Segura E*, et al.* (2010) Reply to Burgdorf et al.: The mannose receptor is not involved in antigen cross-presentation by steady-state dendritic cells. *Proceedings of the National Academy of Sciences* 107(13):E50-E51.

64. Llorca O (2008) Extended and bent conformations of the mannose receptor family. *Cellular and molecular life sciences* 65(9):1302-1310.

65. Leteux C*, et al.* (2000) The cysteine-rich domain of the macrophage mannose receptor is a multispecific lectin that recognizes chondroitin sulfates A and B and

sulfated oligosaccharides of blood group Lewis(a) and Lewis(x) types in addition to the sulfated N-glycans of lutropin. *J Exp Med* 191(7):1117-1126.

66. East L, Rushton S, Taylor ME, & Isacke CM (2002) Characterization of sugar binding by the mannose receptor family member, Endo180. *J Biol Chem* 277(52):50469-50475.
67. Taylor PR, Gordon S, & Martinez-Pomares L (2005) The mannose receptor: linking homeostasis and immunity through sugar recognition. *Trends in immunology* 26(2):104-110.
68. Liu Y*, et al.* (2000) Crystal structure of the cysteine-rich domain of mannose receptor complexed with a sulfated carbohydrate ligand. *J Exp Med* 191(7):1105-1116.
69. Martinez-Pomares L*, et al.* (2006) Carbohydrate-independent recognition of collagens by the macrophage mannose receptor. *Eur J Immunol* 36(5):1074-1082.
70. Napper CE, Drickamer K, & Taylor ME (2006) Collagen binding by the mannose receptor mediated through the fibronectin type II domain. *Biochem J* 395(3):579-586.
71. Jurgensen HJ*, et al.* (2011) A novel functional role of collagen glycosylation: interaction with the endocytic collagen receptor uparap/ENDO180. *J Biol Chem* 286(37):32736-32748.
72. Taylor ME, Bezouska K, & Drickamer K (1992) Contribution to ligand binding by multiple carbohydrate-recognition domains in the macrophage mannose receptor. *J Biol Chem* 267(3):1719-1726.
73. Taylor ME & Drickamer K (1993) Structural requirements for high affinity binding of complex ligands by the macrophage mannose receptor. *J Biol Chem* 268(1):399-404.
74. Gazi U & Martinez-Pomares L (2009) Influence of the mannose receptor in host immune responses. *Immunobiology* .
75. Gazi U*, et al.* (2011) Fungal recognition enhances mannose receptor shedding through dectin-1 engagement. *J Biol Chem* 286(10):7822-7829.
76. Deslee G*, et al.* (2002) Involvement of the mannose receptor in the uptake of Der p 1, a major mite allergen, by human dendritic cells. *J Allergy Clin Immunol* 110(5):763-770.
77. Martinez-Pomares L*, et al.* (1998) A functional soluble form of the murine mannose receptor is produced by macrophages in vitro and is present in mouse serum. *J Biol Chem* 273(36):23376-23380.

78. Martinez-Pomares L*, et al.* (2003) Analysis of mannose receptor regulation by IL-4, IL-10, and proteolytic processing using novel monoclonal antibodies. *J Leukoc Biol* 73(5):604-613.

79. Marodi L, Korchak HM, & Johnston RB, Jr. (1991) Mechanisms of host defense against Candida species. I. Phagocytosis by monocytes and monocyte-derived macrophages. *J Immunol* 146(8):2783-2789.

80. Chakraborty R, Chakraborty P, & Basu MK (1998) Macrophage mannosyl fucosyl receptor: its role in invasion of virulent and avirulent L. donovani promastigotes. *Biosci Rep* 18(3):129-142.

81. Tailleux L, Maeda N, Nigou J, Gicquel B, & Neyrolles O (2003) How is the phagocyte lectin keyboard played? Master class lesson by Mycobacterium tuberculosis. *Trends Microbiol* 11(6):259-263.

82. Nguyen DG & Hildreth JE (2003) Involvement of macrophage mannose receptor in the binding and transmission of HIV by macrophages. *Eur J Immunol* 33(2):483-493.

83. Ezekowitz RA*, et al.* (1991) Uptake of Pneumocystis carinii mediated by the macrophage mannose receptor. *Nature* 351(6322):155-158.

84. Miller JL*, et al.* (2008) The mannose receptor mediates dengue virus infection of macrophages. *PLoS Pathog* 4(2):e17.

85. Zamze S*, et al.* (2002) Recognition of bacterial capsular polysaccharides and lipopolysaccharides by the macrophage mannose receptor. *The Journal of biological chemistry* 277(44):41613-41623.

86. Stahl PD & Ezekowitz RA (1998) The mannose receptor is a pattern recognition receptor involved in host defense. *Curr Opin Immunol* 10(1):50-55.

87. Burgdorf S, Lukacs-Kornek V, & Kurts C (2006) The mannose receptor mediates uptake of soluble but not of cell-associated antigen for cross-presentation. *J Immunol* 176(11):6770-6776.

88. Burgdorf S, Kautz A, Bohnert V, Knolle PA, & Kurts C (2007) Distinct pathways of antigen uptake and intracellular routing in CD4 and CD8 T cell activation. *Science* 316(5824):612-616.

89. Burgdorf S, Scholz C, Kautz A, Tampe R, & Kurts C (2008) Spatial and mechanistic separation of cross-presentation and endogenous antigen presentation. *Nat Immunol* 9(5):558-566.

90. He LZ*, et al.* (2007) Antigenic targeting of the human mannose receptor induces tumor immunity. *J Immunol* 178(10):6259-6267.

91. Allavena P*, et al.* (2010) Engagement of the mannose receptor by tumoral mucins activates an immune suppressive phenotype in human tumor-associated macrophages. *Clin Dev Immunol* 2010:547179.

92. Chieppa M*, et al.* (2003) Cross-linking of the mannose receptor on monocyte-derived dendritic cells activates an anti-inflammatory immunosuppressive program. *J Immunol* 171(9):4552-4560.

93. McKenzie EJ*, et al.* (2007) Mannose receptor expression and function define a new population of murine dendritic cells. *J Immunol* 178(8):4975-4983.

94. Stein M, Keshav S, Harris N, & Gordon S (1992) Interleukin 4 potently enhances murine macrophage mannose receptor activity: a marker of alternative immunologic macrophage activation. *J Exp Med* 176(1):287-292.

95. Doyle AG*, et al.* (1994) Interleukin-13 alters the activation state of murine macrophages in vitro: comparison with interleukin-4 and interferon-gamma. *Eur J Immunol* 24(6):1441-1445.

96. Harris N, Super M, Rits M, Chang G, & Ezekowitz RA (1992) Characterization of the murine macrophage mannose receptor: demonstration that the downregulation of receptor expression mediated by interferon-gamma occurs at the level of transcription. *Blood* 80(9):2363-2373.

97. Hochst B*, et al.* (2012) Liver sinusoidal endothelial cells contribute to CD8 T cell tolerance toward circulating carcinoembryonic antigen in mice. *Hepatology* 56(5):1924-1933.

98. Linehan SA, Martinez-Pomares L, Stahl PD, & Gordon S (1999) Mannose receptor and its putative ligands in normal murine lymphoid and nonlymphoid organs: In situ expression of mannose receptor by selected macrophages, endothelial cells, perivascular microglia, and mesangial cells, but not dendritic cells. *J Exp Med* 189(12):1961-1972.

99. Svensson J*, et al.* (2011) Macrophages at the fetal-maternal interface express markers of alternative activation and are induced by M-CSF and IL-10. *J Immunol* 187(7):3671-3682.

100. Mascarell L*, et al.* (2011) Oral macrophage-like cells play a key role in tolerance induction following sublingual immunotherapy of asthmatic mice. *Mucosal Immunol* 4(6):638-647.

101. Predina J*, et al.* (2013) Changes in the local tumor microenvironment in recurrent cancers may explain the failure of vaccines after surgery. *Proc Natl Acad Sci U S A* 110(5):E415-424.

102. Chopra A (2004) 99mTc-Labeled anti-macrophage mannose receptor (MMR; CD206) nanobody. .

103. Kodumudi KN*, et al.* (2010) A novel chemoimmunomodulating property of docetaxel: suppression of myeloid-derived suppressor cells in tumor bearers. *Clin Cancer Res* 16(18):4583-4594.

104. Klotz L*, et al.* (2009) Increased antigen cross-presentation but impaired cross-priming after activation of peroxisome proliferator-activated receptor gamma is mediated by up-regulation of B7H1. *J Immunol* 183(1):129-136.

105. Schonrich G*, et al.* (1991) Down-regulation of T cell receptors on self-reactive T cells as a novel mechanism for extrathymic tolerance induction. *Cell* 65(2):293-304.

106. Lee SJ*, et al.* (2002) Mannose receptor-mediated regulation of serum glycoprotein homeostasis. *Science* 295(5561):1898-1901.

107. Zehner M*, et al.* (2012) Intraendosomal flow cytometry: a novel approach to analyze the protein composition of antigen-loaded endosomes. *Eur J Immunol* 42(8):2187-2190.

108. Ljunggren HG & Karre K (1985) Host resistance directed selectively against H-2-deficient lymphoma variants. Analysis of the mechanism. *J Exp Med* 162(6):1745-1759.

109. Watt SM, Gilmore DJ, Davis JM, Clark MR, & Waldmann H (1987) Cell-surface markers on haemopoietic precursors. Reagents for the isolation and analysis of progenitor cell subpopulations. *Mol Cell Probes* 1(4):297-326.

110. Froger A & Hall JE (2007) Transformation of plasmid DNA into E. coli using the heat shock method. *J Vis Exp* (6):253.

111. Guimezanes A*, et al.* (2001) Identification of endogenous peptides recognized by in vivo or in vitro generated alloreactive cytotoxic T lymphocytes: distinct characteristics correlated with CD8 dependence. *Eur J Immunol* 31(2):421-432.

112. Urbanek RA*, et al.* (2001) Potent reversible inhibitors of the protein tyrosine phosphatase CD45. *J Med Chem* 44(11):1777-1793.

113. Fecteau S*, et al.* (2001) CTLA-4 up-regulation plays a role in tolerance mediated by CD45. *Nat Immunol* 2(1):58-63.

114. Mellman I, Turley SJ, & Steinman RM (1998) Antigen processing for amateurs and professionals. *Trends Cell Biol* 8(6):231-237.

115. Cochand L, Isler P, Songeon F, & Nicod LP (1999) Human lung dendritic cells have an immature phenotype with efficient mannose receptors. *Am J Respir Cell Mol Biol* 21(5):547-554.

116. Ylostalo JH, Bartosh TJ, Coble K, & Prockop DJ (2012) Human mesenchymal stem/stromal cells cultured as spheroids are self-activated to produce prostaglandin E2 that directs stimulated macrophages into an anti-inflammatory phenotype. *Stem Cells* 30(10):2283-2296.

117. Melief J*, et al.* (2012) Phenotyping primary human microglia: tight regulation of LPS responsiveness. *Glia* 60(10):1506-1517.

118. Movahedi K*, et al.* (2012) Nanobody-based targeting of the macrophage mannose receptor for effective in vivo imaging of tumor-associated macrophages. *Cancer Res* 72(16):4165-4177.

119. Smedsrod B, Melkko J, Risteli L, & Risteli J (1990) Circulating C-terminal propeptide of type I procollagen is cleared mainly via the mannose receptor in liver endothelial cells. *Biochem J* 271(2):345-350.

120. Jen KY*, et al.* (2007) CD45RB ligation inhibits allergic pulmonary inflammation by inducing CTLA4 transcription. *J Immunol* 179(6):4212-4218.

121. Koretzky GA, Picus J, Thomas ML, & Weiss A (1990) Tyrosine phosphatase CD45 is essential for coupling T-cell antigen receptor to the phosphatidyl inositol pathway. *Nature* 346(6279):66-68.

122. Cahir McFarland ED*, et al.* (1993) Correlation between Src family member regulation by the protein-tyrosine-phosphatase CD45 and transmembrane signaling through the T-cell receptor. *Proc Natl Acad Sci U S A* 90(4):1402-1406.

123. Burns CM, Sakaguchi K, Appella E, & Ashwell JD (1994) CD45 regulation of tyrosine phosphorylation and enzyme activity of src family kinases. *J Biol Chem* 269(18):13594-13600.

124. D'Oro U & Ashwell JD (1999) Cutting edge: the CD45 tyrosine phosphatase is an inhibitor of Lck activity in thymocytes. *J Immunol* 162(4):1879-1883.

125. Baker M*, et al.* (2000) Development of T-leukaemias in CD45 tyrosine phosphatase-deficient mutant lck mice. *Embo J* 19(17):4644-4654.

126. Byth KF*, et al.* (1996) CD45-null transgenic mice reveal a positive regulatory role for CD45 in early thymocyte development, in the selection of CD4+CD8+ thymocytes, and B cell maturation. *J Exp Med* 183(4):1707-1718.

127. Tchilian EZ*, et al.* (2001) A deletion in the gene encoding the CD45 antigen in a patient with SCID. *J Immunol* 166(2):1308-1313.

128. Tivol EA*, et al.* (1995) Loss of CTLA-4 leads to massive lymphoproliferation and fatal multiorgan tissue destruction, revealing a critical negative regulatory role of CTLA-4. *Immunity* 3(5):541-547.

129. Parry N*, et al.* (1999) Cyclosporine inhibits long-term survival in cardiac allografts treated with monoclonal antibody against CD45RB. *J Heart Lung Transplant* 18(5):441-447.

130. Fehr T*, et al.* (2010) A CD8 T cell-intrinsic role for the calcineurin-NFAT pathway for tolerance induction in vivo. *Blood* 115(6):1280-1287.

131. Macian F (2005) NFAT proteins: key regulators of T-cell development and function. *Nat Rev Immunol* 5(6):472-484.

132. Macian F*, et al.* (2002) Transcriptional mechanisms underlying lymphocyte tolerance. *Cell* 109(6):719-731.

133. Mise-Omata S, Montagne B, Deckert M, Wienands J, & Acuto O (2003) Mammalian actin binding protein 1 is essential for endocytosis but not lamellipodia formation: functional analysis by RNA interference. *Biochem Biophys Res Commun* 301(3):704-710.

134. Collins S*, et al.* (2008) Opposing regulation of T cell function by Egr-1/NAB2 and Egr-2/Egr-3. *Eur J Immunol* 38(2):528-536.

135. Gibson HM*, et al.* (2007) Induction of the CTLA-4 gene in human lymphocytes is dependent on NFAT binding the proximal promoter. *J Immunol* 179(6):3831-3840.

136. Vaeth M*, et al.* (2012) Dependence on nuclear factor of activated T-cells (NFAT) levels discriminates conventional T cells from Foxp3+ regulatory T cells. *Proc Natl Acad Sci U S A* 109(40):16258-16263.

137. Wu Y*, et al.* (2006) FOXP3 controls regulatory T cell function through cooperation with NFAT. *Cell* 126(2):375-387.

138. Hu H, Djuretic I, Sundrud MS, & Rao A (2007) Transcriptional partners in regulatory T cells: Foxp3, Runx and NFAT. *Trends Immunol* 28(8):329-332.

139. Wing K*, et al.* (2008) CTLA-4 control over Foxp3+ regulatory T cell function. *Science* 322(5899):271-275.

140. Stuart RW & Racke MK (2002) Targeting T cell costimulation in autoimmune disease. *Expert Opin Ther Targets* 6(3):275-289.

141. Perrin PJ, June CH, Maldonado JH, Ratts RB, & Racke MK (1999) Blockade of CD28 during in vitro activation of encephalitogenic T cells or after disease onset ameliorates experimental autoimmune encephalomyelitis. *J Immunol* 163(3):1704-1710.

142. Grosso JF & Jure-Kunkel MN (2013) CTLA-4 blockade in tumor models: an overview of preclinical and translational research. *Cancer Immun* 13:5.

143. Finck BK, Linsley PS, & Wofsy D (1994) Treatment of murine lupus with CTLA4Ig. *Science* 265(5176):1225-1227.

144. van Gelder M, Kinwel-Bohre EP, & van Bekkum DW (1993) Treatment of experimental allergic encephalomyelitis in rats with total body irradiation and syngeneic BMT. *Bone Marrow Transplant* 11(3):233-241.

145. Howard LM*, et al.* (1999) Mechanisms of immunotherapeutic intervention by anti-CD40L (CD154) antibody in an animal model of multiple sclerosis. *J Clin Invest* 103(2):281-290.

146. Cross AH*, et al.* (1995) Long-term inhibition of murine experimental autoimmune encephalomyelitis using CTLA-4-Fc supports a key role for CD28 costimulation. *J Clin Invest* 95(6):2783-2789.

147. Sayegh MH*, et al.* (1995) CD28-B7 blockade after alloantigenic challenge in vivo inhibits Th1 cytokines but spares Th2. *J Exp Med* 181(5):1869-1874.

148. Knoerzer DB, Karr RW, Schwartz BD, & Mengle-Gaw LJ (1995) Collagen-induced arthritis in the BB rat. Prevention of disease by treatment with CTLA-4-Ig. *J Clin Invest* 96(2):987-993.

149. Gerold KD*, et al.* (2011) The soluble CTLA-4 splice variant protects from type 1 diabetes and potentiates regulatory T-cell function. *Diabetes* 60(7):1955-1963.

150. Linsley PS*, et al.* (1992) Immunosuppression in vivo by a soluble form of the CTLA-4 T cell activation molecule. *Science* 257(5071):792-795.

151. Marangoni F*, et al.* (2013) The transcription factor NFAT exhibits signal memory during serial T cell interactions with antigen-presenting cells. *Immunity* 38(2):237-249.

152. Hugues S*, et al.* (2004) Distinct T cell dynamics in lymph nodes during the induction of tolerance and immunity. *Nat Immunol* 5(12):1235-1242.

153. Hugues S, Boissonnas A, Amigorena S, & Fetler L (2006) The dynamics of dendritic cell-T cell interactions in priming and tolerance. *Curr Opin Immunol* 18(4):491-495.

154. Bakocevic N, Worbs T, Davalos-Misslitz A, & Forster R (2010) T cell-dendritic cell interaction dynamics during the induction of respiratory tolerance and immunity. *J Immunol* 184(3):1317-1327.

155. Martin-Cofreces NB*, et al.* (2008) MTOC translocation modulates IS formation and controls sustained T cell signaling. *J Cell Biol* 182(5):951-962.

156. Mittelbrunn M*, et al.* (2009) Imaging of plasmacytoid dendritic cell interactions with T cells. *Blood* 113(1):75-84.

157. Shakhar G*, et al.* (2005) Stable T cell-dendritic cell interactions precede the development of both tolerance and immunity in vivo. *Nat Immunol* 6(7):707-714.

158. Singh SK*, et al.* (2011) Design of neo-glycoconjugates that target the mannose receptor and enhance TLR-independent cross-presentation and Th1 polarization. *Eur J Immunol* 41(4):916-925.

159. Luca ME*, et al.* (2005) Mannosylated PLP(139-151) induces peptide-specific tolerance to experimental autoimmune encephalomyelitis. *J Neuroimmunol* 160(1-2):178-187.

160. Kel J*, et al.* (2007) Soluble mannosylated myelin peptide inhibits the encephalitogenicity of autoreactive T cells during experimental autoimmune encephalomyelitis. *Am J Pathol* 170(1):272-280.

161. Adorini L, Amuchastegui S, & Daniel KC (2005) Prevention of chronic allograft rejection by Vitamin D receptor agonists. *Immunol Lett* 100(1):34-41.

162. Munger KL*, et al.* (2004) Vitamin D intake and incidence of multiple sclerosis. *Neurology* 62(1):60-65.

163. Cantorna MT & Mahon BD (2004) Mounting evidence for vitamin D as an environmental factor affecting autoimmune disease prevalence. *Exp Biol Med (Maywood)* 229(11):1136-1142.

164. Merlino LA*, et al.* (2004) Vitamin D intake is inversely associated with rheumatoid arthritis: results from the Iowa Women's Health Study. *Arthritis Rheum* 50(1):72-77.

165. Asadullah K, Sterry W, & Volk HD (2003) Interleukin-10 therapy--review of a new approach. *Pharmacol Rev* 55(2):241-269.

166. Ghoreschi K*, et al.* (2003) Interleukin-4 therapy of psoriasis induces Th2 responses and improves human autoimmune disease. *Nat Med* 9(1):40-46.

167. Friese MA & Fugger L (2009) Pathogenic CD8(+) T cells in multiple sclerosis. *Ann Neurol* 66(2):132-141.

168. Tsai S, Shameli A, & Santamaria P (2008) CD8+ T cells in type 1 diabetes. *Adv Immunol* 100:79-124.

169. Skapenko A, Leipe J, Lipsky PE, & Schulze-Koops H (2005) The role of the T cell in autoimmune inflammation. *Arthritis Res Ther* 7 Suppl 2:S4-14.

7 ABBREVIATIONS

$1,25(OH)_2D_3$. 1α,25(OH)2Vitamin D3

4-NPP. *4-Nitrophenylphosphate*

ABTS. 2,2'-azino-bis(3-ethylbenzothiazoline-6-sulphonic acid

AdLOG. Adenovirus expressing Luciferase OVA GFP

Amp. *Ampicillin*

AP1. *Activator protein 1*

APC. Antigen presenting cell, Allophycocyanin, *Antigen-presenting cell*

BMDC. *Bone marrow-derived Dendritic cell*

BSA. *Bovine serum albumin*

CD. *Cluster of differentiation*

CFSE. *Carboxyfluorescein succinimidyl ester*

CpG. *CpG-dinucleotide*, *CpG-dinucleotide*

CR. *Cystein rich domain*

CRD. Carbohydrate recognition domain

Csk. *C-terminal Src kinase*

CTL. *Cytotoxic T lymphocyte*

CTLA-4. *Cytotoxic T-lymphocyte antigen 4*

CTLD. *C-type lectin-like carbohydrate recognition domain*

DAG. *Diacyl glycerol*

DC. *Dendritic cell*

DCs. *Dendritic cells*

DMEM. Dulbecco's modified Eagle's medium

DTT. *Dithiothreitol*

EAE. Experimental allergic encephalo-myelitis

EDTA. Ethylenediaminetetraacetic acid

Egr. *Early growth response protein*

ELISA. Enzyme-linked immunosorbent assay

ER. Endoplasmic reticulum

FACS. Fluorescence-activated cell sorting

FC. *Fold change*

FCS. *Fetal calf serum*

FDR. *False discovery rate*

FITC. Fluorescein

FNII. *Fibronectin type II domain*

Foxp3. *Forkhead box P3*

GalNAc. N-Acetylgalactosamine

GFP. Green-fluorescent protein

GM-CSF. Granulocyte-macrophage colony-stimulating factor

HEK. *Human embryonic kidney cell*

HEK-MR. *HEK cells expressing the MR*

HEPES. 4-(2-hydroxyethyl)-1-piperazineethanesulfonic acid

ICAM. Intercellular adhesion molecule 1

ICOS. *Inducible T cell costimulator*

ICOSL. *Inducible T cell costimulator ligand*

IFN-g. *Interferon-gamma*

IFNR. *Interferon receptor*

IKK. Inhibitor of nuclear factor-kappa B kinase

IL. *Interleukin*

IMDM. *Iscove's modified Dulbecco's medium*

$InsP_3$. *Inositol-1,4,5-triphosphate*

ITAM. Immunoreceptor tyrosine-based activation motif

Jmjd3. Jumonji domain containing 3

Kana. *Kanamycin*

kDa. *kilo Dalton*

LAT. *Linker for the activation of T cells*

Lck. *Lymphocyte-specific protein tyrosine kinase*

MACS. *Magnatic activated cell sorting*
MAPK. *Mitogen-activated protein kinase*
M-CSF. *Macrophage colony-stimulating factor*
MFI. Mean fluorescent intensity
MHC. *Major histocompatibility complex*
MHC I. *MHC class I molecule*
MHC II. *MHC class II molecule*
MOI. *Multiplicity of infection*
MR. *Mannose Receptor*
$MR^{-/-}$. *MR knockout*
MS. *Multiple sclerosis*

NFAT. *Nuclear factor of activated T cells*
NF-kB. Nuclear factor-kappa B
NK. *Natural killer cell*

OVA. *Ovalbumin*

PAMP. *Pathogen-associated molecular pattern*
PBMC. *Peripheral blood mononuclear cells*
PBS. *Phosphate buffered saline*
PBST. Phosphate buffered saline Tween-20
PD. Programmed cell death
PD-L. Programmed cell death ligand
PE. R-Phycoerythrin
Pen/Strep. *Penicillin/Streptomycin*
PGS. *Partek Genomics Suite*
PKC. *Protein kinase C*
PLCg1. *Phospholipase C gamma 1*
PPARg. *Peroxisome proliferator-activated receptor gamma*
PRR. *Pattern-recognition receptor*
PtdIns(4,5)P_2. Phosphatidylinositol-4,5-bisphosphate

PTPN22. *Protein tyrosine phosphatase, non-receptor type 22*
PVDF. Polyvinylidenfluorid

RA. Rheumatoid arthritis
RAS. *Rat sarcoma*
RCB. *Red cell lysis buffer*
RT. *Room temperature*

SCID. *Severe-combined immunodeficiency*
sCTLA-4. Soluble chimeric CTLA-4 protein
SDS. *Sodium dodecyl sulfate*
SF1670. *N-(9,10-Dioxo-9,10-dihydro-phenanthren-2-yl)-2,2-dimethyl-propioamide*
SLE. Systemic lupus erythematosus
SLP76. Scr homology 2 domain-containing leukocyte phosphoprotein of 76kDa
Src. *Sarcoma*

T1D. *Type 1 diabetes*
TAM. *Tumor-associated macrophage*
TAP. *Transporter associated with antigen processing*
TBS. *Tris buffered saline*
TBST. *Tris buffered saline Tween-20*
TCR. *T cell receptor*
TGF-b. *Transforming growth factor-beta*
T_H. *T helper type 1 cells*
T_H2. *T helper type 2 cell*
TLR. *Toll-like receptor*
TNF. *Tumor necrosis factor*

wt. *Wildtype*

Y394. *Tyrosine residue 394*
Y505. *Tyrosine residue 505*

ZAP-70. Zeta-chain-associated protein kinase of 70 kDa